Practical approach to XANES data analysis:

Shortcuts to understand local structure and chemistry from XANES spectra

Carlo Meneghini

carlo.meneghini@uniroma3.it

https://www.elettra.trieste.it/Conferences/2019/SILS/

XAFS is a local sensitive, chemical selective probe which may provide structural, electronic and even magnetic details

Subjective (Absorber) view of the local atomic structure in your sample

XAFS is a local sensitive, chemical selective probe which may provide structural, electronic and even magnetic details

- Applicable to materials in **any aggregation state:** gas, liquid, solid, single crystals, powders, amorphous, nanostructures, etc....
- Measurable from **bulk** to the highest **diluted** samples (micro- and nano-molar)
- **Versatile** probe (bulk, surfaces, layered structures, quantum structures, etc...)
- **Simple** experimental set-up and easy data collection
- **Fast** (quick XAFS) and **ultrafast** (dispersive) data collection
- **Directional sensitivity** (polarized XAS): to probe structural anisotropy
- **Element selective** Magnetic state sensitive (**XMCD**)

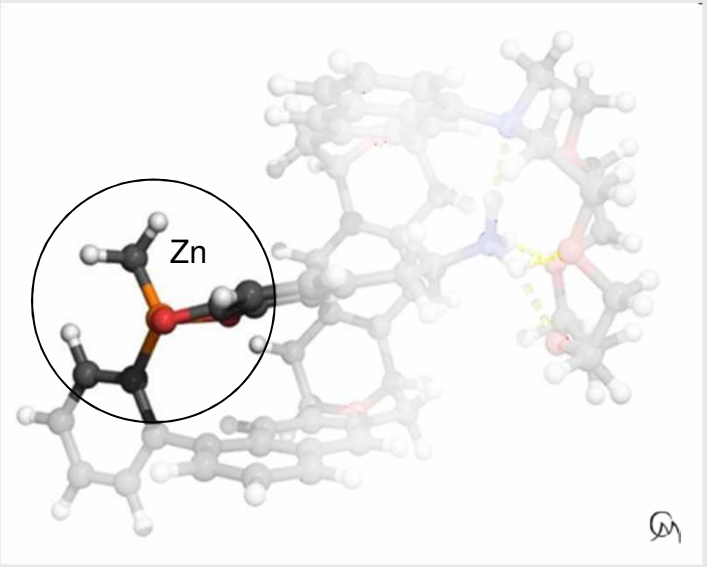

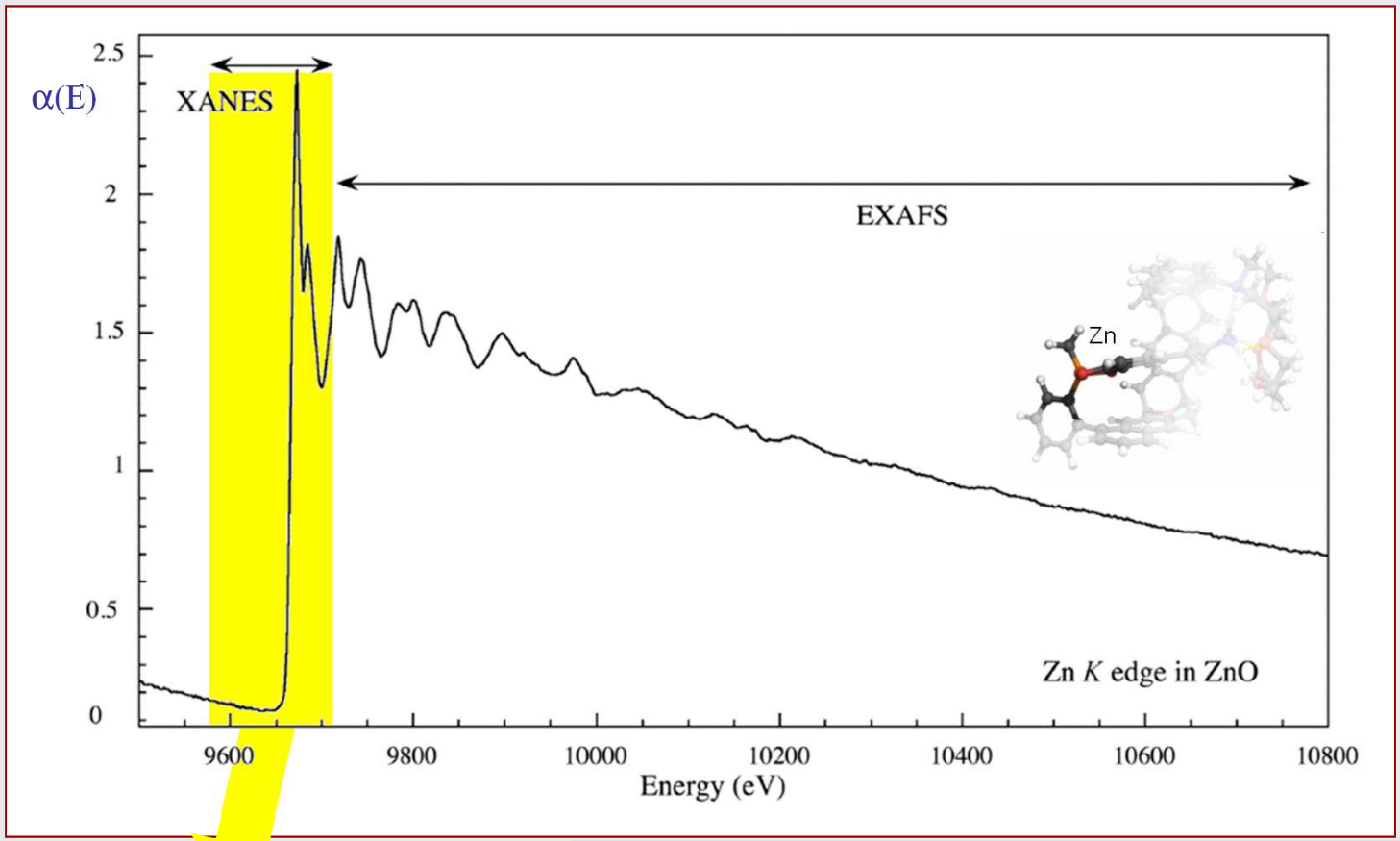

XANES region:

- **Hard theory**
- **lack of an analytical expression**
- long computation time

EXAFS region: simple analytical formula suited for data fitting and *easy* structural refinement

$$\chi(k) = \frac{1}{k}\sum_j A_j(k, r_j) sin(2kr_j + \psi_j(k))$$

$$A_j(k, r_j) = S_o^2 \frac{N_j}{r_j^2} |f_j(k, r)|\ e^{-2k^2\sigma_j^2}\ e^{-2r_j/\lambda}$$

Advantages of XANES based probes

XANES signal is **stronger** than EXAFS

Damping of XANES signal due to **structural disorder** is weak

Simpler/faster data collection respect to EXAFS

Restricted **energy range**

Info on: **Electronic structure** (empty DoS) and **structural topology**

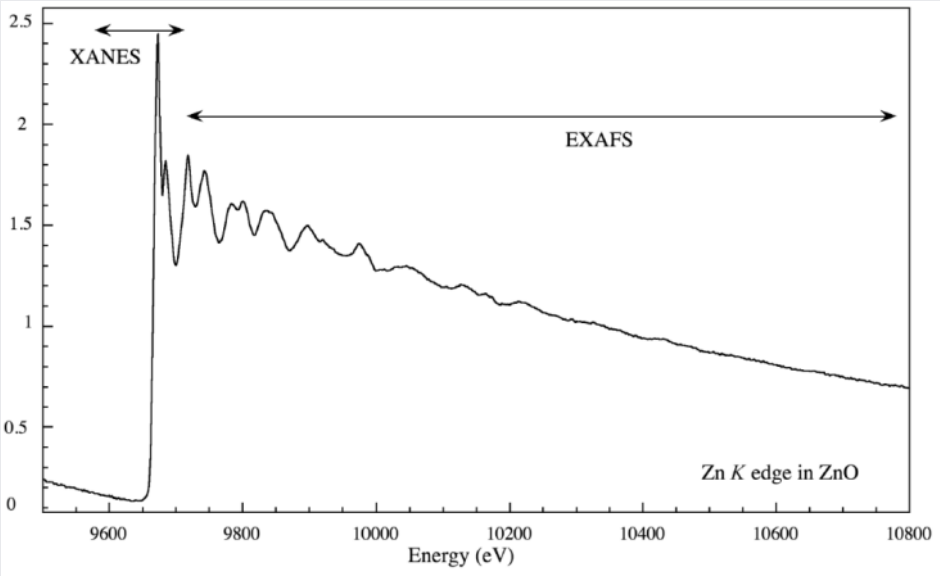

Applications of XANES spectroscopy systematically increases

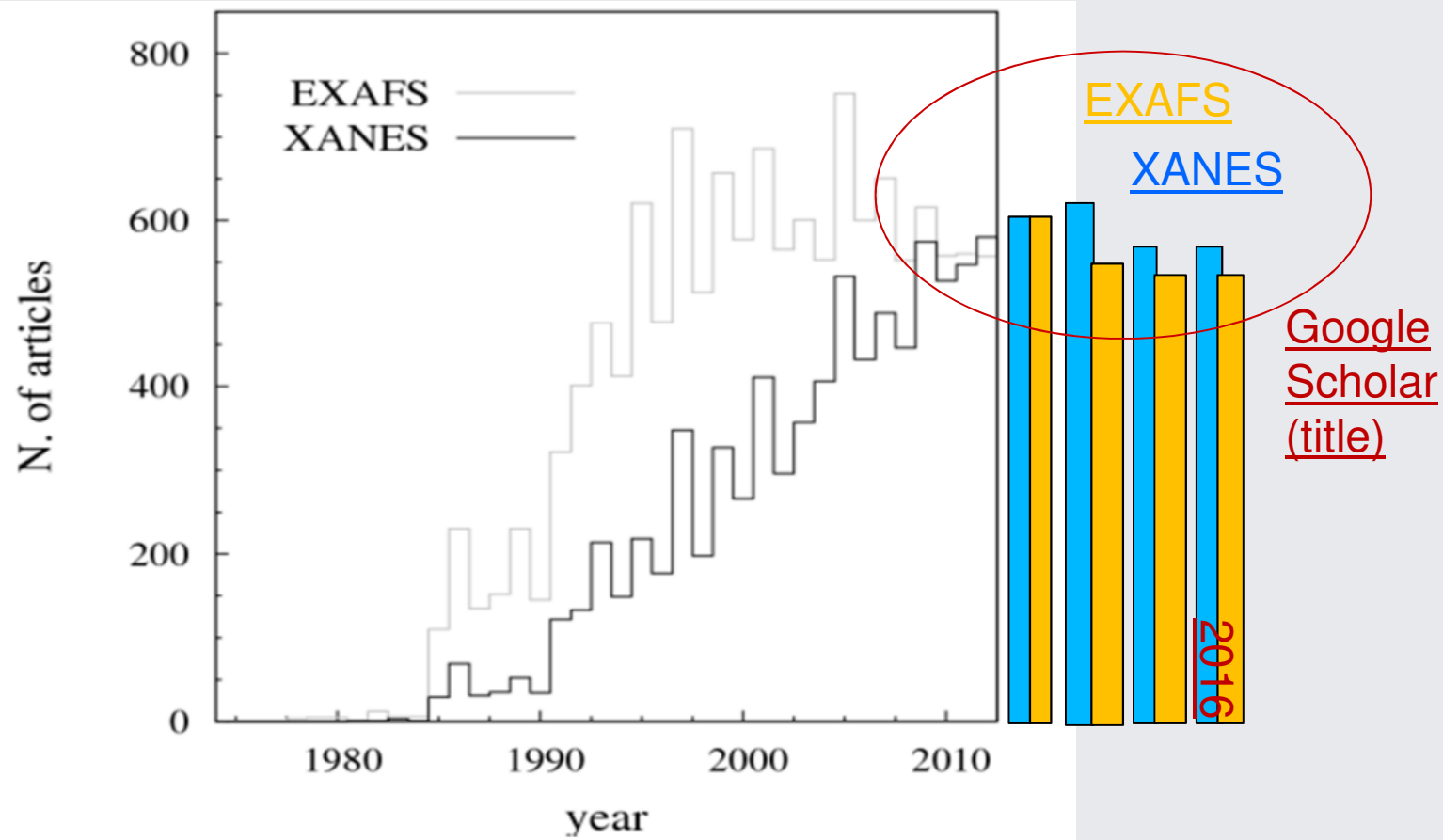

Fig. 1. Results of database search on ISI-web of knowledge using "EXAFS" ("XANES") in *Topic* or *Title* fields.

XANES signal is dense of electronic, structural and magnetic and information

XANES signal is stronger than EXAFS:

- less sensitive to data statistics, sample quality, beam intensity,
- can be measured on less concentrated samples,
- can be measured faster than EXAFS (time resolved experiments),
- can be measured at low energies (i.e. Carbon, Oxygen, Nitrogen K-edges.

XANES theory is complex

Damping of XANES signal due to structural disorder is weak:

- Applications to extreme condition studies: High **T**, High **P**, High **H**....

Electronic structure (DoS) and structural topology:

- XANES features are specially sensitive to the valence state, coordination chemistry, ligand symmetry of the absorber.
- Can be used as fingerprint for chemical speciation in mixtures and inhomogeneous systems.

XANES are prone to simple interpretation for simple and fast (semi-)quantitative analysis

Restricted energy range around the edge:

- Measurements at low energies (i.e. Carbon, Oxygen, Nitrogen K-edges)
- Fast data collection (time resolved XAS)
- XANES Microprobes (mapping) with sub-micrometer resolution

Chemical selective Magnetic information

- X ray Magnetic Circular Dichroism (XMCD) signal is an element specific probe for magnetism
- Sum rules at $L_{2,3}$ edges allow distinguishing orbital and spin contributions to the magnetic moment of the photoabsorber

Deeper insight into the XANES region

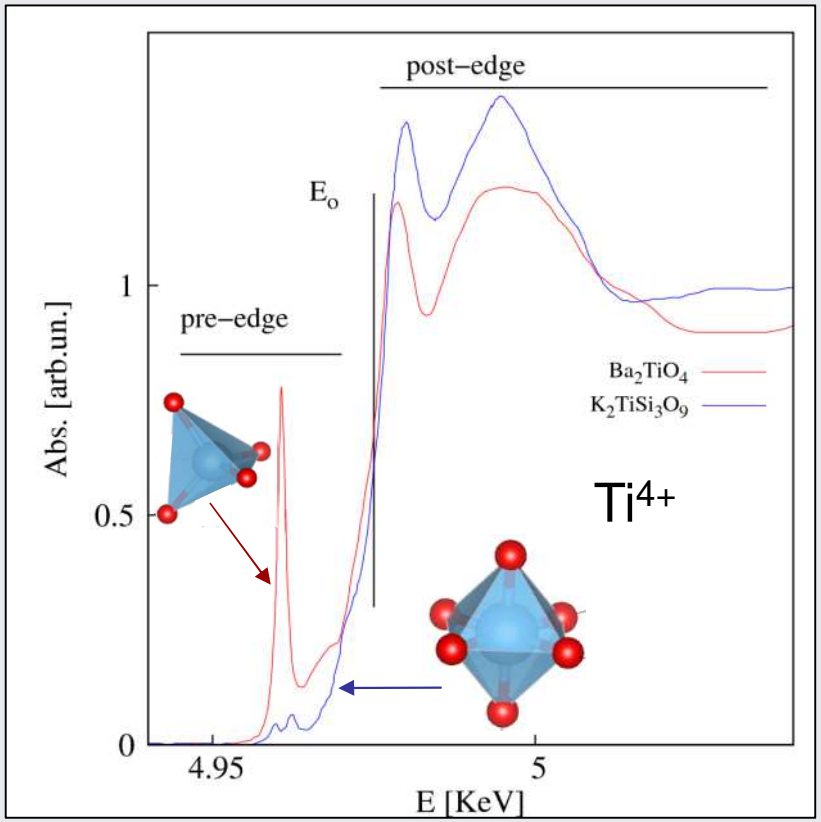

Local symmetry and XANES in Ti^{4+} compounds

XANES features are strongly related to the coordination chemistry & geometry: number, kind and symmetry of ligands

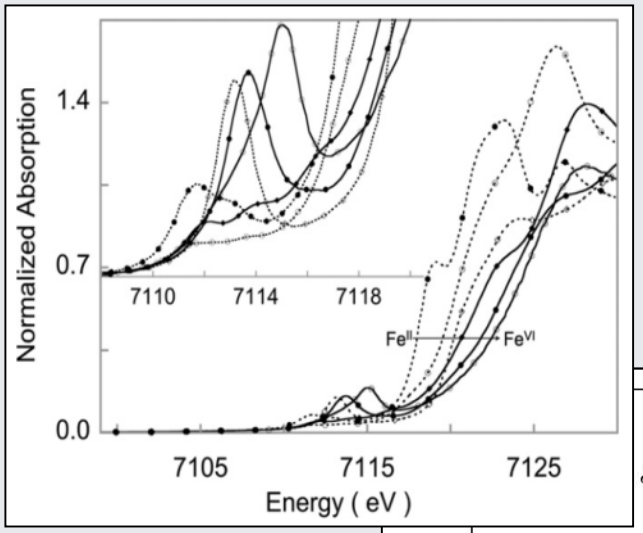

Fe K edges: representative XANES Fe in complexes

R. Sarangi, Coord. Chem. Rev. **257** 459–472 (2013)

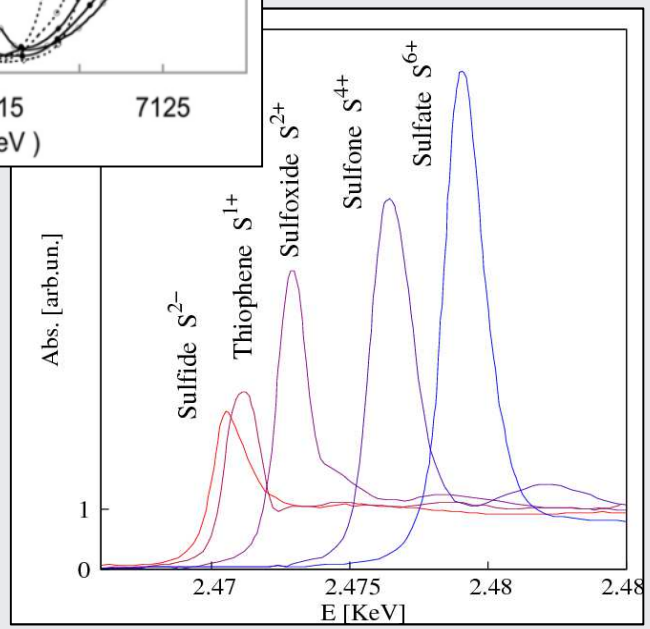

Sulphur K edges: chemical shift as a function of valence state of S-ions

Absorption Edges (energy position and shape) definitively depend on the oxidation state of the absorber

Origin of the XANES features

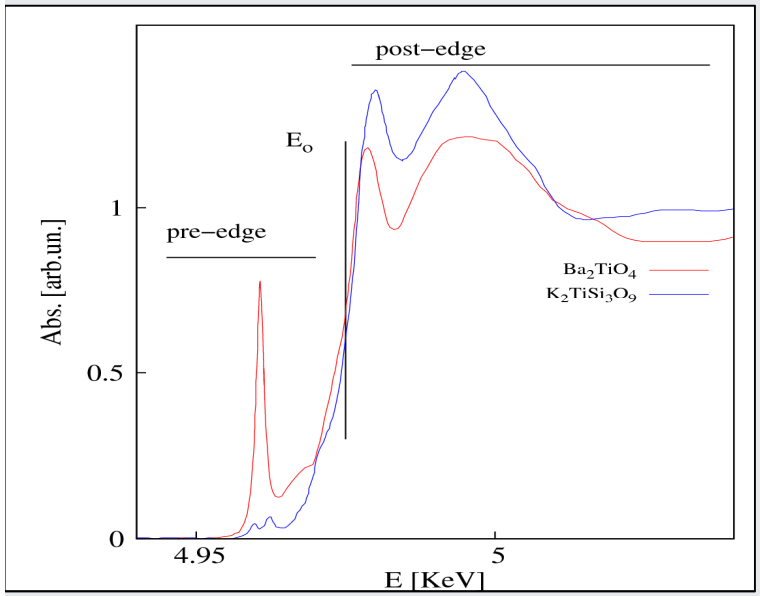

Pre-edge

caused by electronic transitions (mainly dipole allowed) to **empty bound states** near the Fermi level.

Provide information about absorber local geometry and electronic state around the absorber: number of neighbours, ligand symmetry, valence state

Edge (E_o)

defines the onset of **continuous states** (not the Fermi level !)

E_o is a function of the absorber oxidation state & binding geometry. It may also increase by several eV per oxidation unit

Post-edge (XANES)

multiple scattering features (FMS)

The analysis may provide finest details about local atomic structure and geometry.

The Pre-edge region

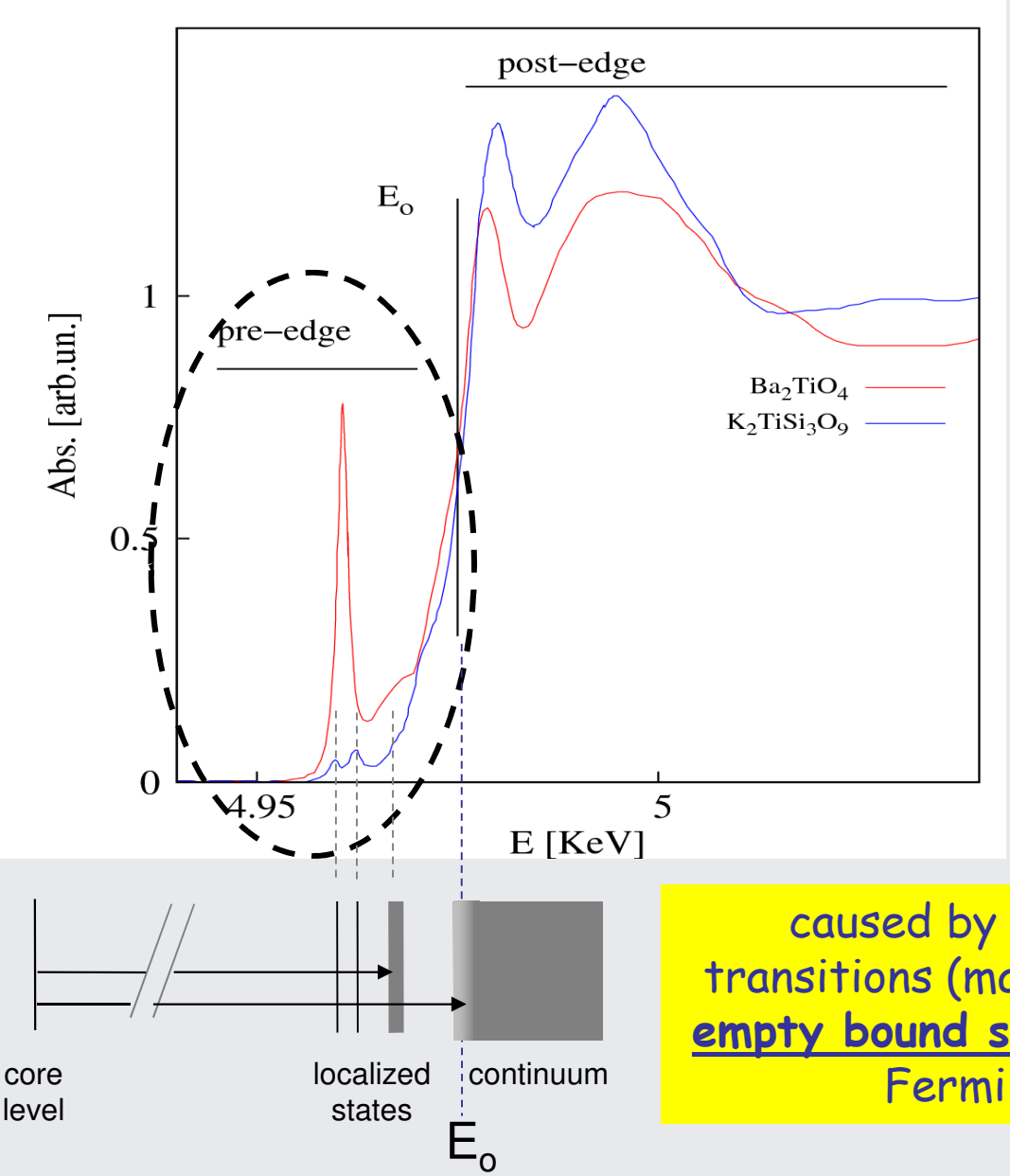

caused by electronic transitions (mainly dipole) to **empty bound states** near the Fermi level.

K pre-edges 3d metal oxides: intensity & empty electronic states

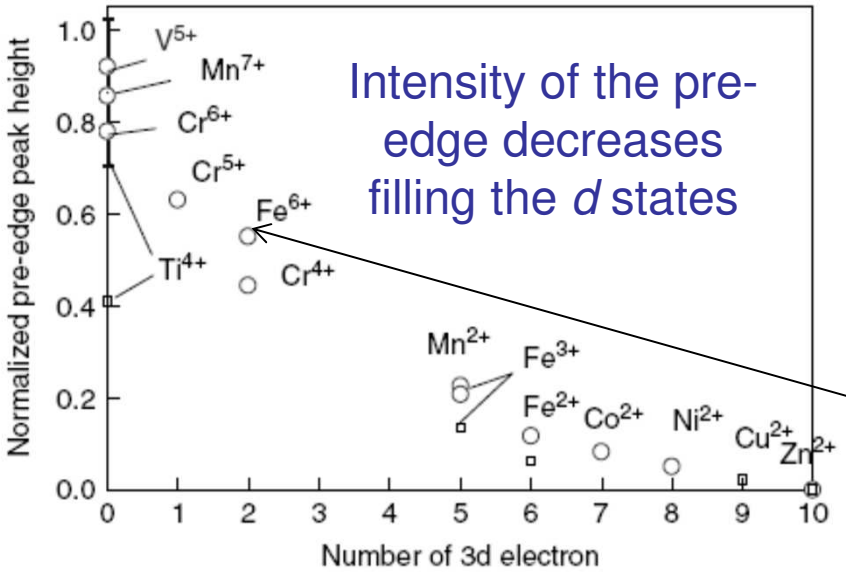

Example:
Pseudo Tetrahedral Metal Complexes ***M*(B(3-isopropyl-pyrazol-1-yl)4)2**

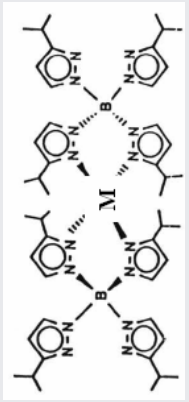

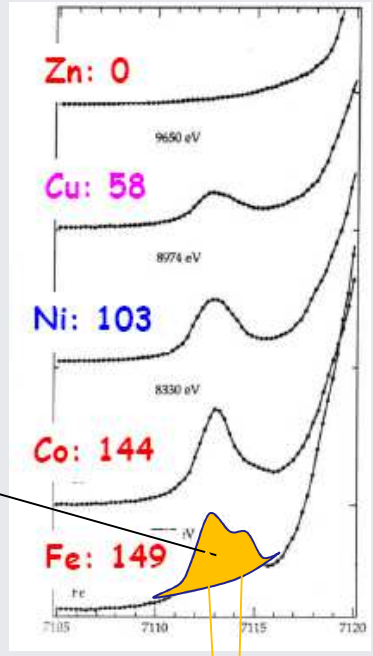

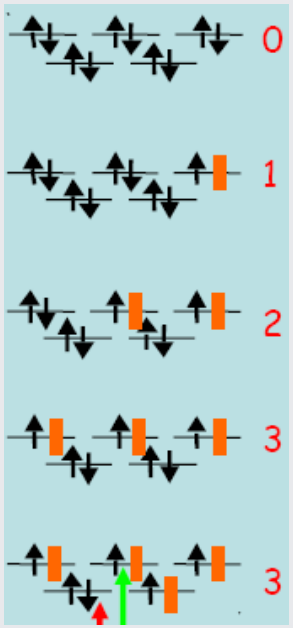

Pre-edge features are caused by electronic transitions (mainly dipole) to **empty states** close to the Fermi level.

K pre-edges 3d metal oxides:

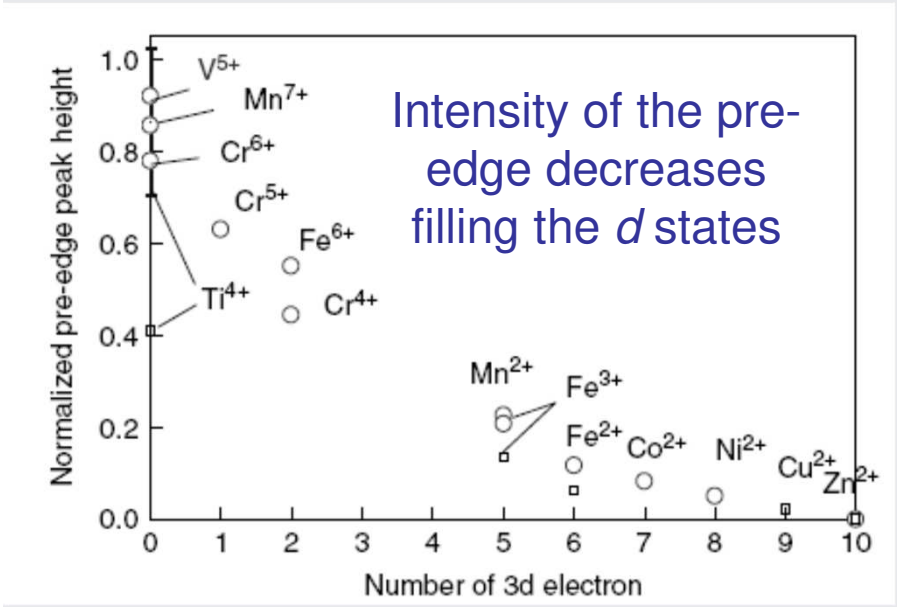

Example:

Pseudo Tetrahedral Metal Complexes ***M*(B(3-isopropyl-pyrazol-1-yl)4)2**

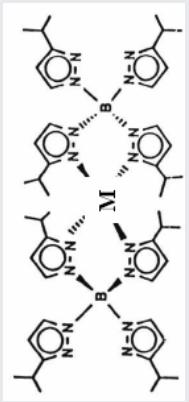

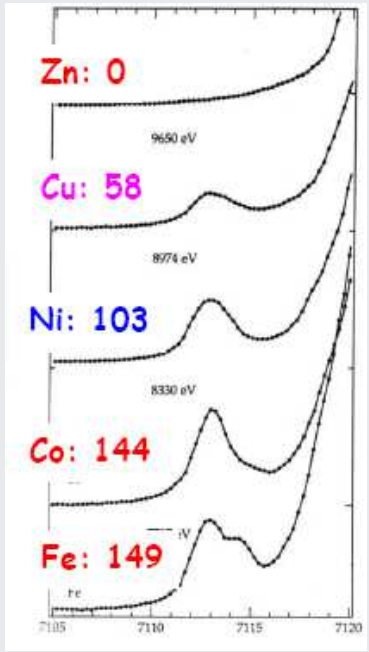

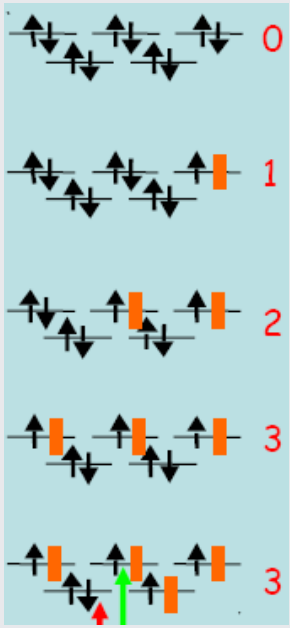

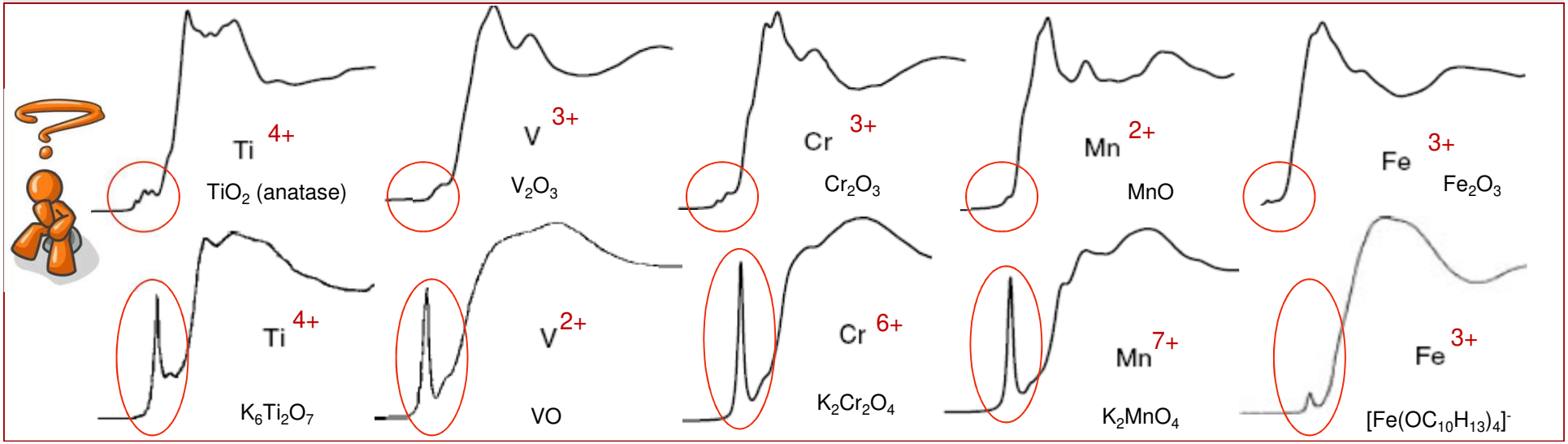

Fe K edges in minerals

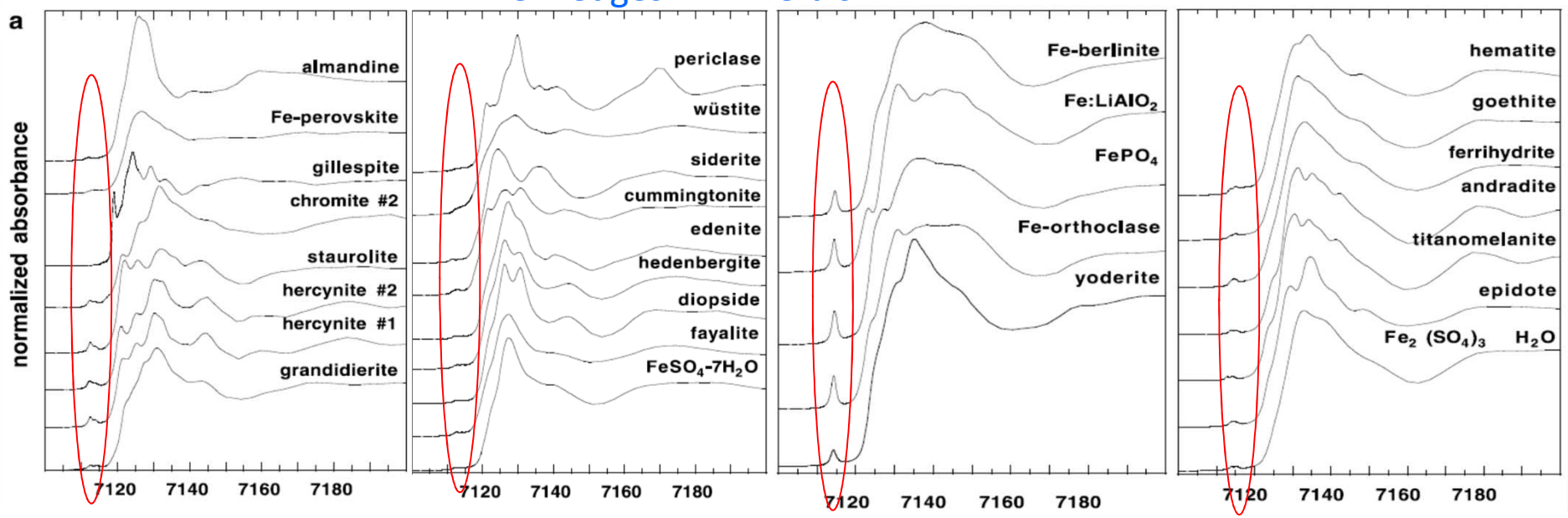

Fe^{2+} in 4, 5, 6 coord. sites | Fe^{2+} in 6 coord. sites | Fe^{3+} in 4, 5 coord. sites | Fe^{3+} in 6 coord. sites

M. Wilke, F. Farges et al. *American Mineralogist, Volume 86, pages 714–730, 2001*

Ti K edge spectra in Ti^{4+} compounds

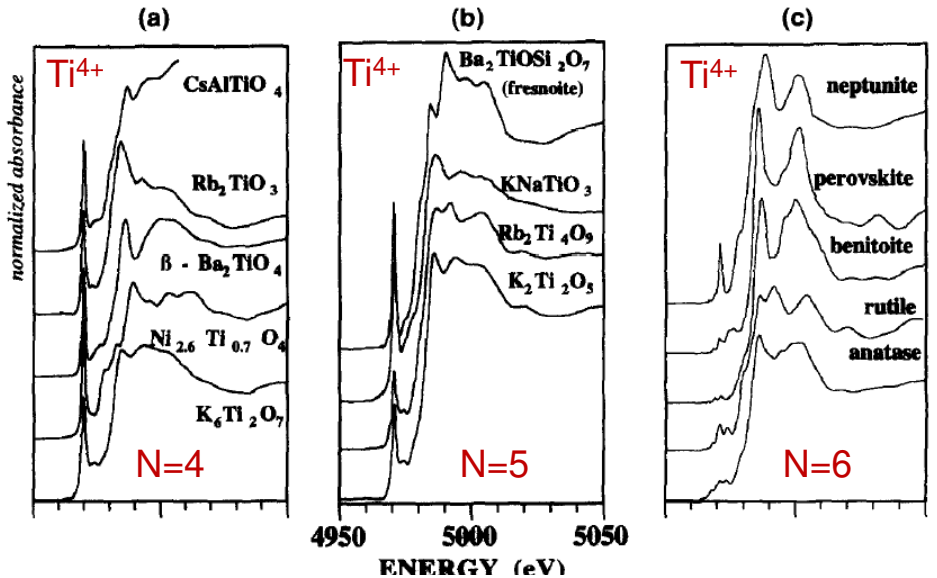

Farges F, Brown GE, Rehr JJ. *Geochim. Cosmochim. Acta* 1996; 60: 3023.

Fe K pre-edge may look different as a function of Fe **oxidation** state and **coordination** number

Ti K pre-edge peak in **4-**, **5-** and **6-**fold coordinated **Ti^{4+}** compounds have **different shape**

Pre-edge features signal the transitions to bound electronic levels below the continuum threshold

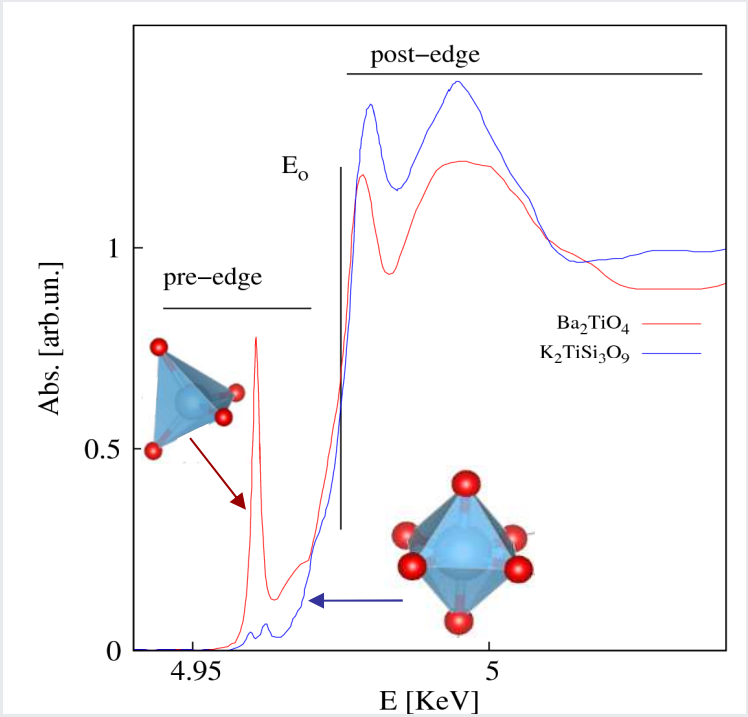

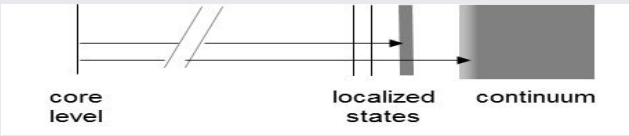

The XANES of the **same ions**, even in the **same oxidation state**, may behave **differently** in different compounds!

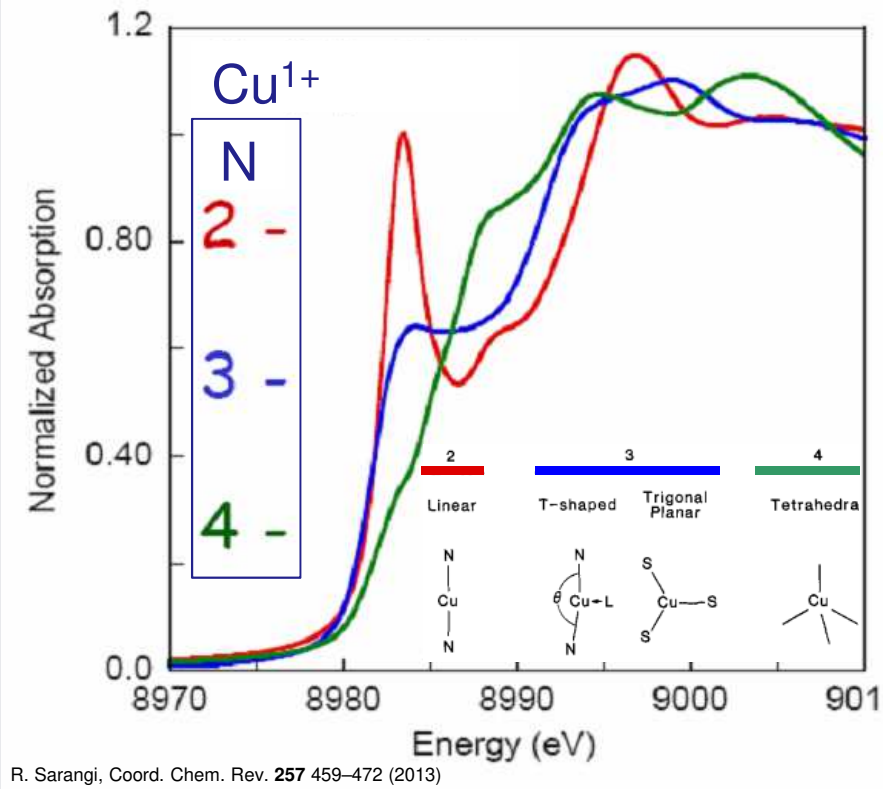

R. Sarangi, Coord. Chem. Rev. **257** 459–472 (2013)

Pre-edge features signal the transitions to bound electronic levels below the continuum threshold

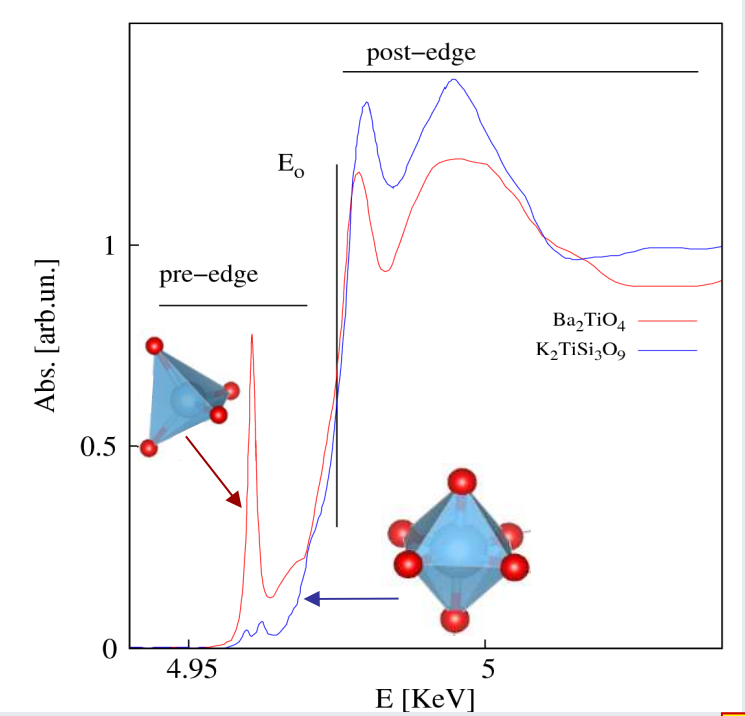

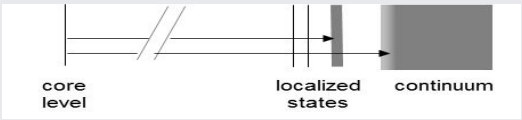

The XANES of the same ions, even in the same oxidation state, may behave differently in different compounds

… depending on **oxidation state** and **coordination geometry** of the absorber

Quantitative Models: multiplet theory

Semi-quantitative approaches:

- Comparison with model compounds
- Molecular orbital symmetry (group theory)

Selection of normalized pre-edge features

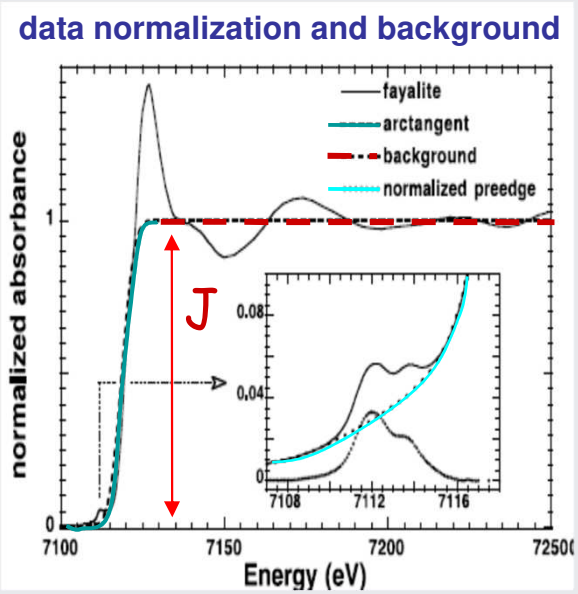

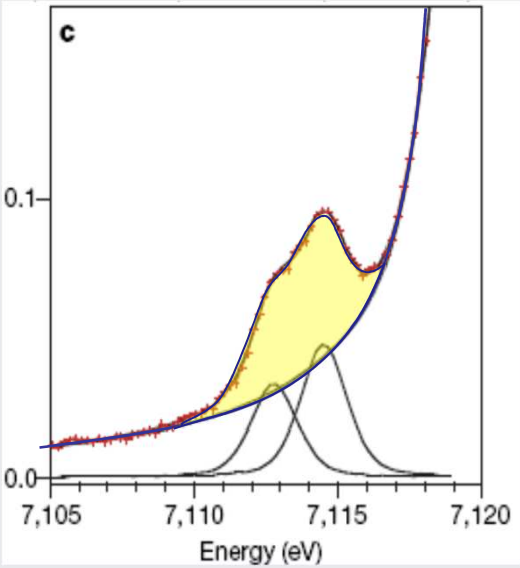

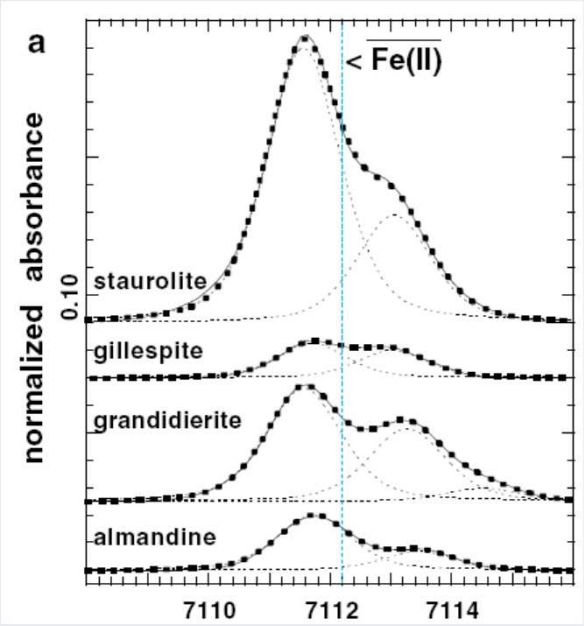

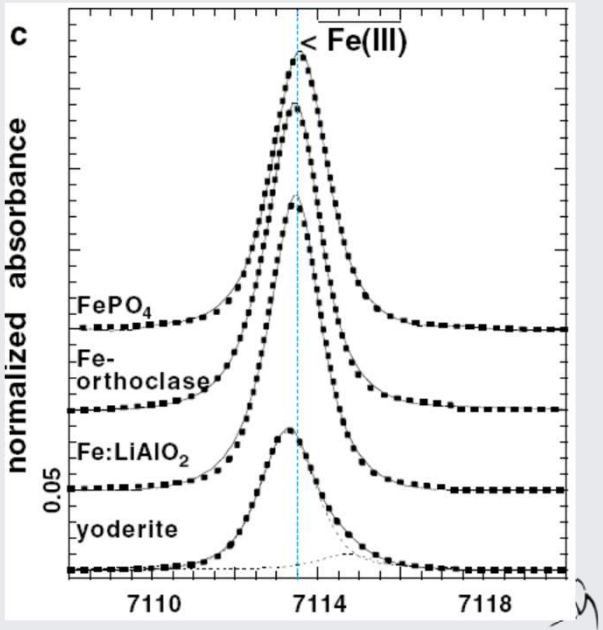

normalization: Jump = 1

arctangent: transitions to continuum states,

peaks: transitions to localized states:

Pseudo-Voigt shaped peaks take into account for the convolution of true peak shape (Lorentzian contribution) with the experimental energy resolution (Gaussian contribution)

M. Wilke, F. Farges et al. *American Mineralogist, Volume 86, pages 714–730, 2001*

The Iron case: the average valence and coordination chemistry from the pre-edge peak shape/position

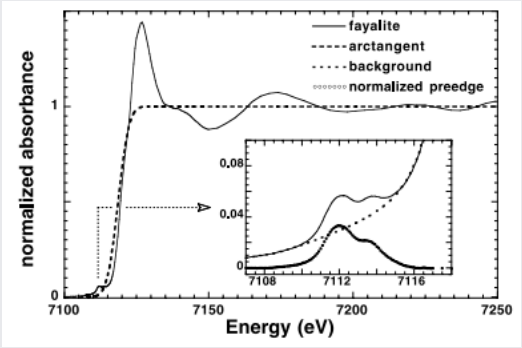

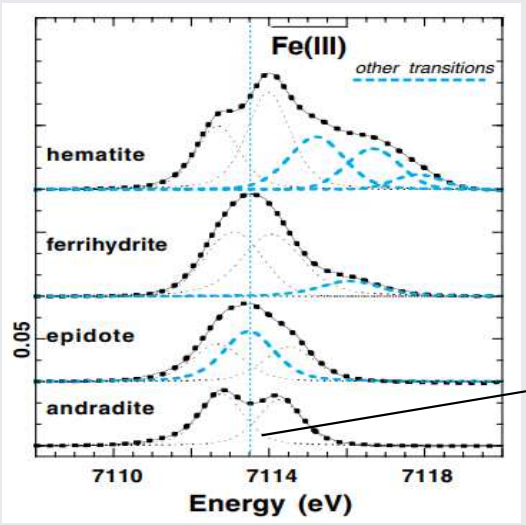

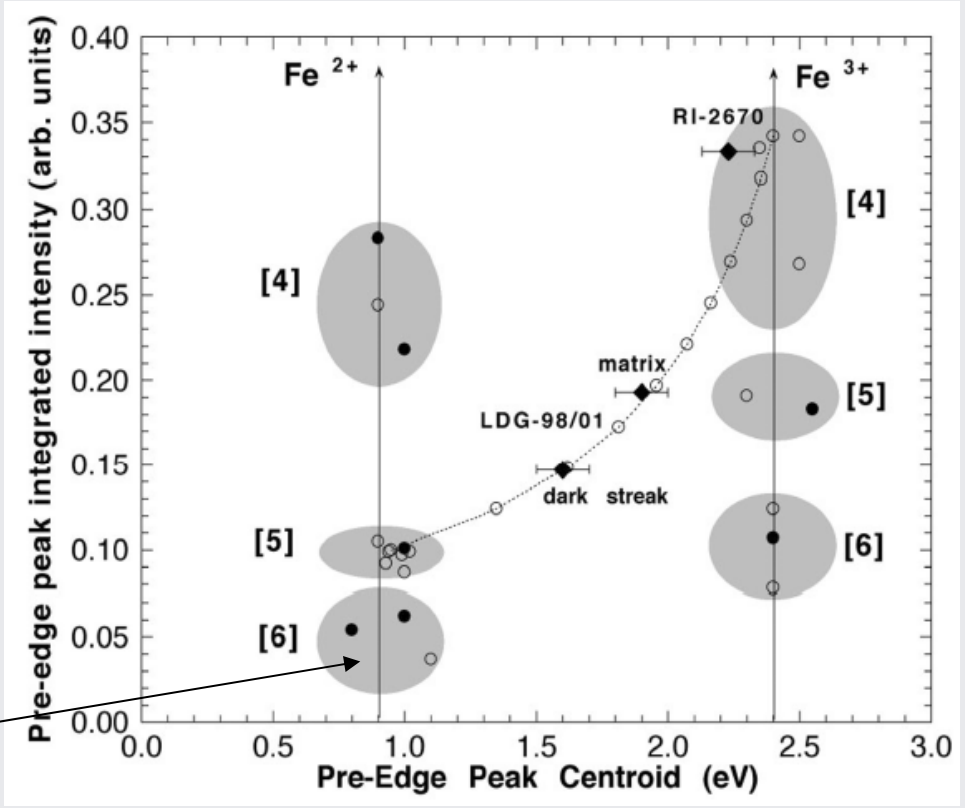

American Mineralogist, Volume 86, pages 714–730, 2001

Oxidation state and coordination of Fe in minerals: An Fe *K*-XANES spectroscopic study

MAX WILKE,[1,*] FRANÇOIS FARGES,[1,2] PIERRE-EMMANUEL PETIT,[3] GORDON E. BROWN JR.,[2,4] AND FRANÇOIS MARTIN[5]

850 cit. (sept.2019, Scholar Google)

It is possible to understand the Fe **coordination number** looking at the intensity/area of the pre-edge peaks in comparison with reference compounds data

The case of Fe in metallo-proteins:

Biophysics

Ibuprofen/warfarin induce V to VI Fe coordination transition in HSA

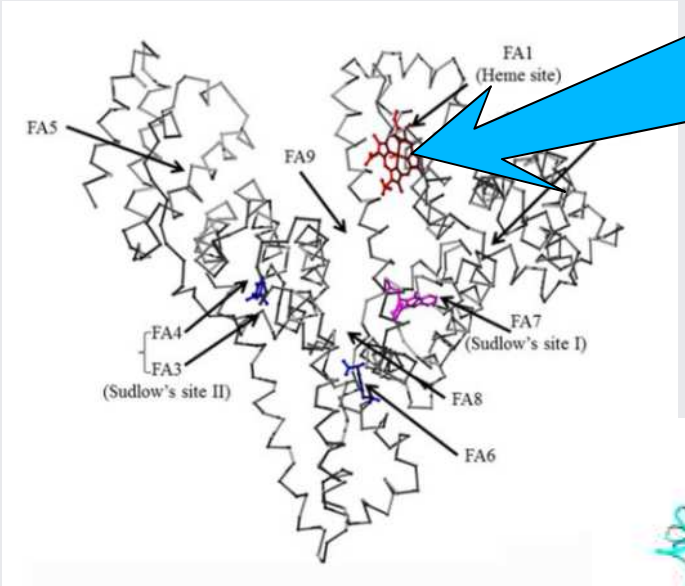

Human Serum Albumin

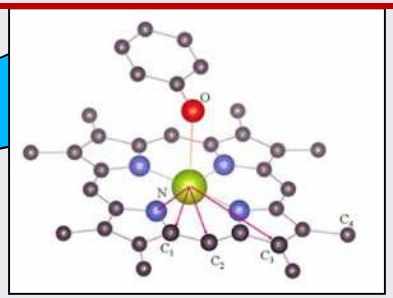

Heme (Fe) site

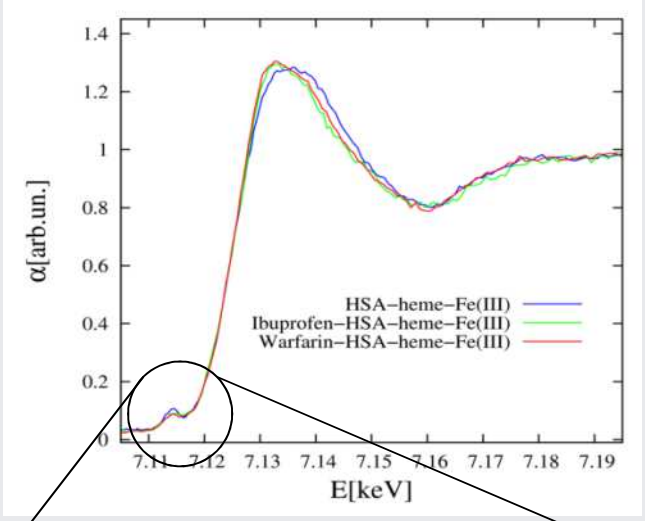

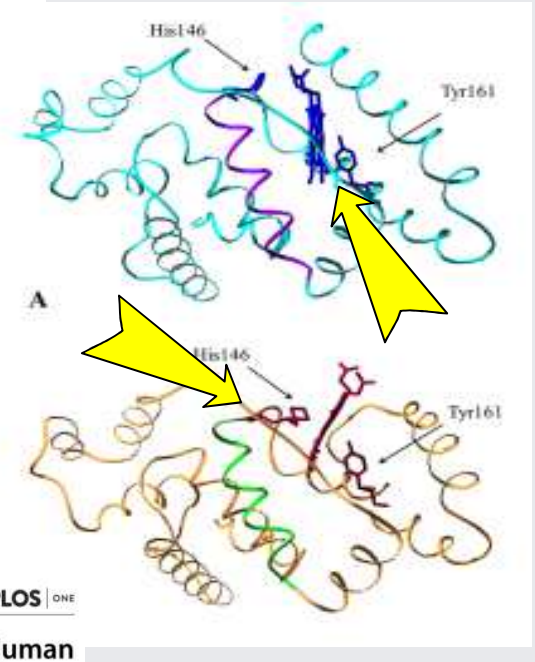

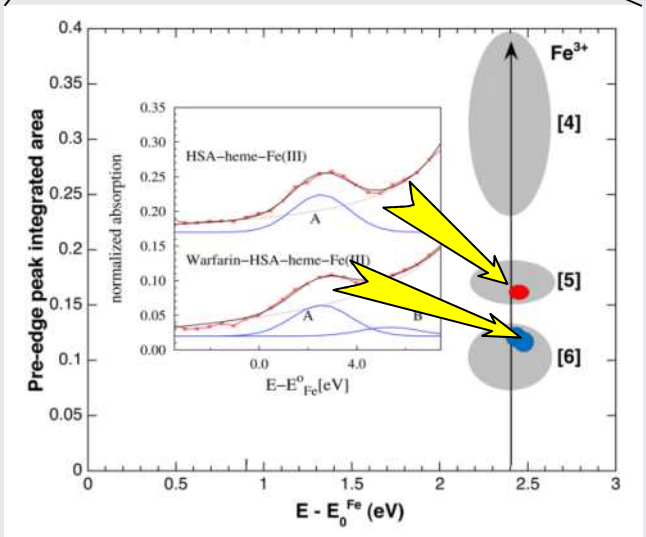

OPEN ACCESS Freely available online

PLOS ONE

The Five-To-Six-Coordination Transition of Ferric Human Serum Heme-Albumin Is Allosterically-Modulated by Ibuprofen and Warfarin: A Combined XAS and MD Study

Carlo Meneghini[1*], Loris Leboffe[1,2*], Monica Bionducci[1], Gabriella Fanali[3], Massimiliano Meli[4], Giorgio Colombo[4], Mauro Fasano[3], Paolo Ascenzi[2,5*], Settimio Mobilio[1]

Fe in archaean rocks

Geophysics

reference samples with different Fe^{3+} over total Fe (ΣFe) content

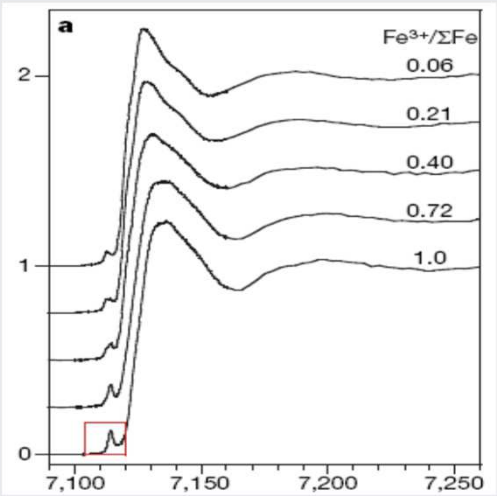

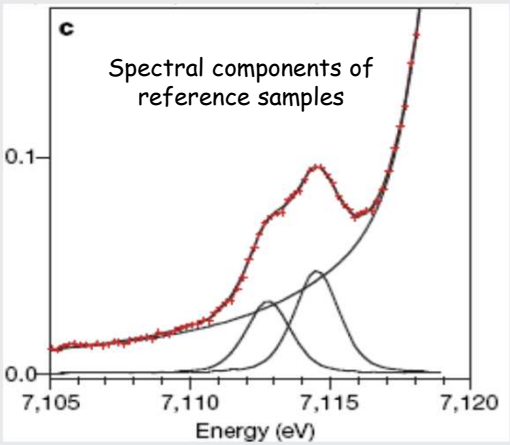

Andrew J. Berry Vol 455|16 October 2008|doi:10.1038/nature07377

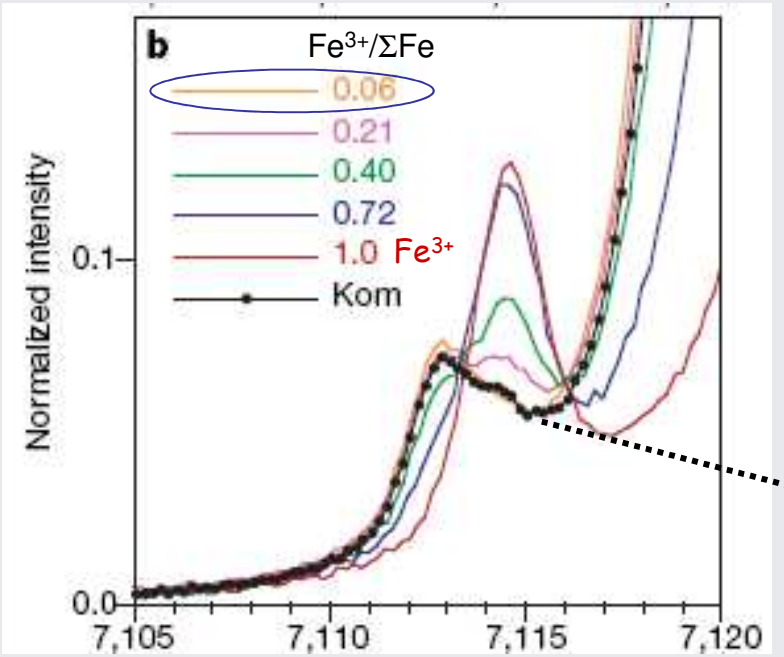

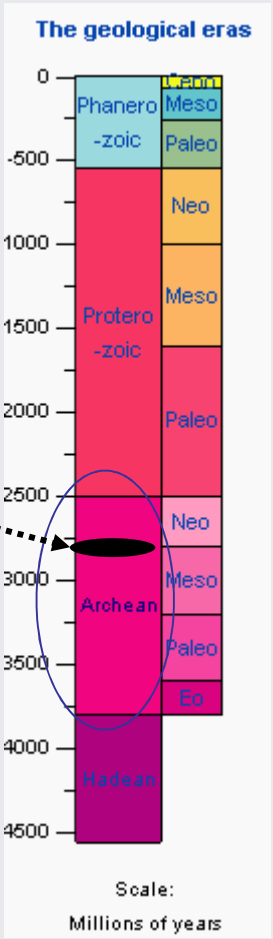

Samples: small inclusions (D~15 μm) of Belingwe komatiite in olivine minerals

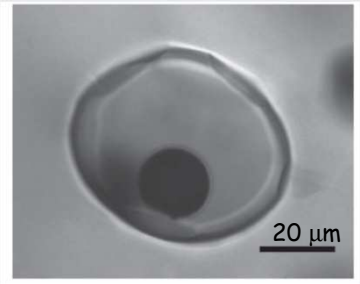

… results support the identification of the Belingwe komatiite as a product of high mantle temperatures (~1,700 °C), rather than melting under hydrous conditions (3–5-wt% water), confirming the existence of anomalously hot mantle in the Archaean era.

Titanium: the average valence and coordination chemistry from the pre-edge peak shape/position

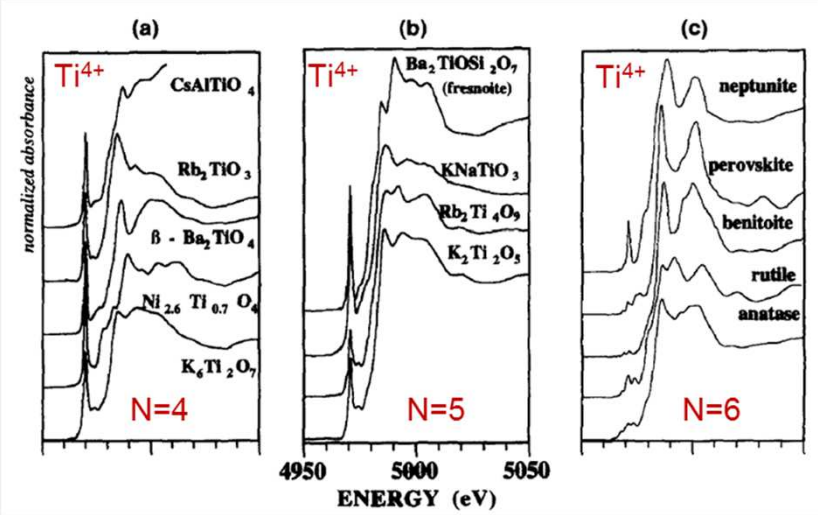

It is possible to understand the absorber **coordination number** looking at the intensity/area of the pre-edge peaks in comparison with reference compounds data

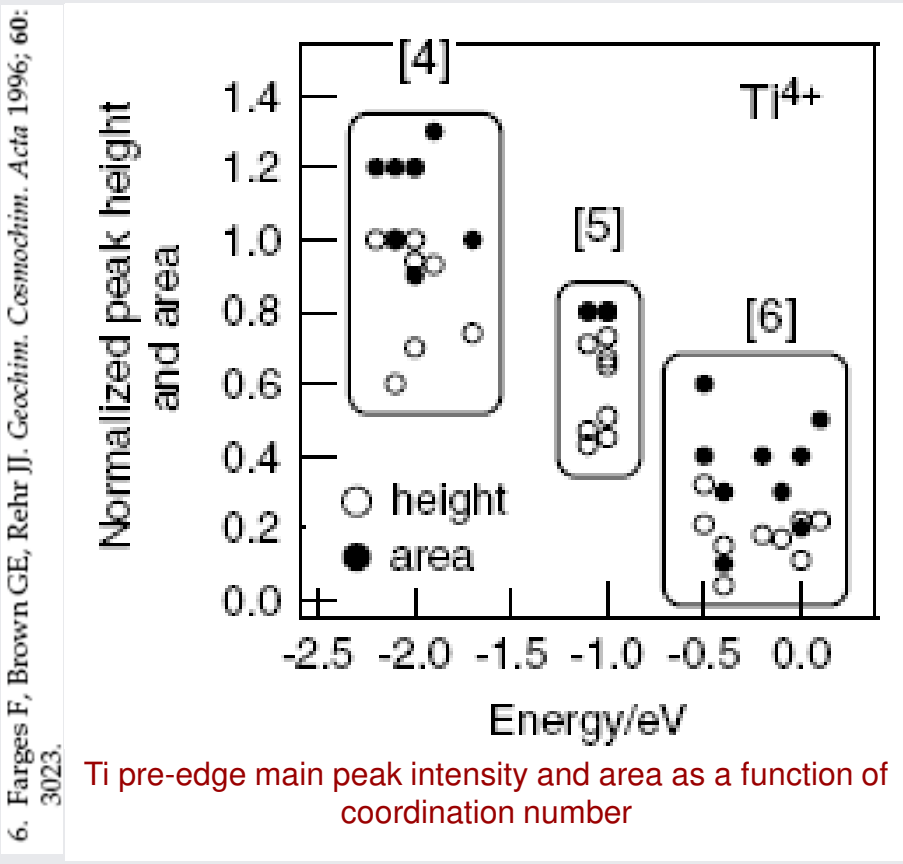

Ti pre-edge main peak intensity and area as a function of coordination number

…. and the Vanadium

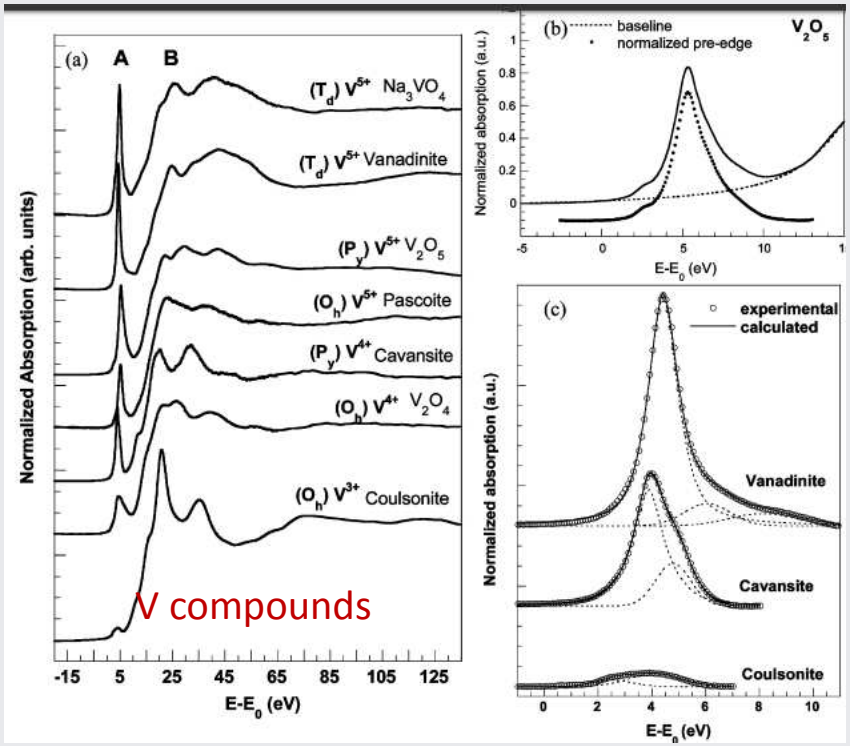

J. Phys. Chem. B **2007**, *111*, 5101−5110 5101

New Methodological Approach for the Vanadium K-Edge X-ray Absorption Near-Edge Structure Interpretation: Application to the Speciation of Vanadium in Oxide Phases from Steel Slag

Perrine Chaurand,*,† Jérôme Rose,† Valérie Briois,‡ Murielle Salome,§ Olivier Proux,||

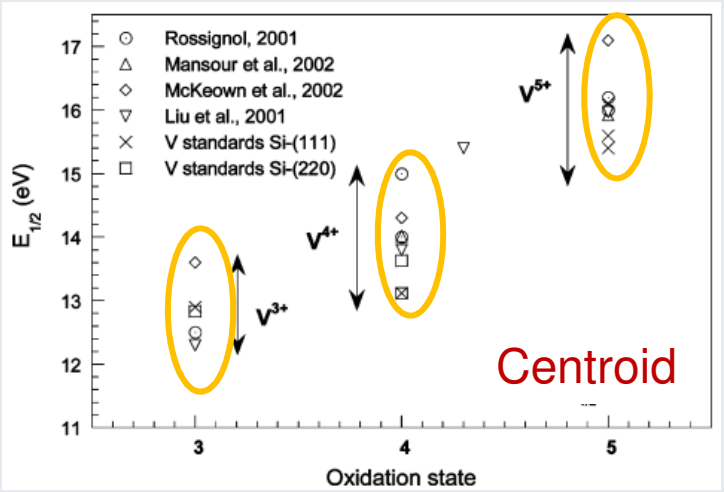

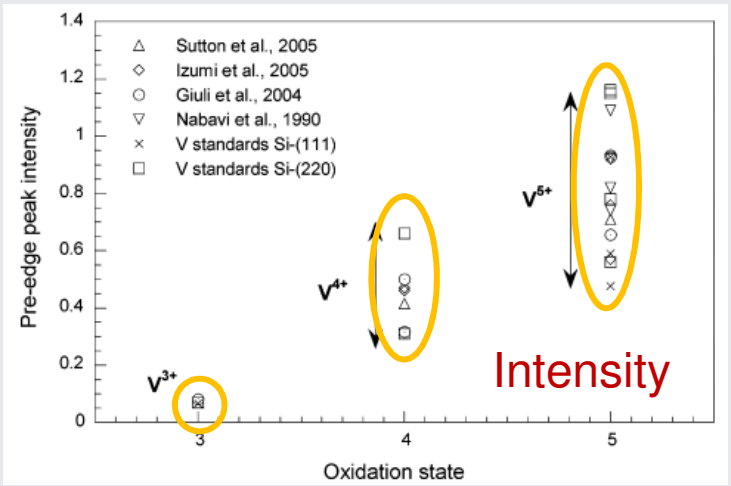

and the Copper…

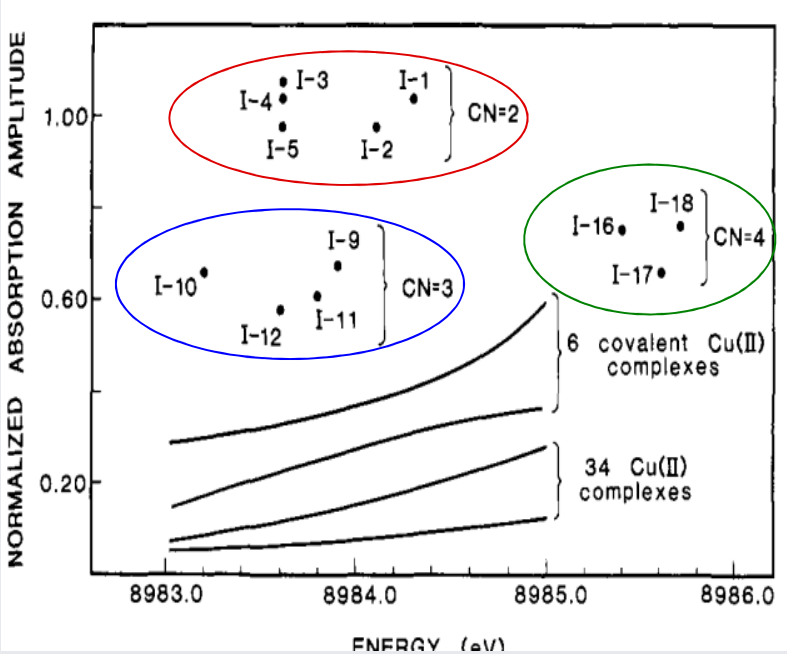

J. Am. Chem. Soc., Vol. 109, No. 21, 1987 6437

Ligand geometry in Cu complexes

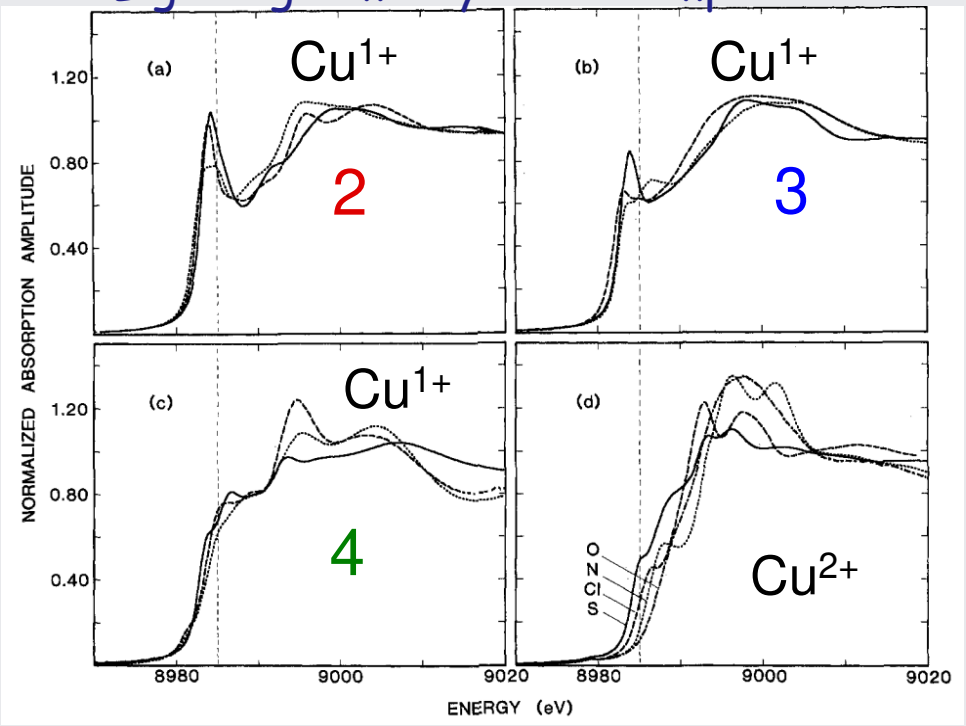

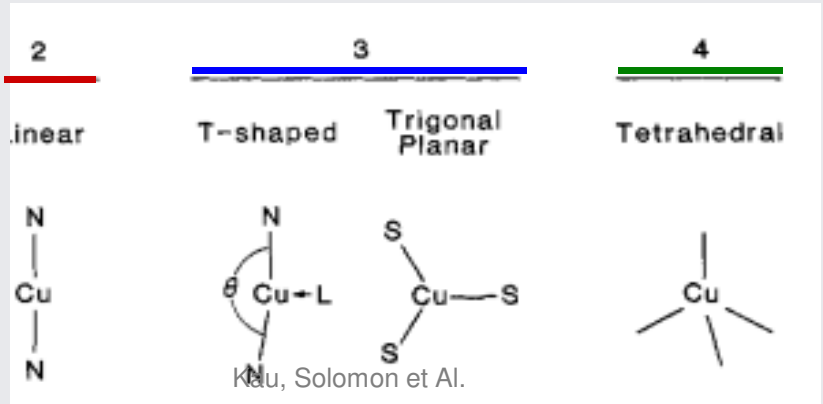

Kau, Solomon et Al.

K edges of 3d metal oxides... origin of the pre-edge peaks

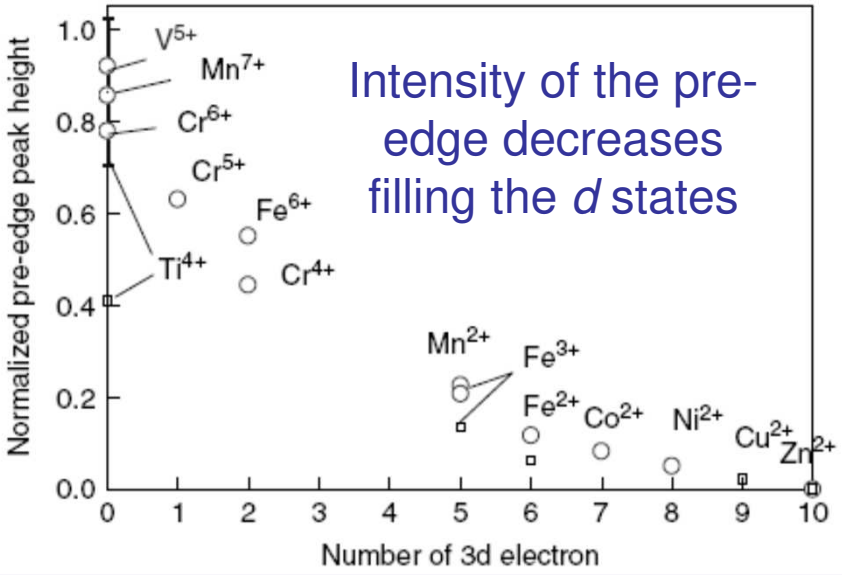

Example:

Pseudo Tetrahedral Metal Complexes ***M*(B(3-isopropyl-pyrazol-1-yl)4)2**

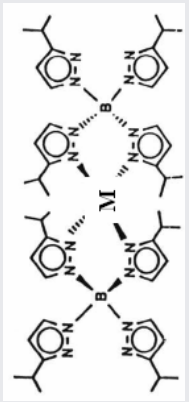

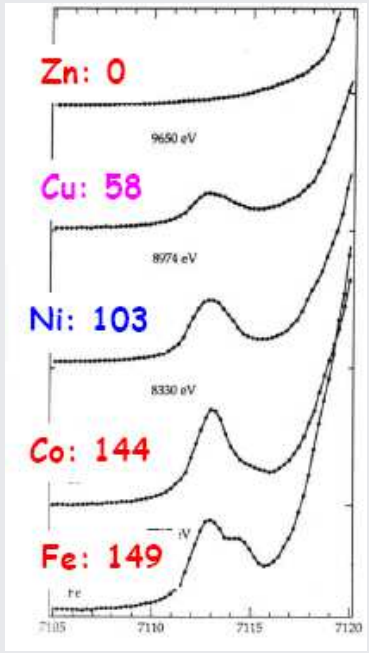

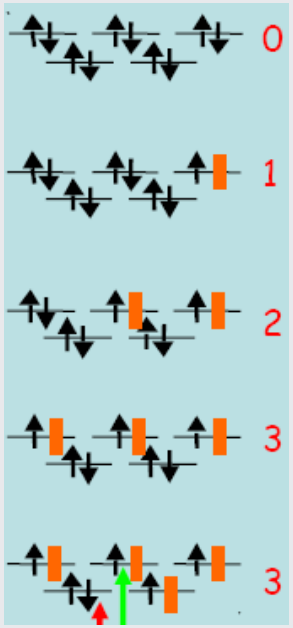

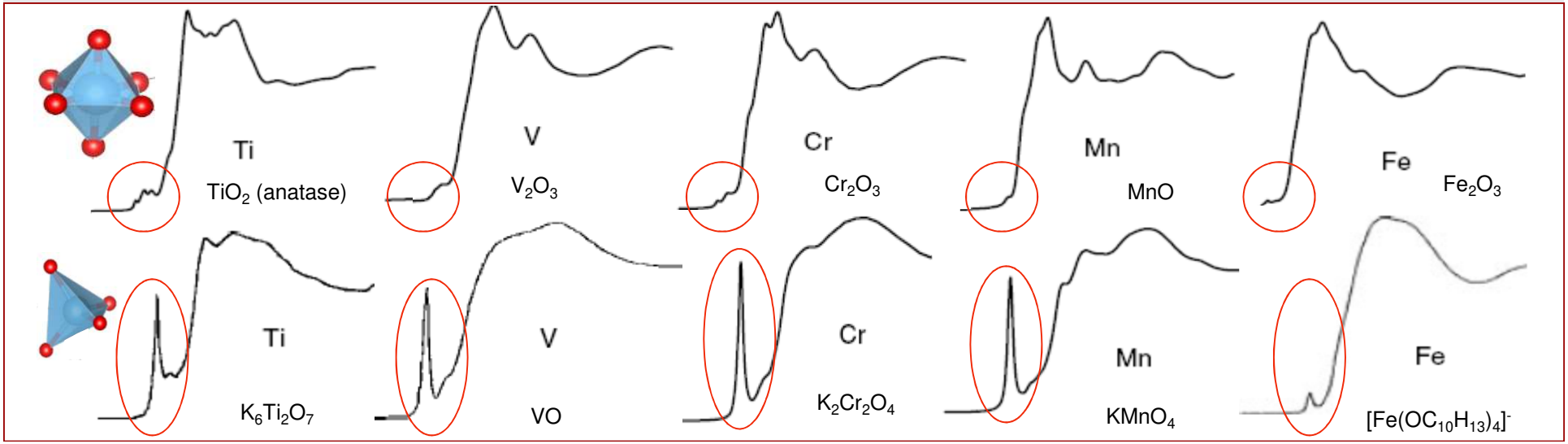

K edge: mainly s -> p transitions

I_{sd} (quadrupole) ~ 10^{-2} I_{sp} (dipole)

Hybridization mixes *p-d* states then dipole allowed transitions occur to empty p-components of hybrid *pd* levels

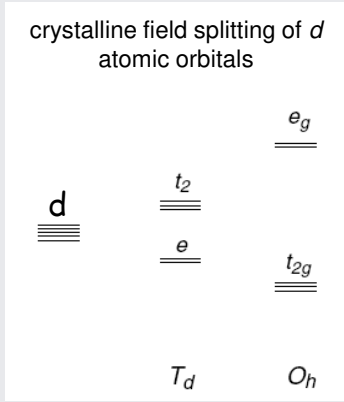

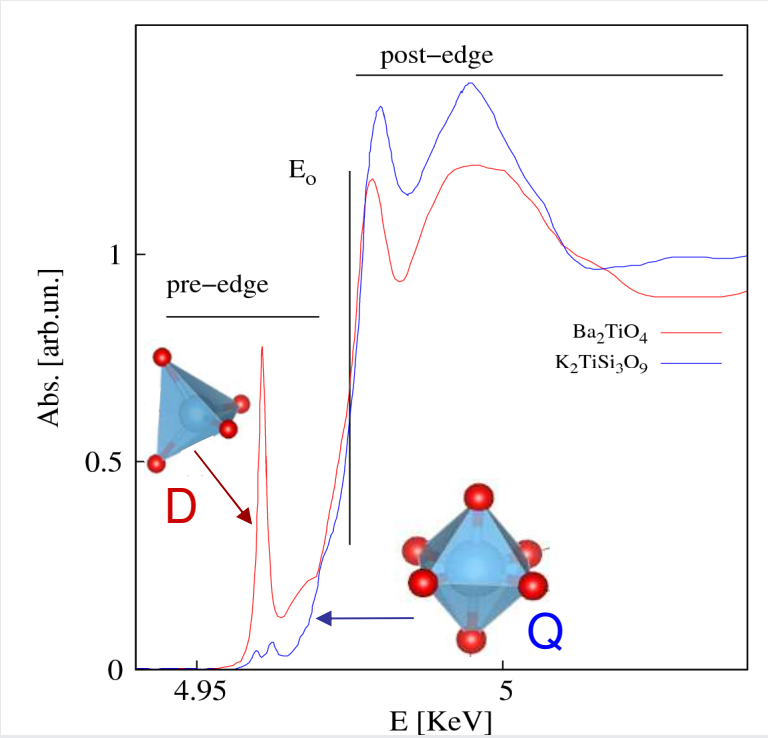

Table 1. Lists of irreducible representations and the relating functions in T_d, O_h, and D_{4h} point groups

	T_d	
	p	d
A_1		$x^2+y^2+z^2$
A_2		
E		$(2z^2-x^2-y^2, x^2-y^2)$
T_1	(R_x, R_y, R_z)	
T_2	(x, y, z)	(xz, yz, xy)

	O_h	
	p	d
A_{1g}		$x^2+y^2+z^2$
A_{2g}		
E_g		$(2z^2-x^2-y^2, x^2-y^2)$
T_{1g}	(R_x, R_y, R_z)	
T_{2g}		(xz, yz, xy)
A_{1u}		
A_{2u}		
E_u		
T_{1u}	(x, y, z)	
T_{2u}		

Yamamoto *X-Ray Spectrom.* 2008; **37**: 572–584

Geometrical origin of pre-edge peaks in Ti oxides

Hybridization mixes *p-d* states then dipole allowed transitions occur to **empty** p-components of hybrid *pd* levels

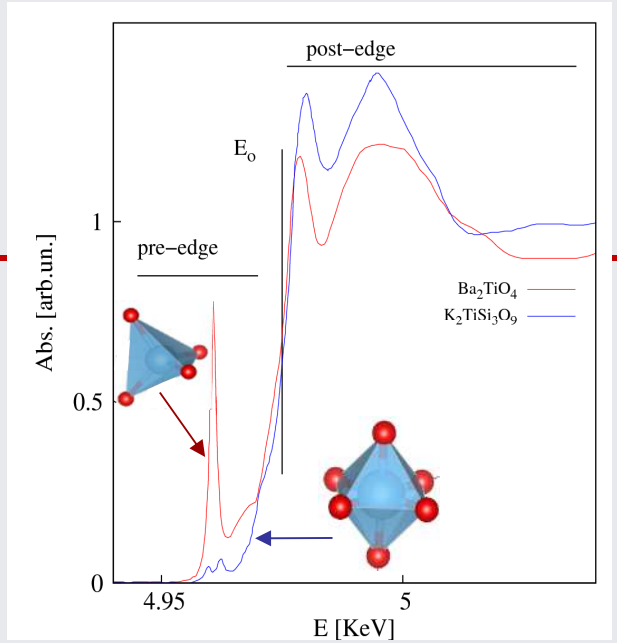

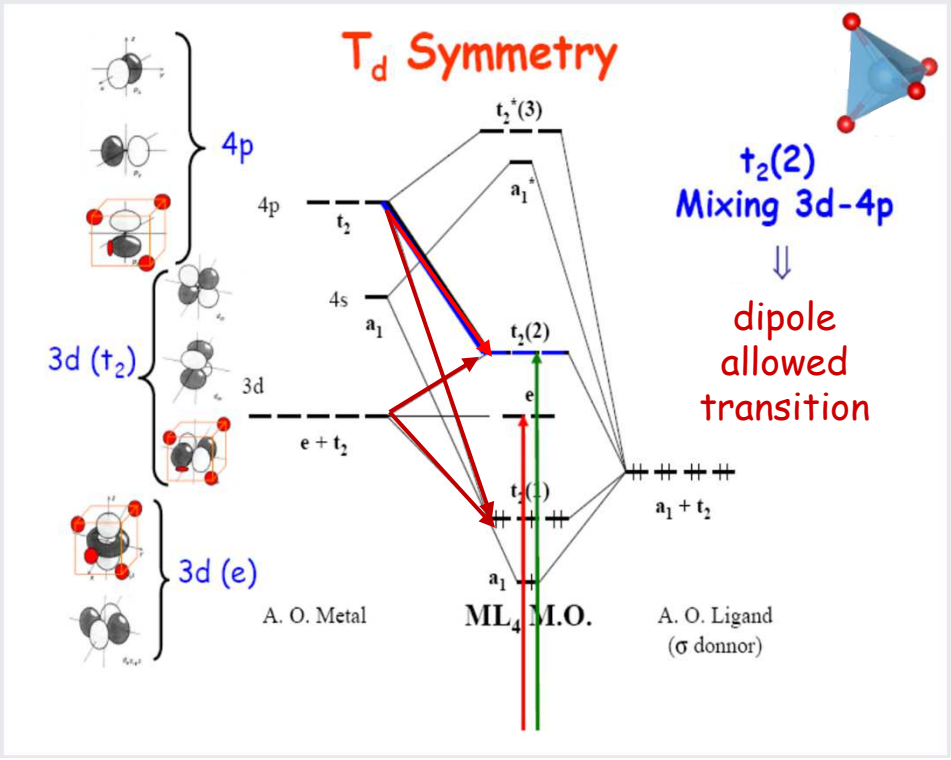

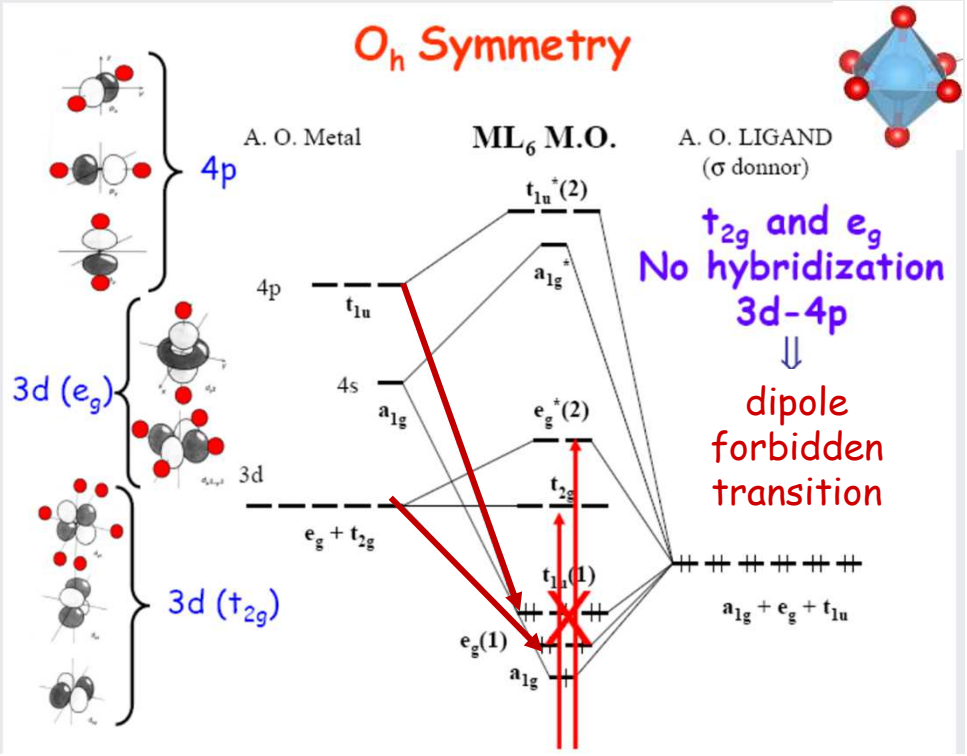

p-d mixing and sensitivity to local symmetry of TiO_6 units

Off centre displacement and stretching of the octahedron decreases the local symmetry (non-centro-symmetric) allowing some degree of *p-d* mixing, this affect the pre-edge peaks intensity

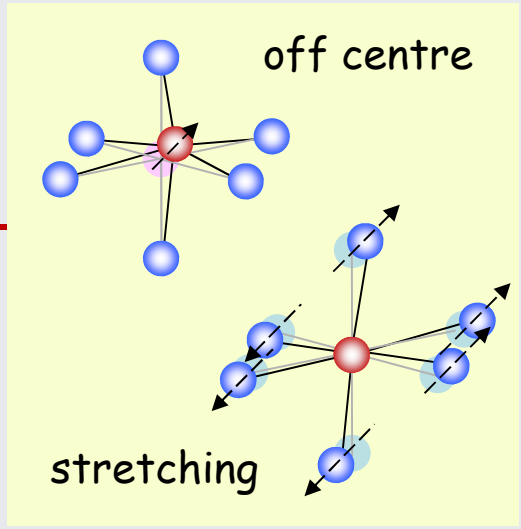

Regular TiO_6

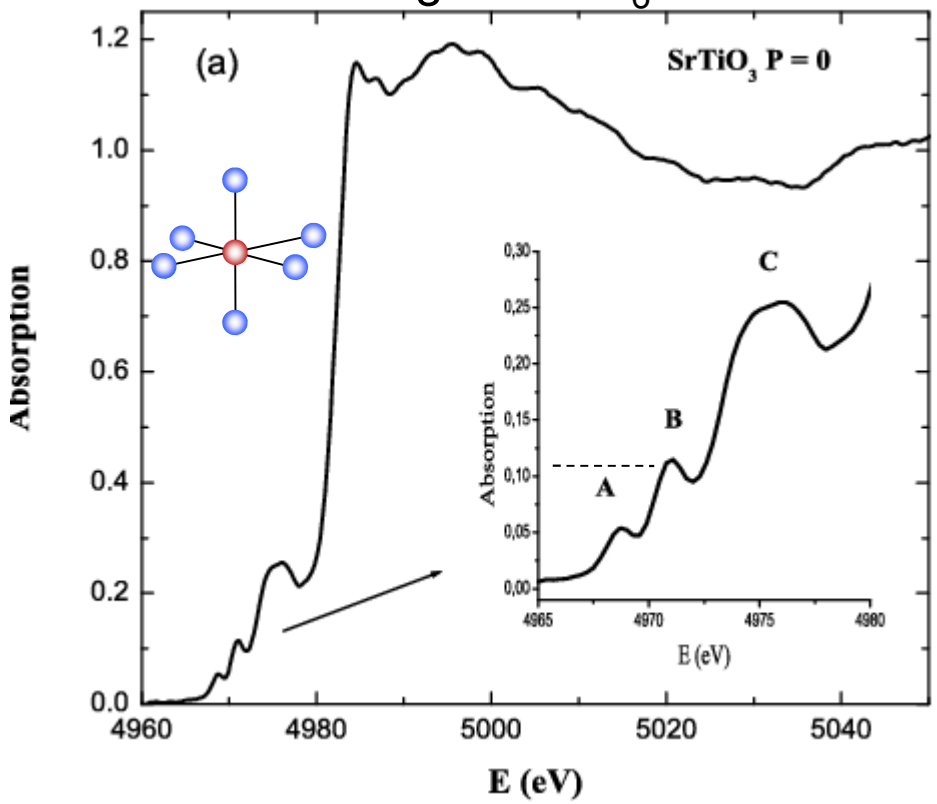

Distorted TiO_6

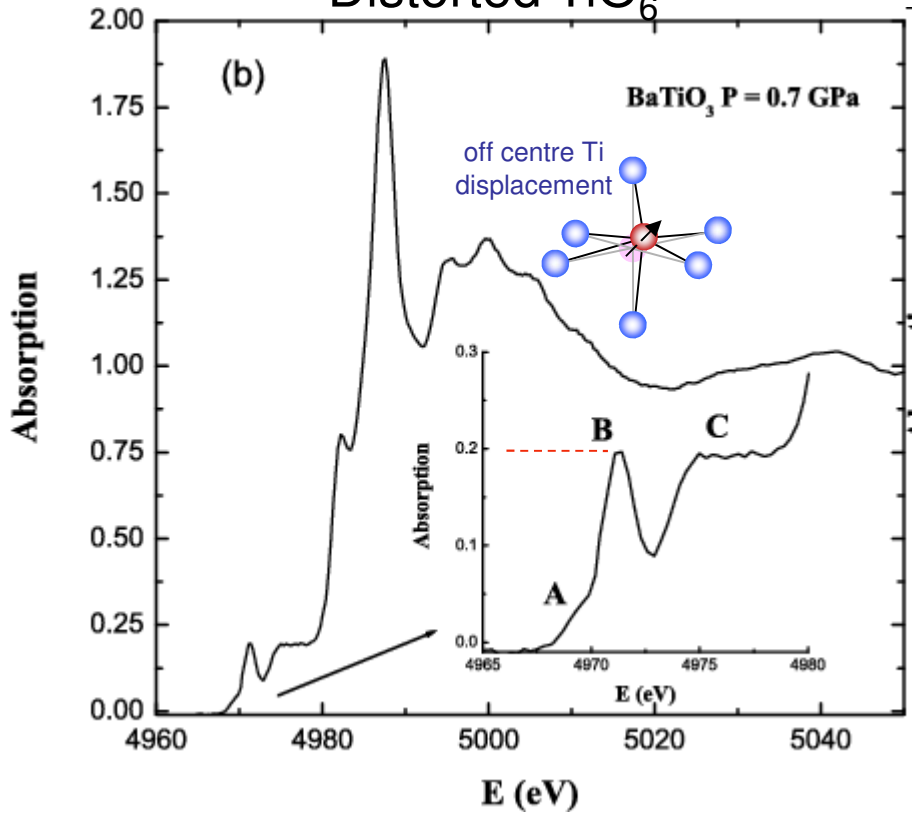

p-d mixing and sensitivity to local symmetry of TiO_6 units

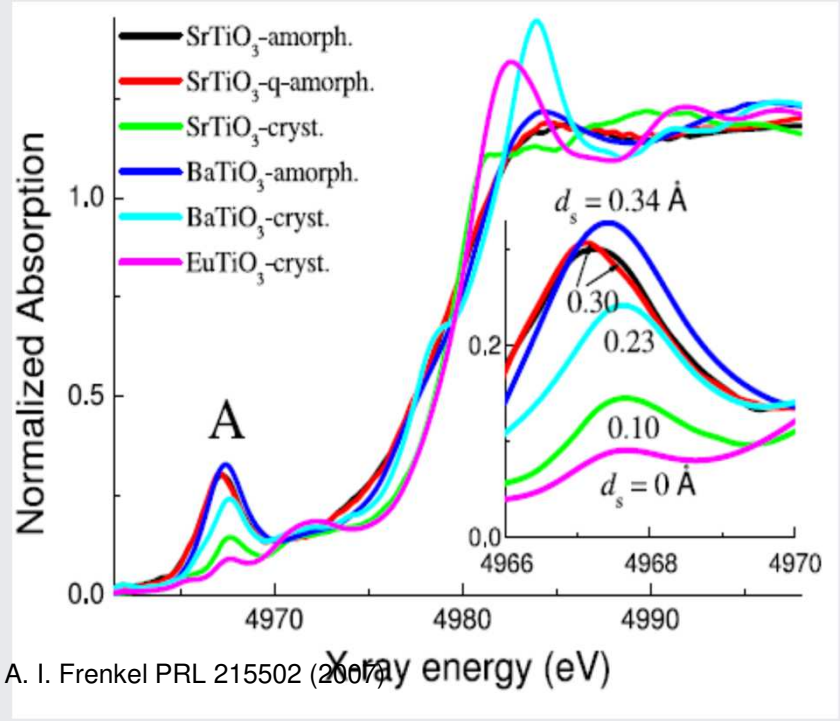

A. I. Frenkel PRL 215502 (2007)

In perovskite structures [1] the area of peak A is proportional to the square of the off center displacement:

$$A = \gamma\, d^2 / 3$$

for Ti $\gamma = 11.2\text{-}13.6$ eV/Å

the displacement d contains a static plus a dynamic contribution:

$$d^2 = d_s^2 + d_t^2$$

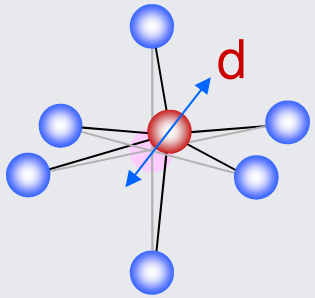

[1] R.V. Vedrinskii et al. J. Phys. Condens. Matter **10**, 9561 (1998).

Example: hydrostatic pressure reduces TiO_6 distortions in $BaTiO_3$ and suppress ferroelectricity

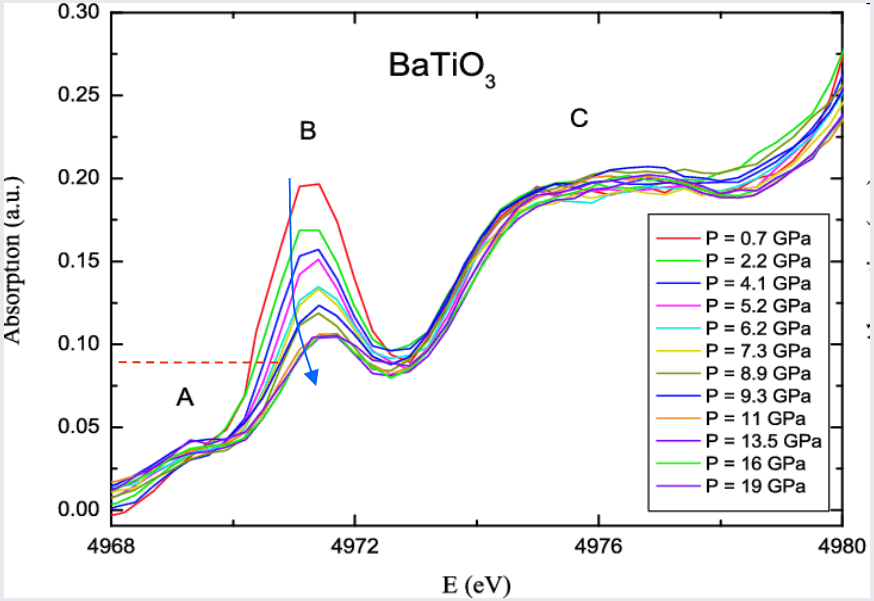

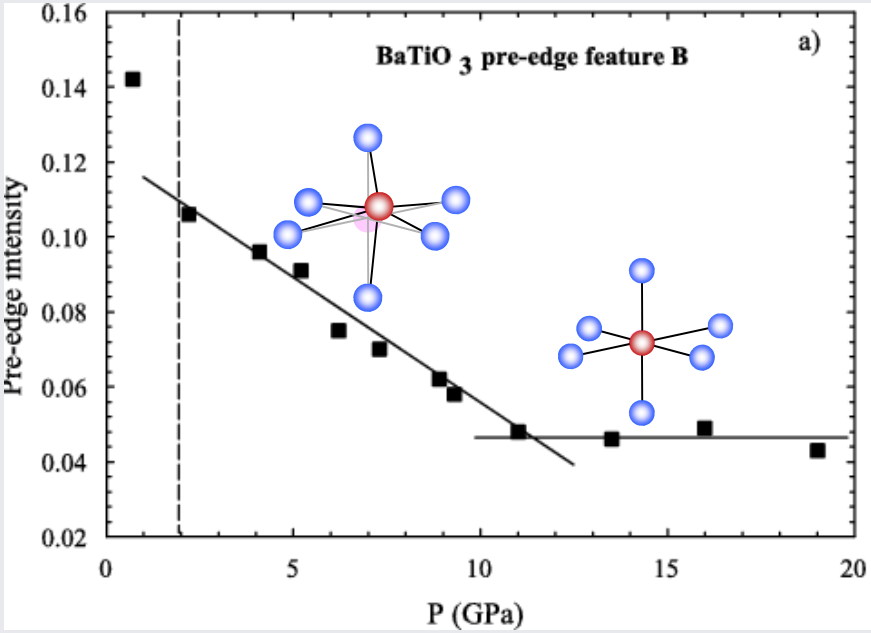

The decrease of B peak intensity signals the reduction of Ti atom displacement.

Above 10 GPa Ti must be at the center of a regular oxygen octahedron,

the hybridization of the Ti 3*d* electronic states with the 2*p* electronic states of the surrounding oxygen is at the minimum

Europhys. Lett., **74** (4), pp. 706–711 (2006)
DOI: 10.1209/epl/i2006-10020-2 J. P. Itié et al.

The Edge region: Shape and position

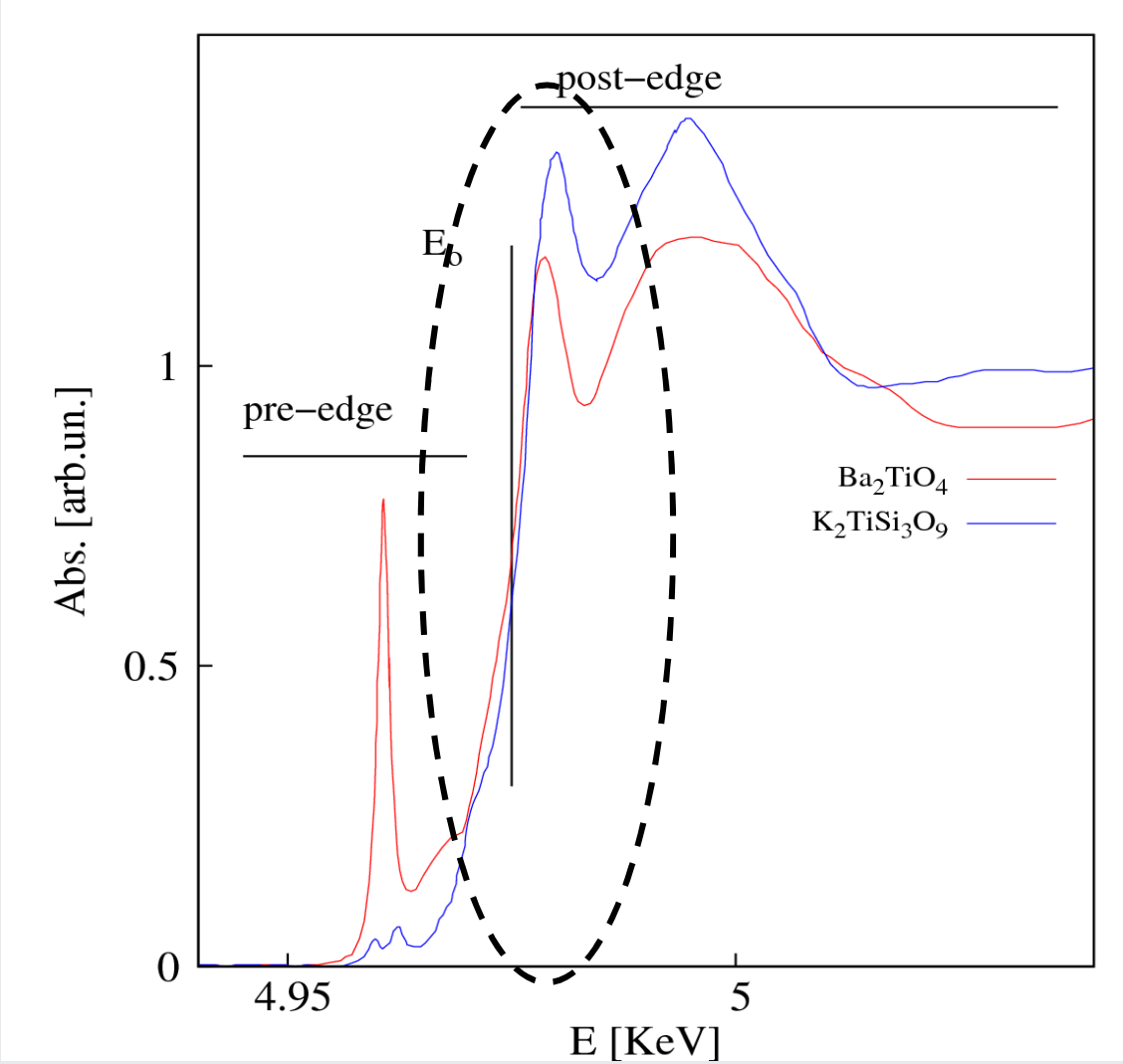

The edge position

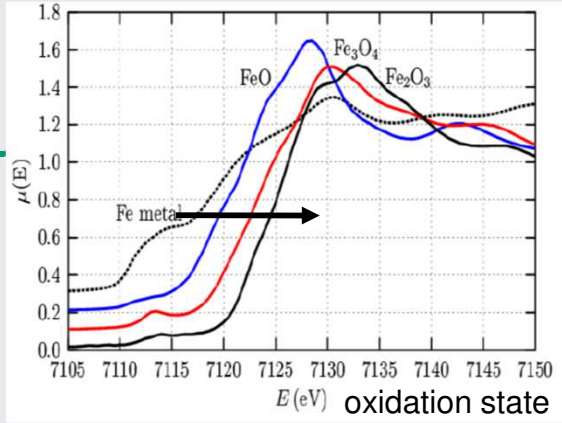

Shape of the edge

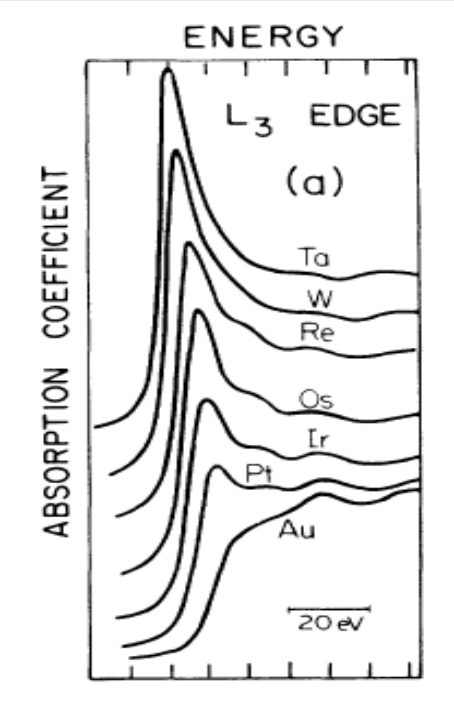

DoS

Edge region: a valuable fingerprint for chemical speciation (coordination geometry and oxidation state)

Sulphur K edges in organic compounds having different functionalities

Edge shape = chemical environment

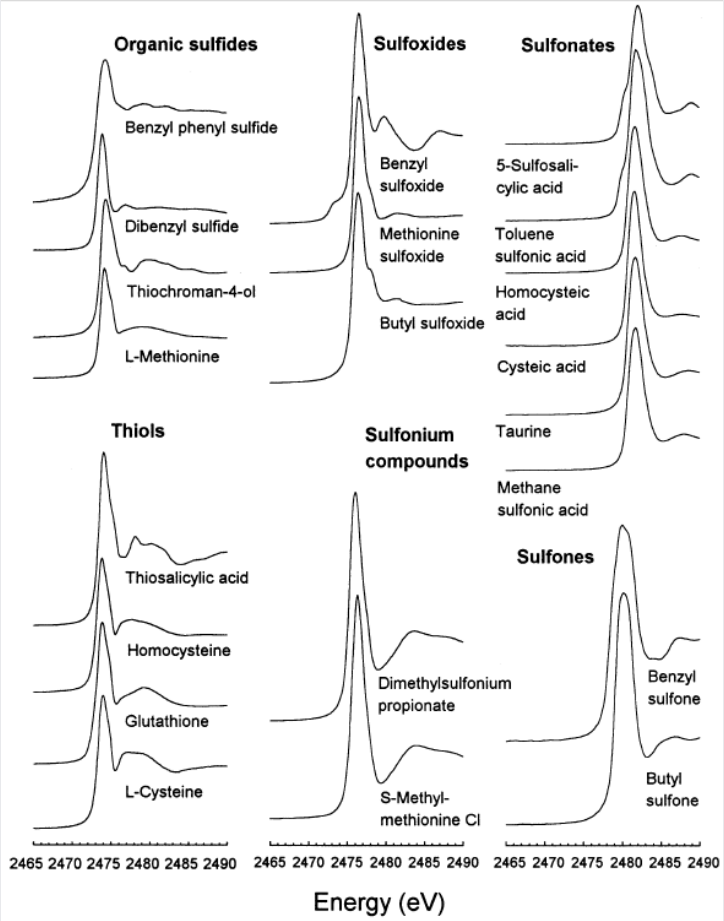

A. Vairavamurthy / Spectrochimica Acta Part A 54 (1998) 2009–2017

Chemical shift = oxidation state

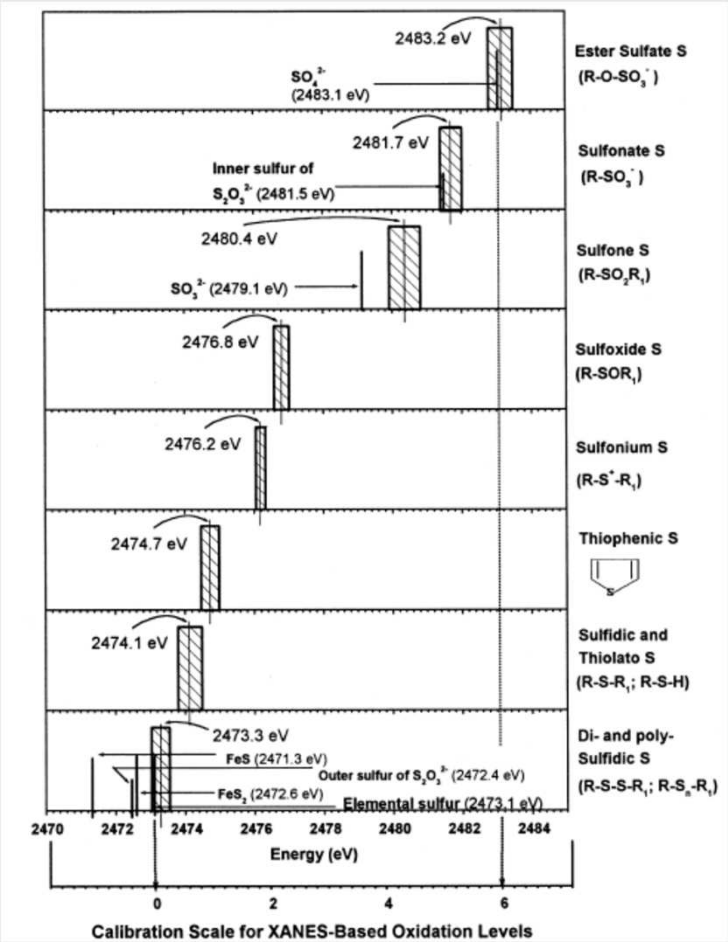

Edge region: a valuable fingerprint for chemical speciation

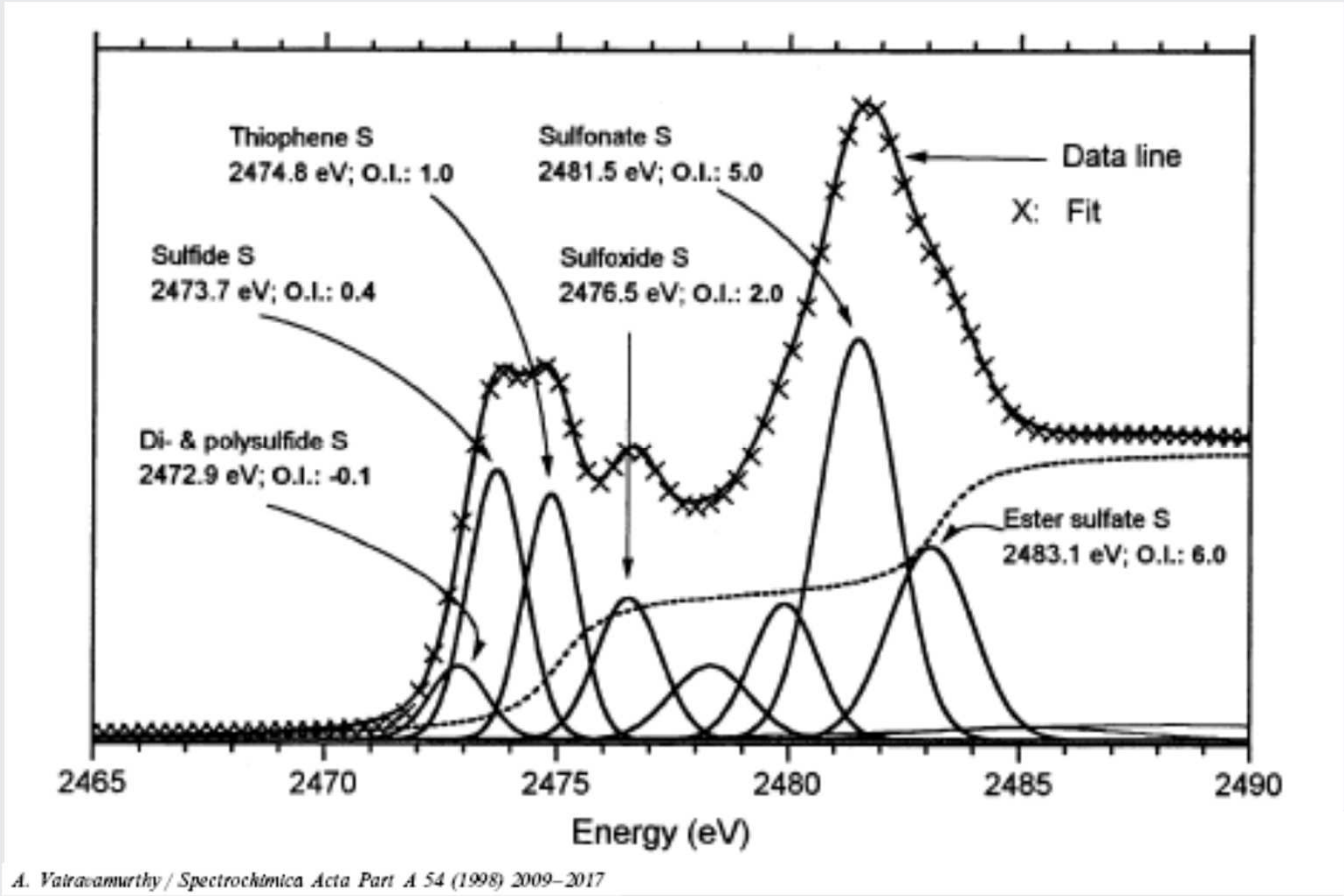

chemical speciation of Sulphur in complex humic substances

The chemical shift reveals the absorber oxidation state…

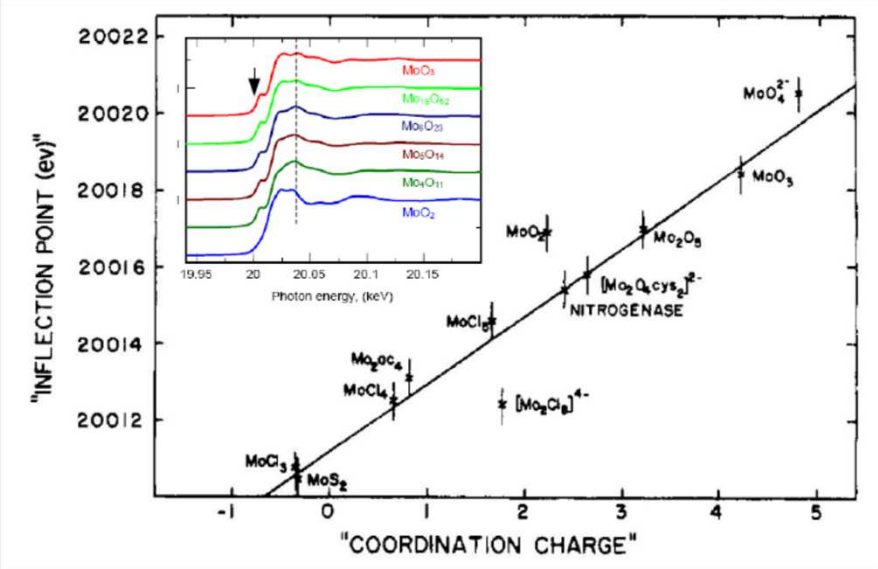

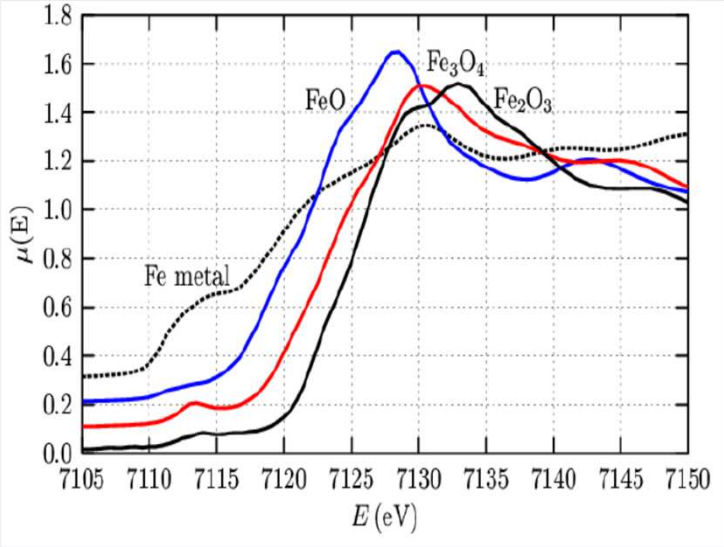

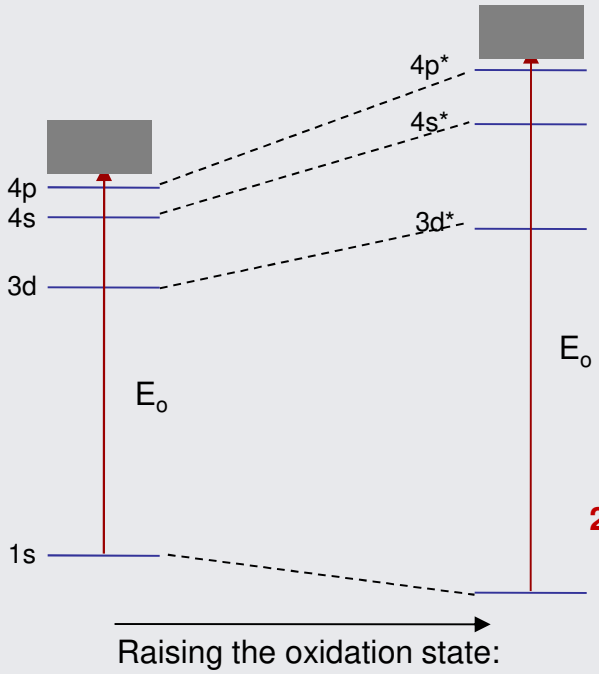

1) shorter bonds (Coulomb)

↓

destabilization of antibonding (empty) levels

2) decreases the screening

↓

stabilization of core level

Higher oxidation state

implies

High energy shift of the resonances

$L_{2,3}$ edge white lines: a probe for occupancy of d band in *n*d elements (n=3, 4, 5)

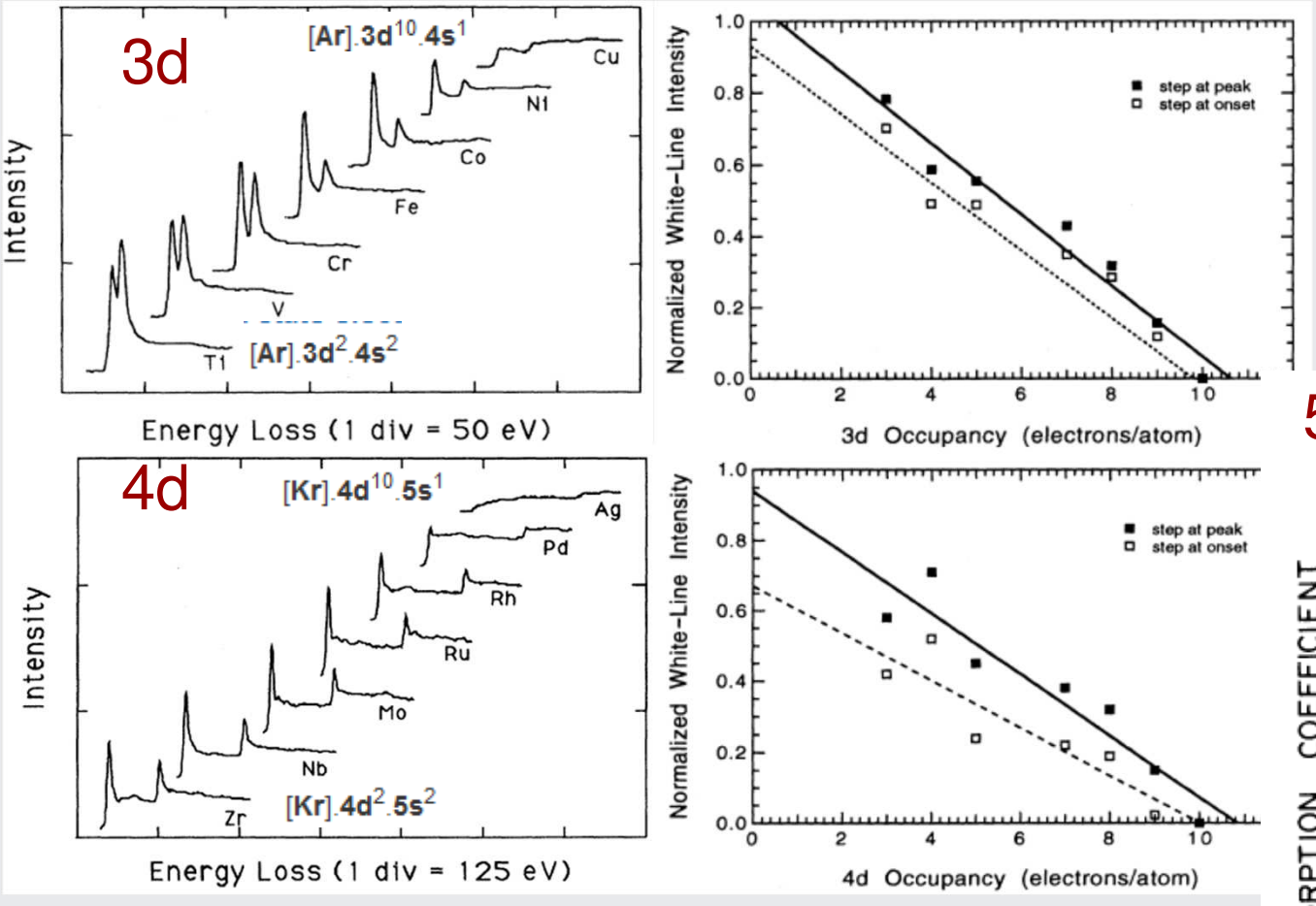

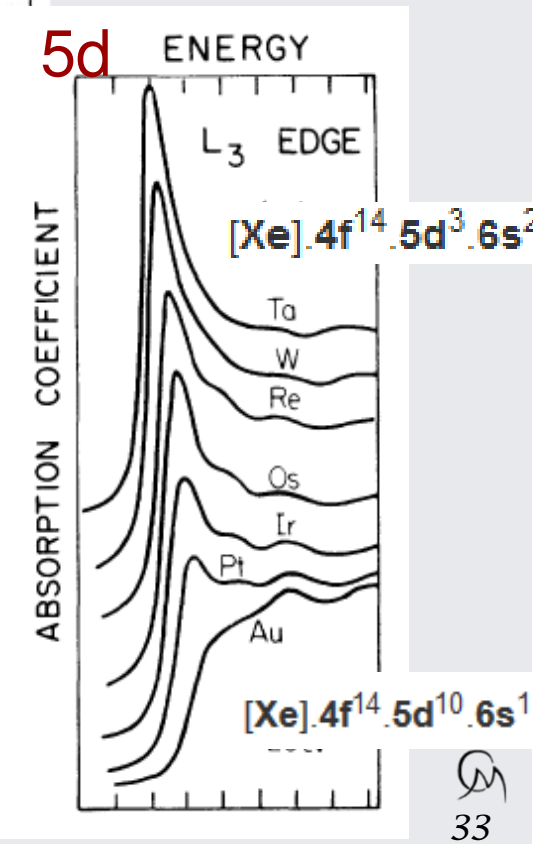

PHYSICAL REVIEW B VOLUME 47, NUMBER 14 1 APRIL 1993-II

White lines and *d*-electron occupancies for the 3*d* and 4*d* transition metals

D. H. Pearson,* C. C. Ahn, and B. Fultz

Example: Pt L_2 edge white line in Pt_xGe_y intermetallic compounds

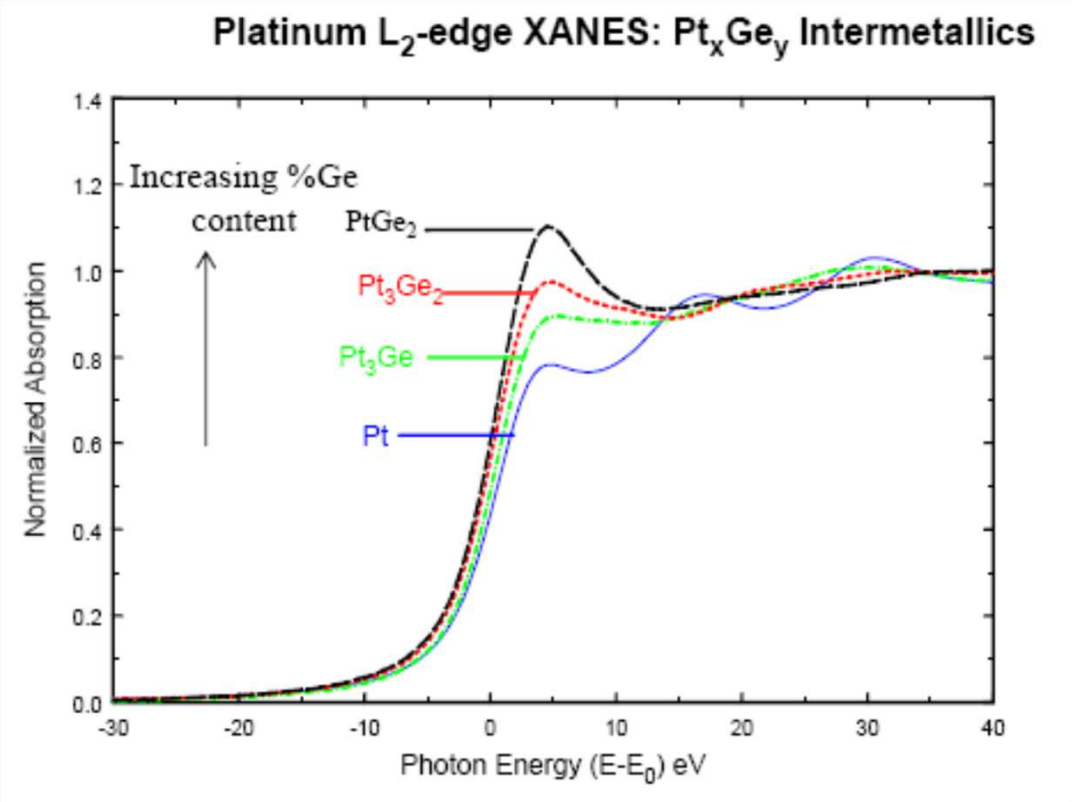

- Transition is $2p$ to $5d$: Pt d-band full, so "no" intensity at edge.
- PtGe intermetallics: charge transfer from d-band of Pt to Ge, resulting in significant intensity at edge.
- Use as signature of Pt-Ge intermetallic formation.

Example: Charge transfer in Cu-Au thin film alloy

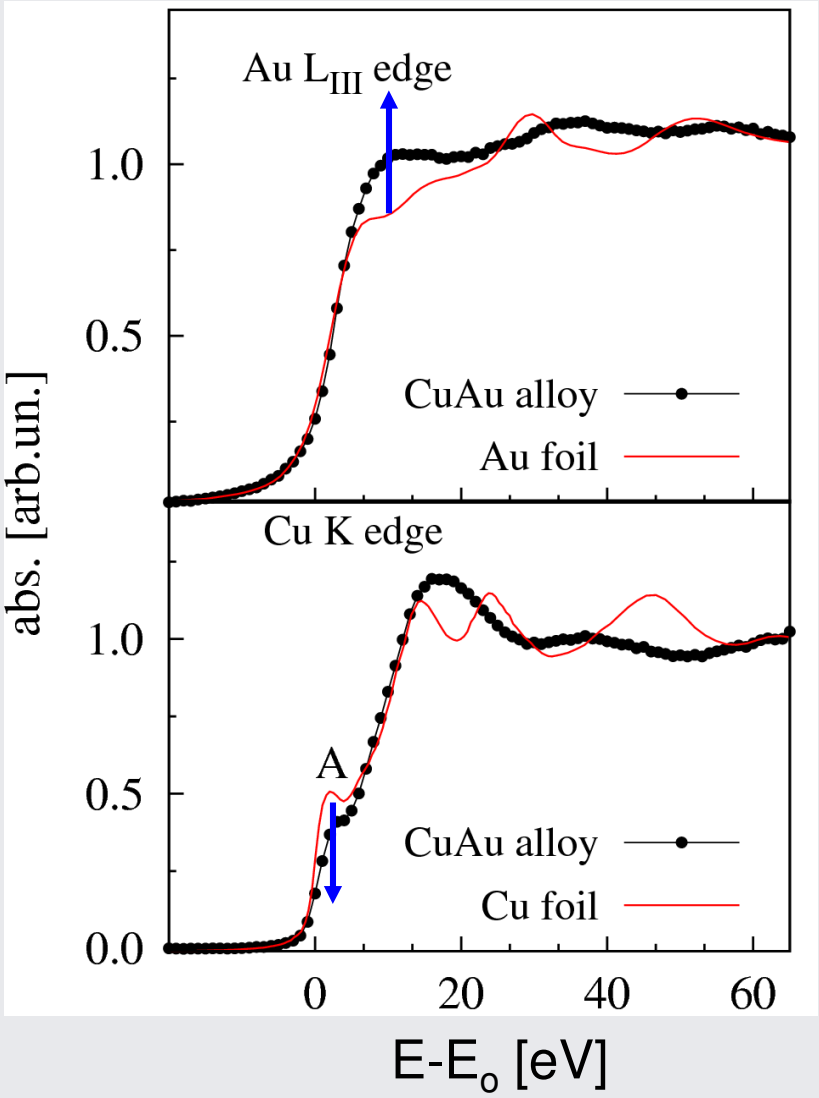

e^- migrate **from Au** (increasing density of empty states)

to Cu (decreasing density of empty states)

Meneghini et al. Corrosion effects in CuAu thin films (to be published)

Analysis of mixtures: Linear Combination Analysis

$$\mu^{th} = \sum_j \alpha_j \mu^{ref_j}$$

$$R^2 = \sum_i \left(\mu^{exp}(E_i) - \mu^{th}(E_i)\right)^2$$

F. Bardelli et al. Geoch. & cosmochem. acta 2011

As adsorption in Natural Calcite samples

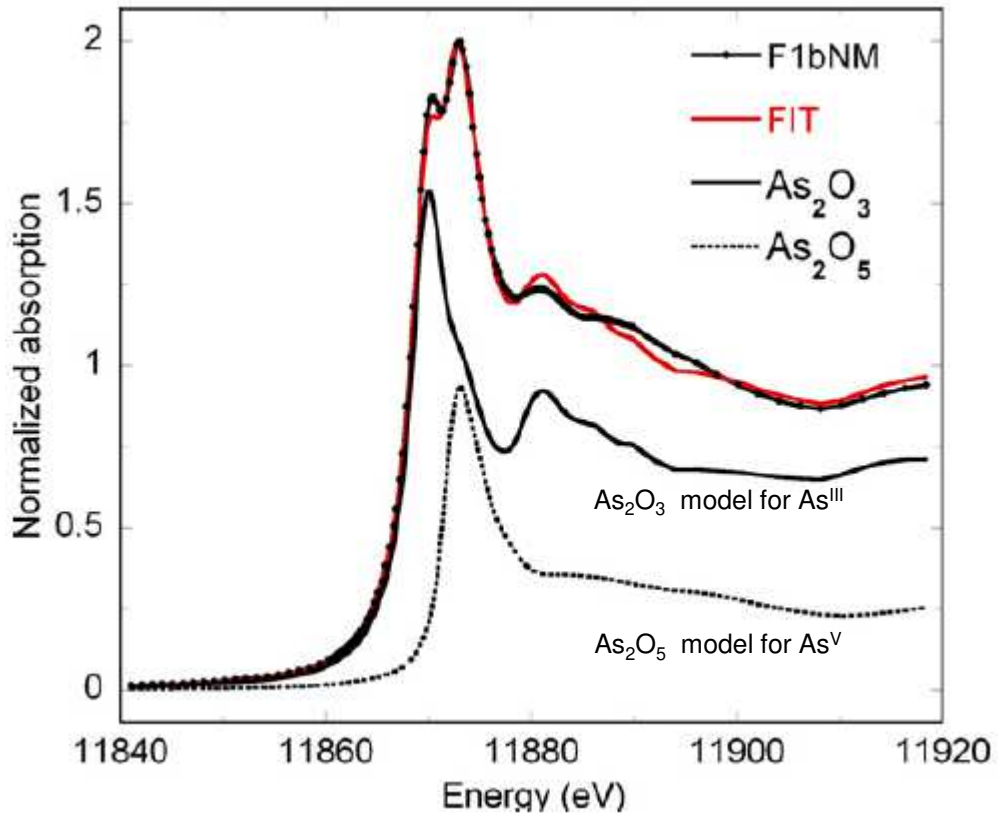

Analysis of mixtures: Linear Combination Analysis

$$\mu^{th} = \sum_j \alpha_j \mu^{ref_j}$$

$$R^2 = \sum_i \left(\mu^{exp}(E_i) - \mu^{th}(E_i)\right)^2$$

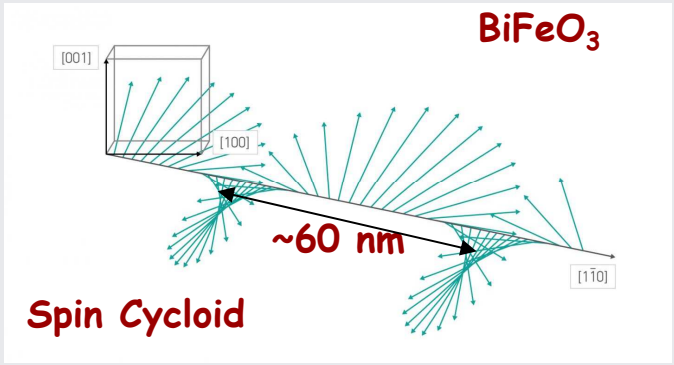

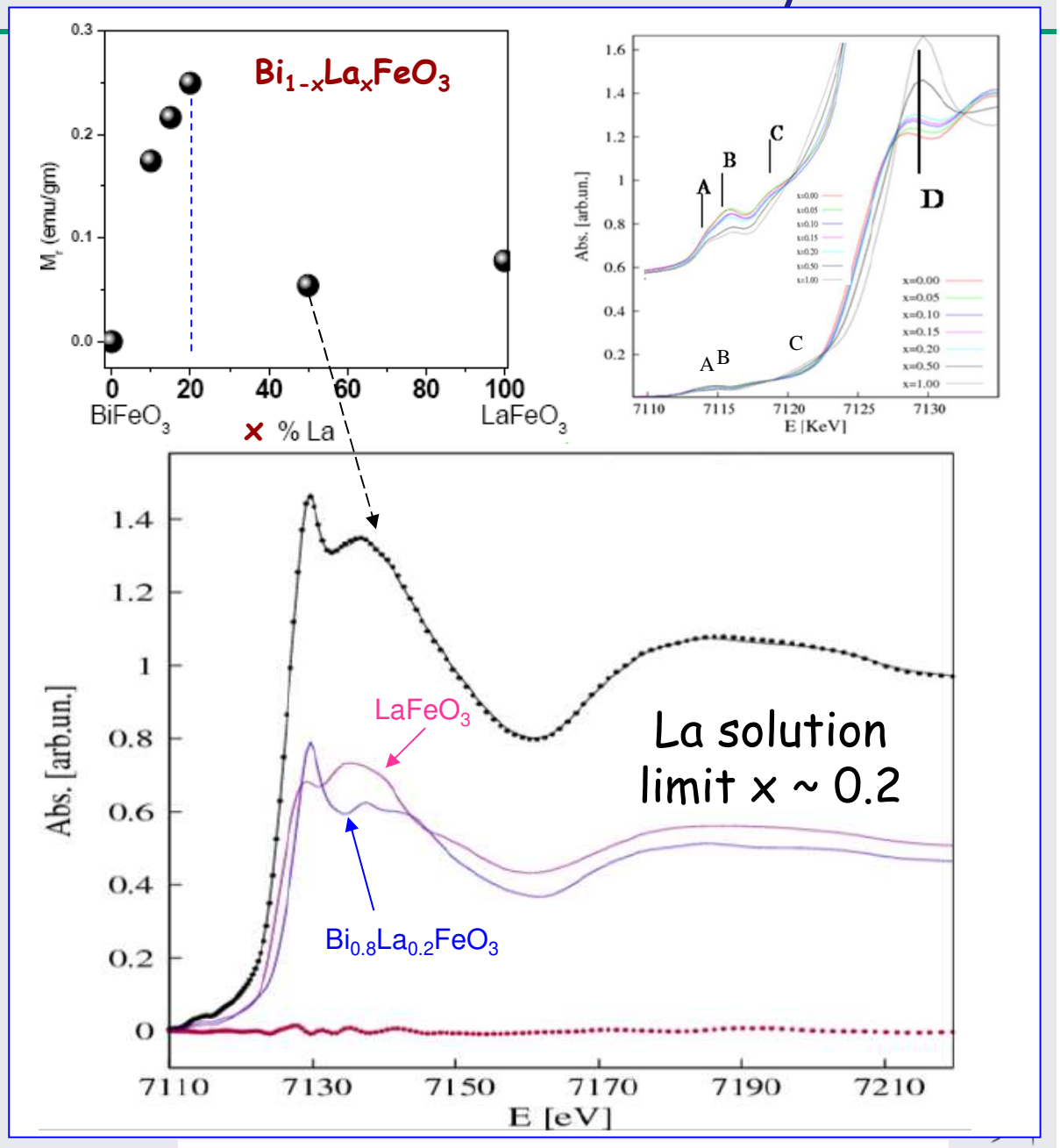

Deepti Kothari *et al* 2010 *J. Phys.: Condens. Matter* **22** 356001

Advanced materials: looking for magneto-electric coupling

Ferromagnetism: a property of certain materials which possess a spontaneous **magnetic** polarization

Ferroelectricity: a property of certain materials which possess a spontaneous **electric** polarization

Magneto-electric coupling: magnetic control of ferroelectricity and/or electric control of ferromagnetism may open the way to new devices

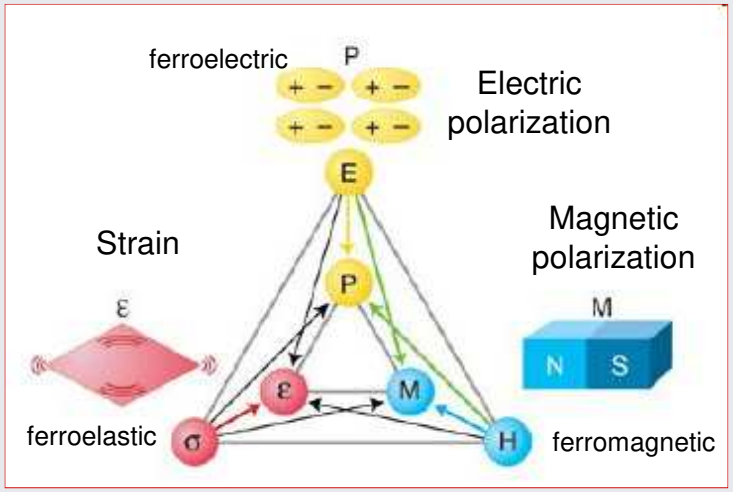

Advanced materials: looking for magneto-electric coupling

$BaTiO_3$

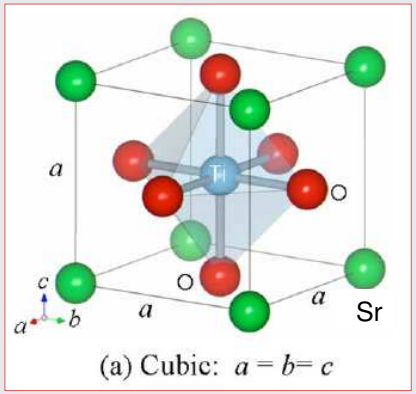

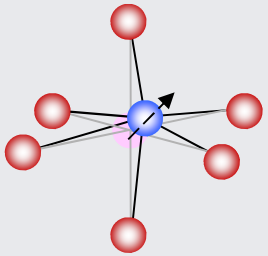

$BaTiO_3$ is **ferroelectric**: off center displacement of Ti^{4+} ions produces a permanent electric dipole in TiO_6 molecules

$BaTiO_{3-\delta}$

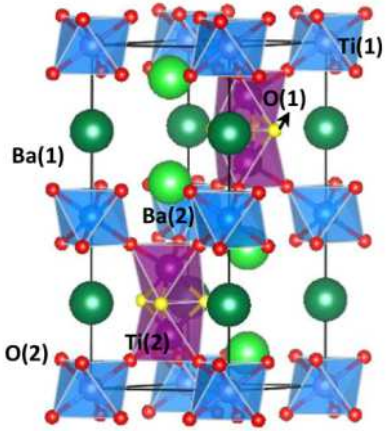

doping with magnetic ions (Fe) may provide some magnetoelectric coupling and stabilize the ferroelectric phase

$BaTi_{0.95}Fe_{0.05}O_{3-\delta}$

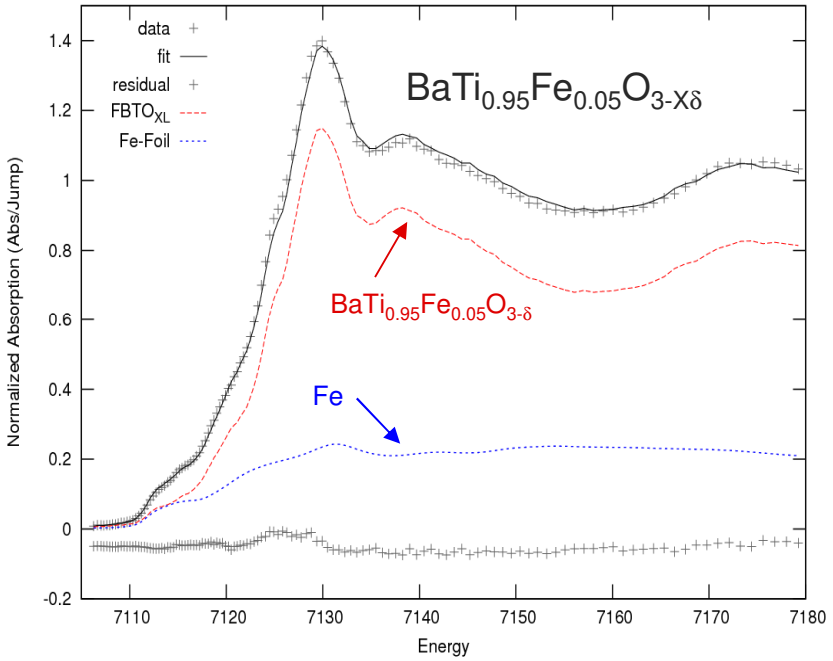

Large Oxygen vacancies causes the Fe ions segregating as metallic Fe^0 phase, the sample is no more homogeneous at the short range scale, wrong magneto-electric understanding

Note: XRD can't show Fe crystalline phase because 1% of Fe^0

T. Chakraborty, C. Meneghini, G. Aquilanti, S. Ray, J. Phys.: Condens. Matter 25 (2013) 23600
T. Chakraborty, C. Meneghini, G. Aquilanti, S. Ray, Advanced Functional Materials, Submitted

XANES - LCA for Catalysis

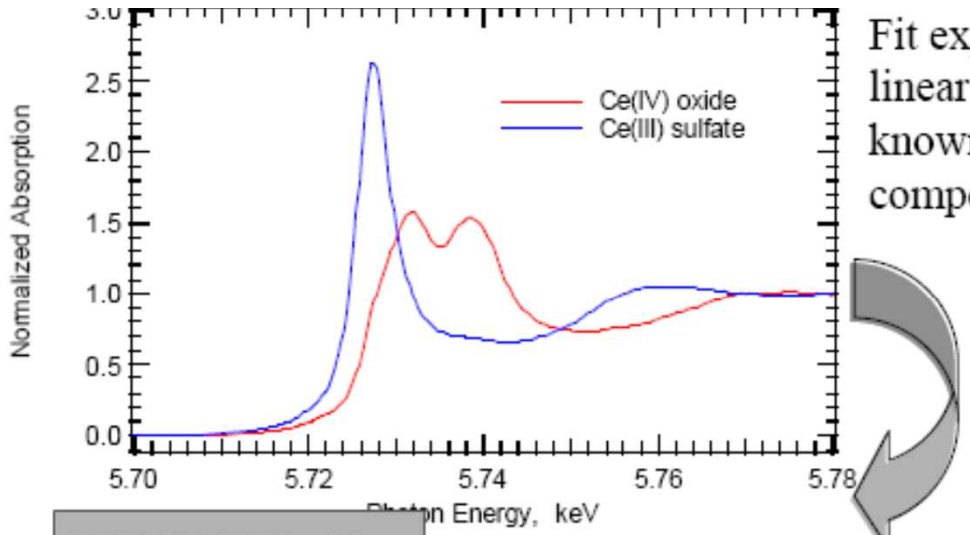

Fit experimental data to linear combination of known reference compounds

TPR-XANES of *in situ* reduction of $Ce_{0.7}Zr_{0.3}$ oxide

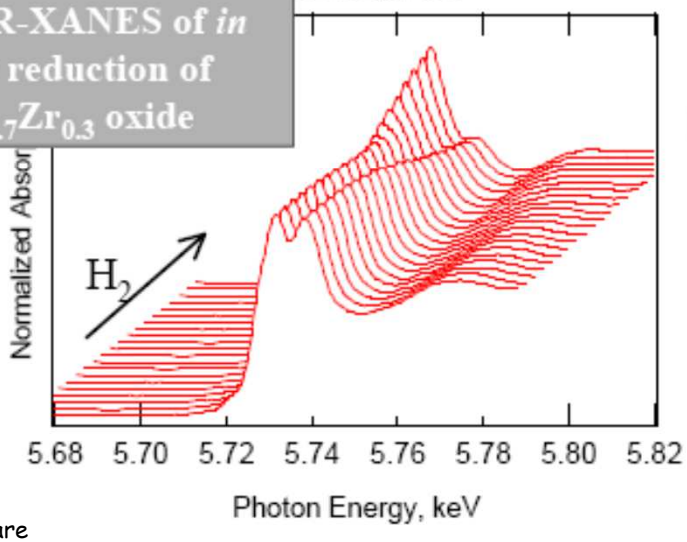

LC-XANES fit to determine amount of Ce(III) and Ce(IV) present as function of temperature

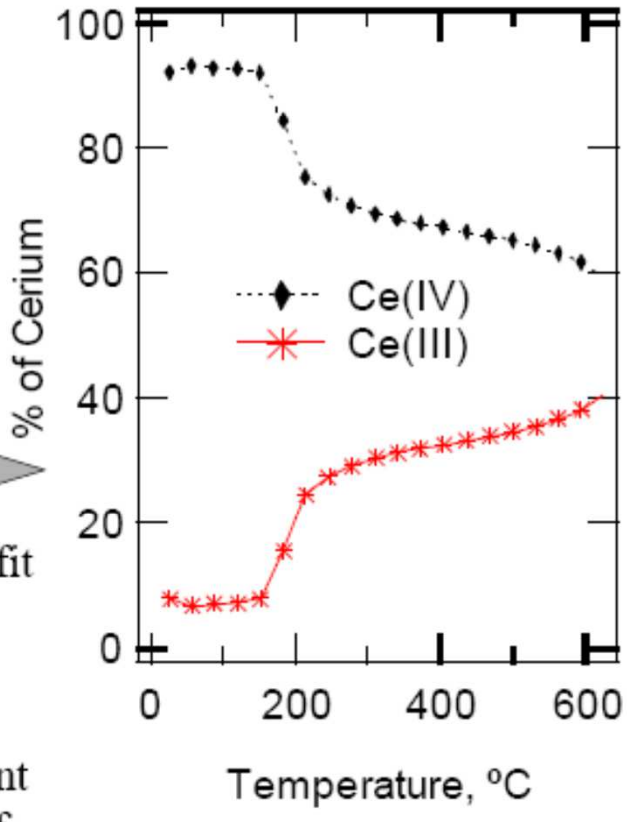

Simon R. Bare

Principal component analysis (PCA)

*Determination of molybdenum surface environment of molybdenum/titania catalysts by EXAFS, XANES and PCA. Mikrochimica Acta 109 (1992) 281.

PCA, based on linear algebra e statistical methods, is widely used in pattern recognition problems. Each reference spectrum (component) represent a vector, the data are reproduced by vectorial sum. The algorithms automatically determine (statistics) the relevant components (principal) out a given ensamble and reject the others

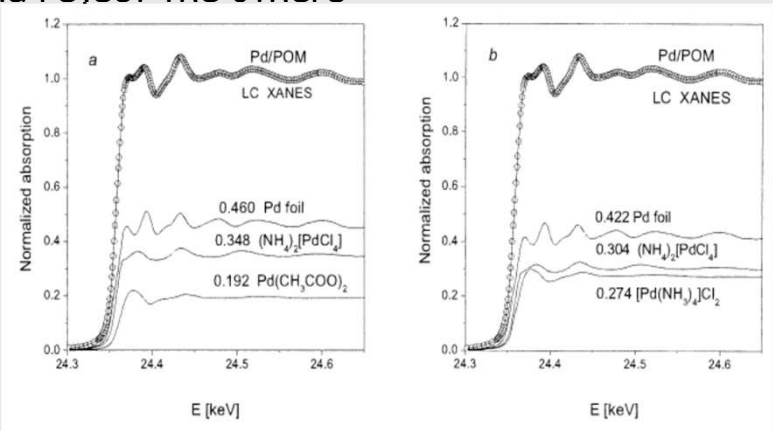

J.W. Sobczak J. of All. and Comp. 362 (2004) 162
Local structure of a Pd-doped polymer

Automatic procedure to select principal components on the basis of their statistical relevance

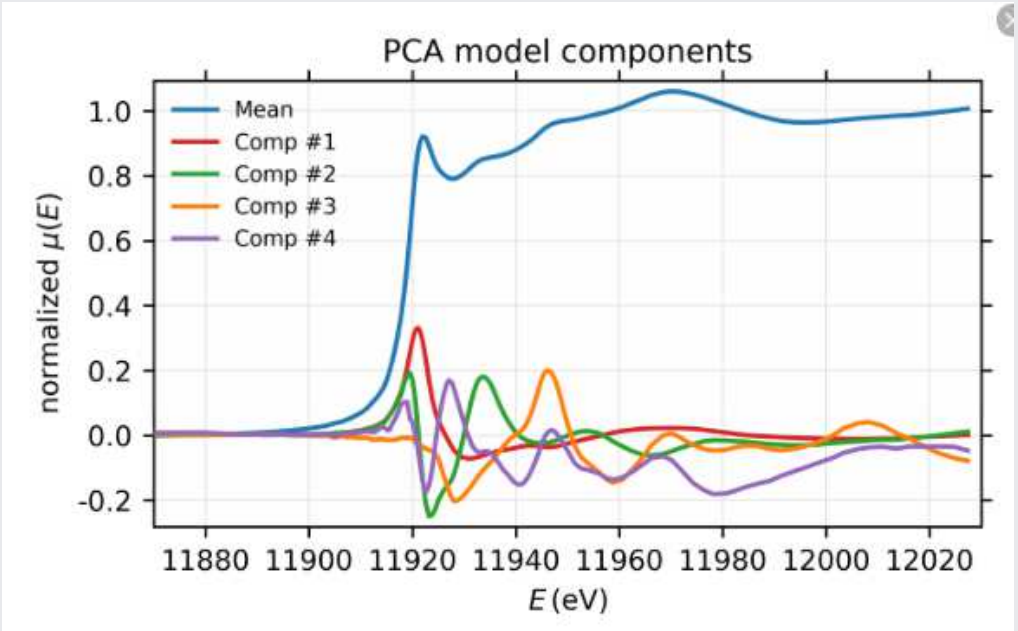

Warning

- Components maybe not "physical"
- Which standards are required?
- Which standards are unphysical?
- Is the final fit reasonable?

- Use all the a-priori knowledge on the sample (physics, chemistry, etc…)
- Check carefully the results

How to calculate the XANES signal

Test the structural models

Fermi Golden Rule

$$\sigma(\omega) = \alpha \frac{4\pi}{\omega} \sum_f | < \Psi_i | H_i | \Psi_f > |^2 \delta(\hbar\omega + E_i - E_f)$$

atomic absorption cross section

Ground state

Interaction Hamiltonian

Final state

photon energy

Electric Dipole

$$\sigma(\omega) \approx \sum_f | < \psi_f; \Psi_f^{N-1} | \hat{\epsilon} \cdot \vec{r} | \psi_i; \Psi_i^{N-1} > |^2 \delta(E_f - E_i - \hbar\omega)$$

One electron

$$\sigma(\omega) \approx \sum_f | < \Psi_i^{N-1} | \Psi_i^{N-1} > |^2 | < \psi_f | \hat{\epsilon} \cdot \vec{r} | \psi_i > |^2 \delta(E_f - E_i - \hbar\omega)$$

Many body effects

S_0^2

Muffin-Tin approximation

$$V(\vec{r}) = V_I + V_{II} + V_{III}$$

$$V_I(\vec{r}) = \sum_j v^J_{R_j}(\vec{r} - \vec{R}_j)$$

I region

$$V^j_I(\vec{r}) = \sum_L v^j_L(r) Y_L \vec{r} \; ; L = 1, m$$

Only the L=0 is considered: spherical symmetry

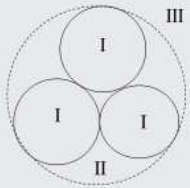

II region

$$\sigma(\omega) \approx \sum_f S_0^2 | < \psi_f | \hat{\epsilon} \cdot \vec{r} | \psi_i > |^2 \delta(E_f - E_i - \hbar\omega)$$

$$\Psi^i_I = \sum_L B^i_L R^i_\ell(r_i) Y_{\ell m}(\hat{r}_i)$$

III regi

V_{III} is a spherical avera
It depends to the physi

In the extended continuum scheme V
to continuum and bound s

$$\sigma(\omega) \approx \sum_{\underline{L}, L, m_\gamma, m_o} \left| B^0_L(\underline{L}) \right|^2 \left| \left\langle R^0_L(\vec{r_o}) | r_o Y_{lm_\gamma}(\hat{r_o}) | \phi_{l_o}(r_o) Y_{L_o}(\hat{r}_o) \right\rangle \right|^2$$

Total scattering amplitude

Radial part of the final state at r_o (the w.f. is localized)

EM interaction (dipole approximation)

Initial state

Selection rules $l = l_o+1, l_o-1$

From the Lippmann-Schwinger equation and using the Green's theorem:

$$B^i_L(\underline{L}) - t^i_l \sum_{j \neq i} \tilde{G}^{ij}_{LL'} B^j_{L'}(\underline{L}) =$$

Total scattering amplitude of momentum L at the site i

Scattering of waves coming from neighbour scattering

The scattering amplitude at the site i with an
amplitude of the exciting wave J plus the
neighbouring sites

Tyson, Hodgson, Natoli, Benfatto Phys. Rev. B 465997 (1992)

$$\sigma(\omega) \approx \sum_{\underline{L}, L, m_\gamma, m_o} \left| B^0_L(\underline{L}) \right|^2 \left| \left\langle R^0_L(\vec{r_o}) | r_o Y_{lm_\gamma}(\hat{r_o}) | \phi_{l_o}(r_o) Y_{L_o}(\hat{r}_o) \right\rangle \right|^2$$

$$\sigma(\omega) = \sigma^a_{l_o, l_o+1} \chi_{l_o+1} + \sigma^a_{l_o, l_o-1} \chi_{l_o-1}$$

Atomic part

$$M^{l_o}_l = \int_o^{R_{MT_i}} \phi_{l_o}(r) R^i_l(r) d\vec{r}$$

Rarial dipole matrix element, the integral just inside the MT volume die to the localization of the w.f.

$M^{l_o}_{l_o \pm 1}$ The dipole allowed transition

$$\sigma^a_{l_o, l_o \pm 1} \approx (M^{l_o}_{l_o \pm 1})^2 \Im m(t_{l_o \pm 1})$$

$sin^2 \delta^0_l$

$$\chi_l = \frac{1}{(2l+l) \sin^2 d_l} \sum_m \Im m \; \tau^{oo}_{lm\,lm}$$

Structural part

exact solution $\tau^{oo}_{LL'} = [(I - T_a G)^{-1} T_a]^{oo}_{LL'}$

The matrix inversion allows obtaining all the structural and electronic information about the atomic cluster

MS expansion

$$(I - T_a G)^{-1} = \sum_{n=0} (T_a G)^n$$

$$\tau = T_a + T_a G T_a G T_a + T_a G T_a G T_a G T_a + ...$$

EXAFS region

Muffin-Tin approximation

$$\mu(E) \propto \mu^{at}\Im\{\frac{1}{sin^2\delta^0_{L_0}}\frac{1}{2L_0+1}\sum_{m_0}[T((1-GT)^{-1})^{0,0}_{L_0,L_0}\}$$

$$(I-GT)^{-1} \cong \sum_n (GT)^n$$

$$\chi(k) = \frac{1}{k}\sum_j A_j(k,r_j)sin(2kr_j+\psi_j(k))$$

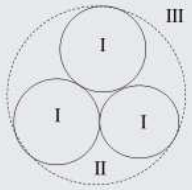

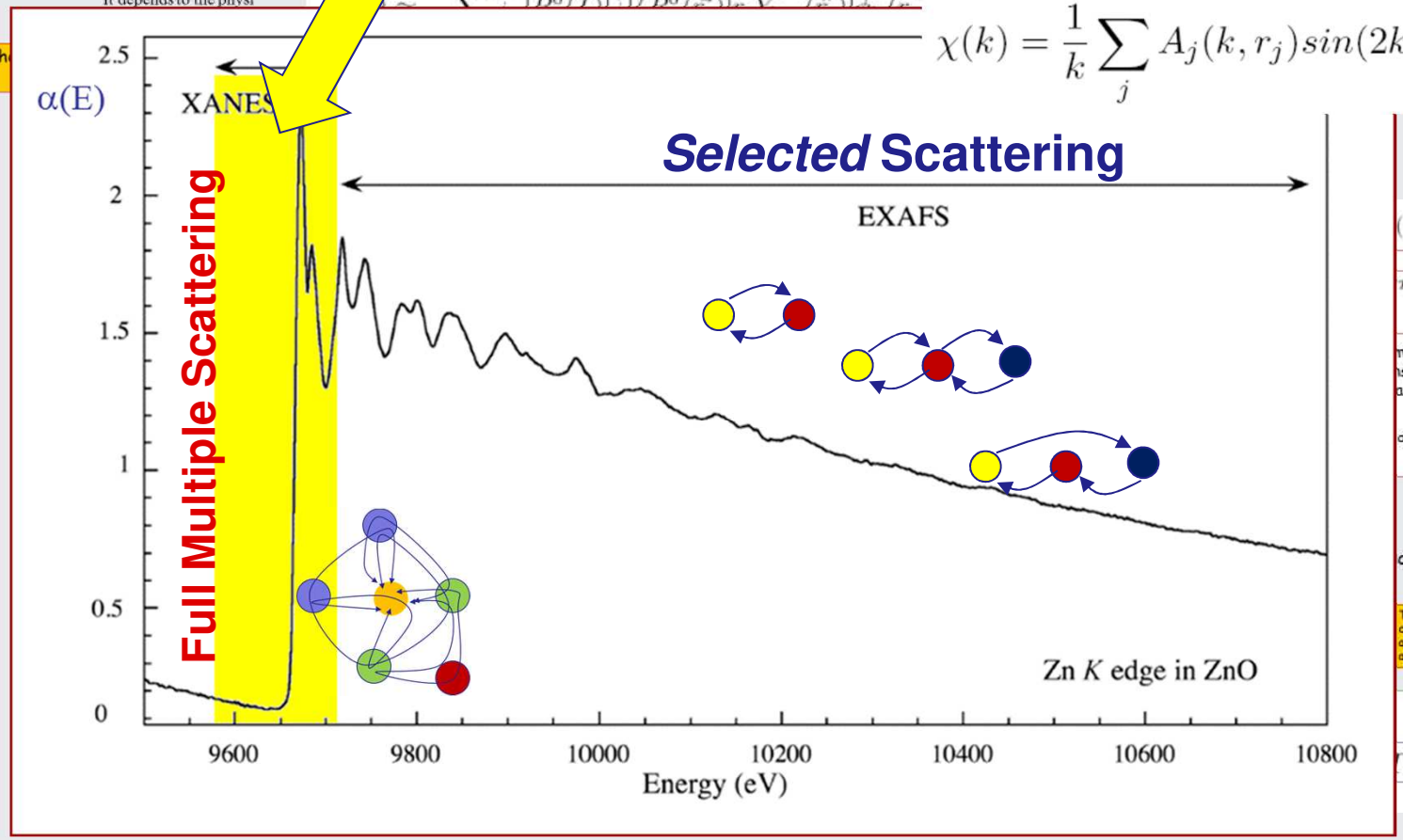

a. Models for the atomic potentials (Exchange and correlation)

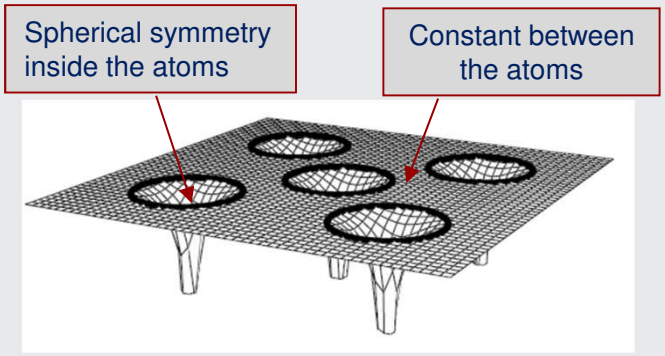

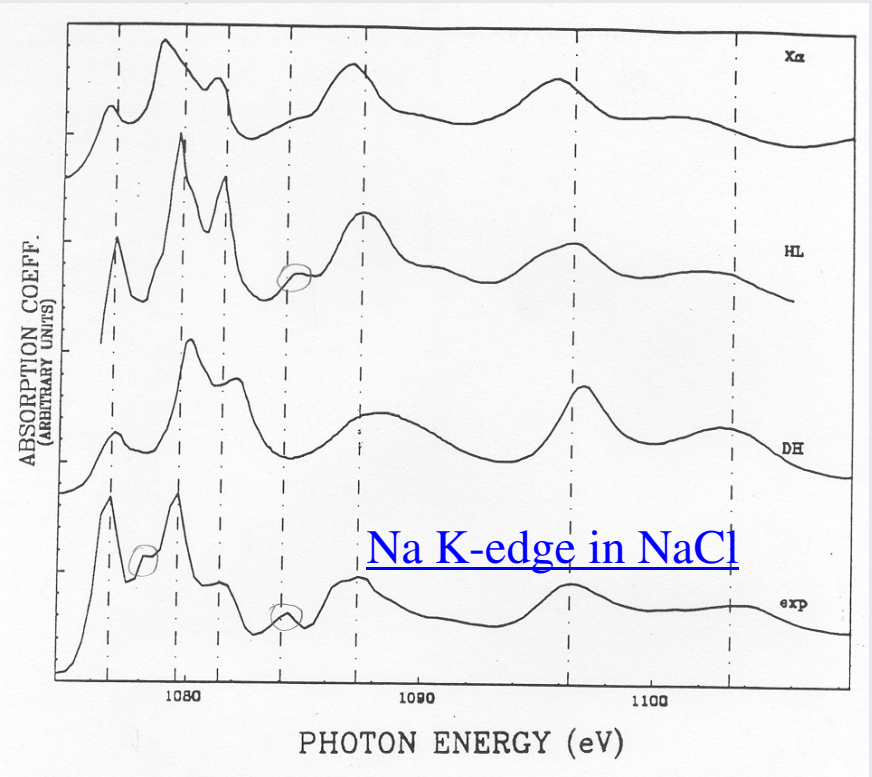

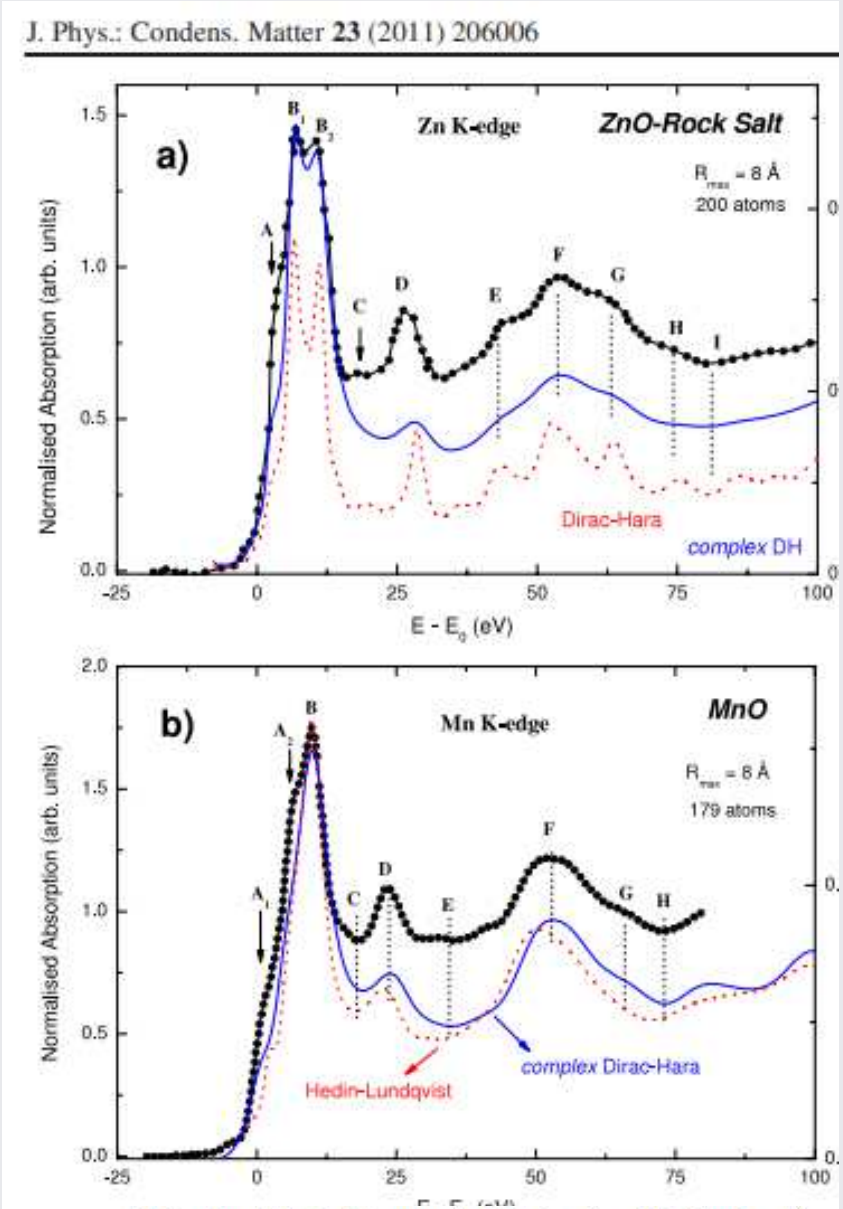

b. Calculate the Full Multiple Scattering: $(I-TG)^{-1}$

Size of the Atomic clusters

- Memory requirements: ~ N^2
- CPU time ~ N^3

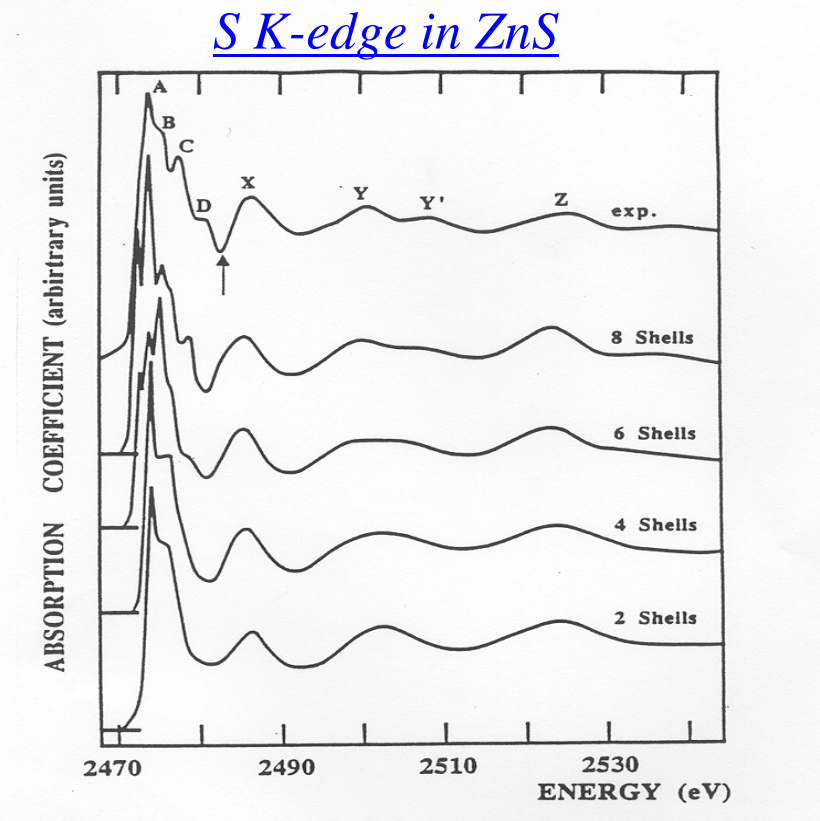

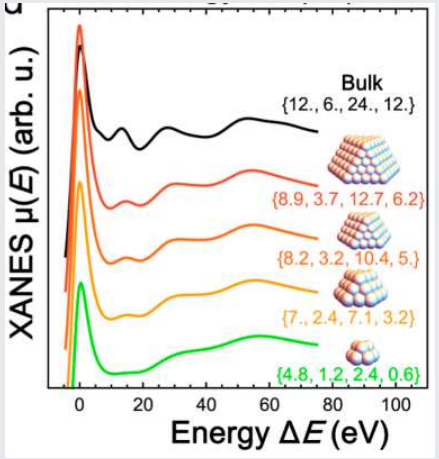

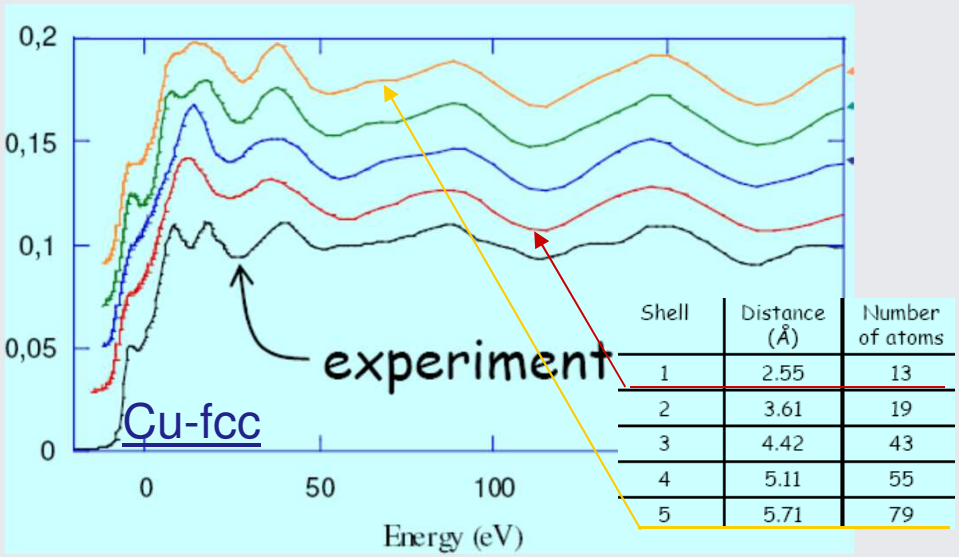

Shell	Distance (Å)	Number of atoms
1	2.55	13
2	3.61	19
3	4.42	43
4	5.11	55
5	5.71	79

Toward a quantitative interpretation of XANES

XANES development

Lee & Pendry Phys. Rev. B 11, 2795 (1975) (initial theory)

C.R. Natoli et al. Phys. Rev. A, 22, (1980) (first calculations)

First-principles calculation of x-ray absorption-edge structure in molecular clusters
C. R. Natoli, D. K. Misemer, S. Doniach, and F. W. Kutzler

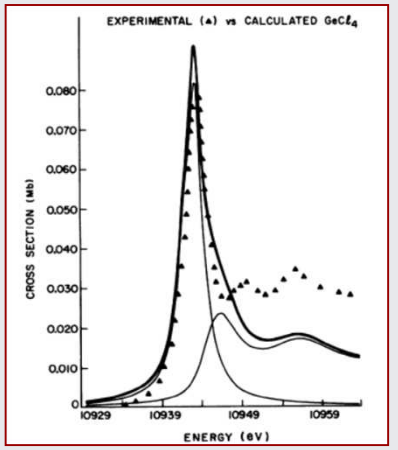

Theory

Tyson, Hodgson, Natoli, Benfatto Phys. Rev. B 465997 (1992)

A. Filipponi et al. Phys. Rev. B 52, 12122 (1995)

Ankudinov et al. Phys Rev. B 58, 7565 (1998)

J. Rehr Rev. Mod. Phys. 72, 621 (2000)

programs for XANES:

C. R. Natoli and M. Benfatto	CONTINUUM, MXAN	freeware	
J. Rehr, Ankudinov	FEFFx (x=6,8,9)	freeware	Licence
Y. Joly	FDMNES	freeware	

FEFF 8

Ibuprofen/warfarin induce 5 to 6 Fe coordination transition in HSA

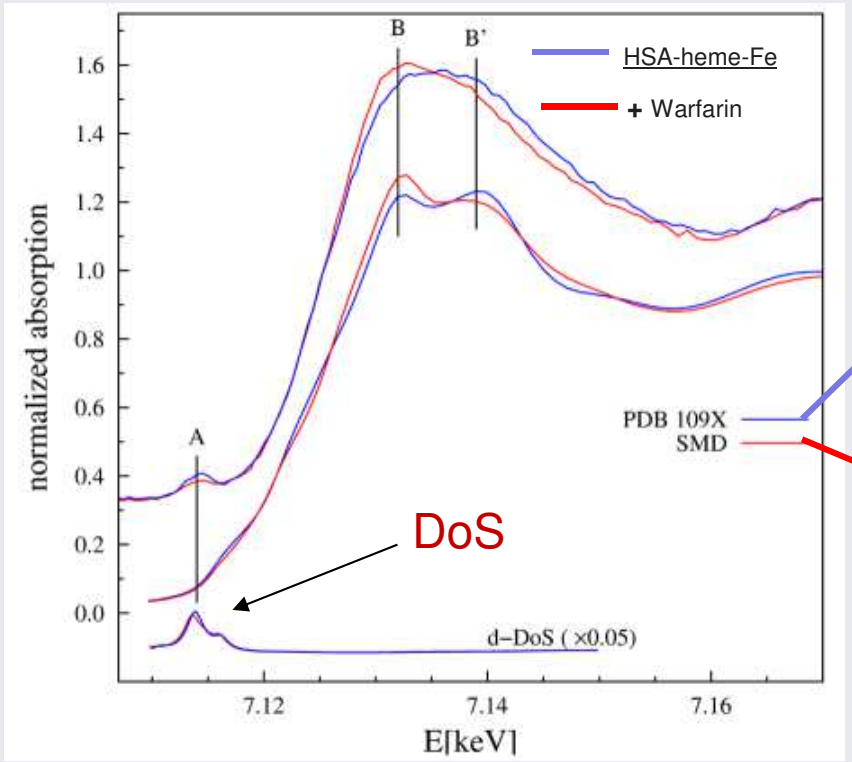

5

6

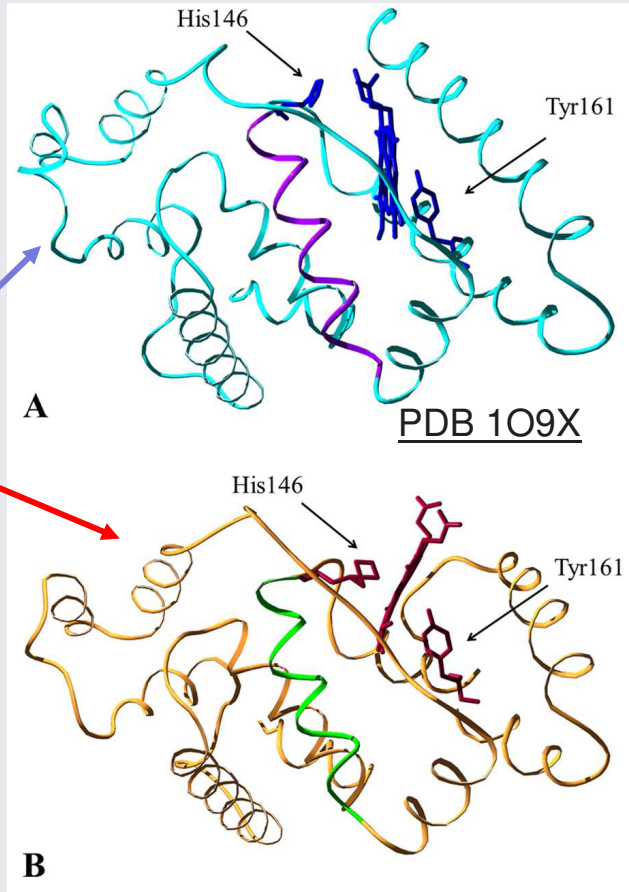

HSA-heme-Fe(III) obtained via MD

FMS: Atomic clusters of 4.5 Å
V= H.L.

OPEN ACCESS Freely available online
PLOS ONE

The Five-To-Six-Coordination Transition of Ferric Human Serum Heme-Albumin Is Allosterically-Modulated by Ibuprofen and Warfarin: A Combined XAS and MD Study

Carlo Meneghini[1*], Loris Leboffe[1,2*], Monica Bionducci[1], Gabriella Fanali[3], Massimiliano Meli[4], Giorgio Colombo[4], Mauro Fasano[3], Paolo Ascenzi[2,5*], Settimio Mobilio[1]

FEFF 8

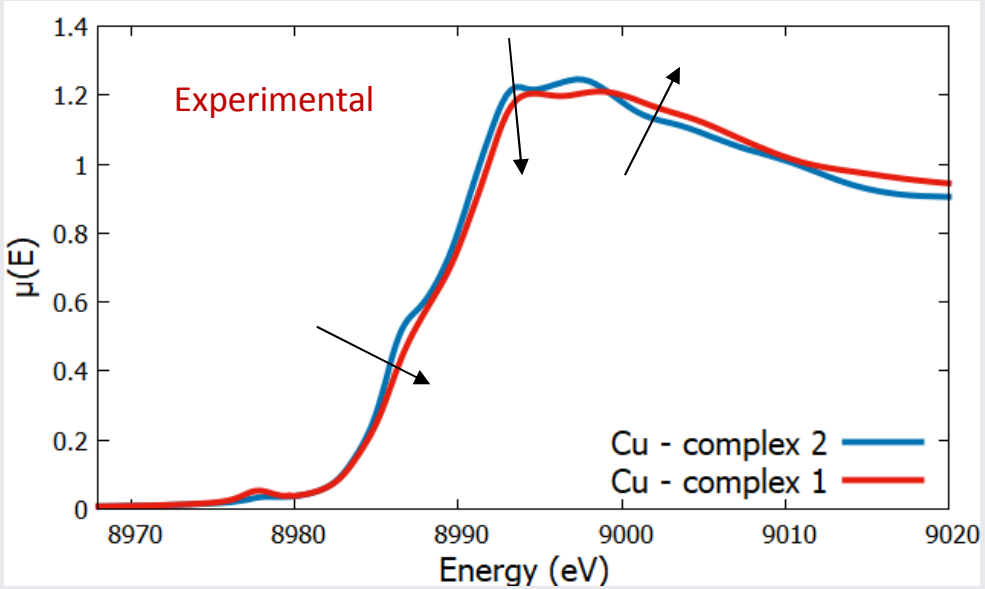

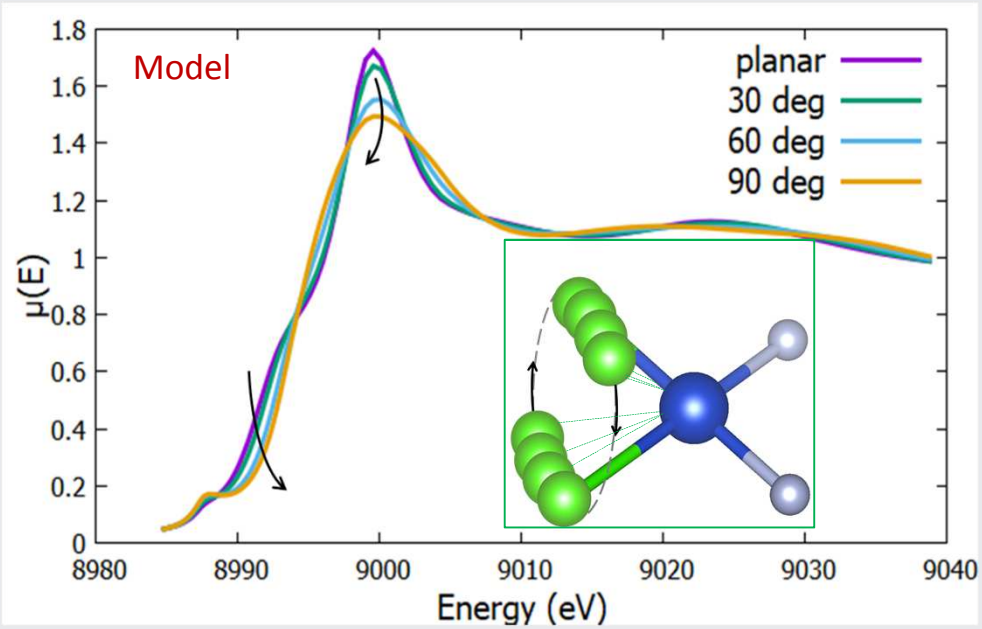

Cu-complex for cancer therapy

Cu-complex 1

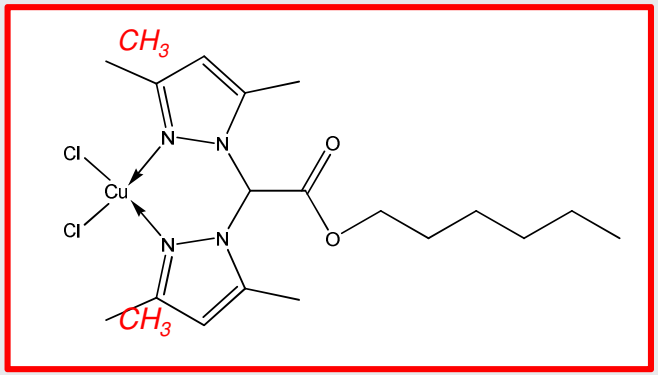

Hexyl bis(3,5-dimethyl-1H-pyrazol-1-yl)acetate

Cu-complex 2

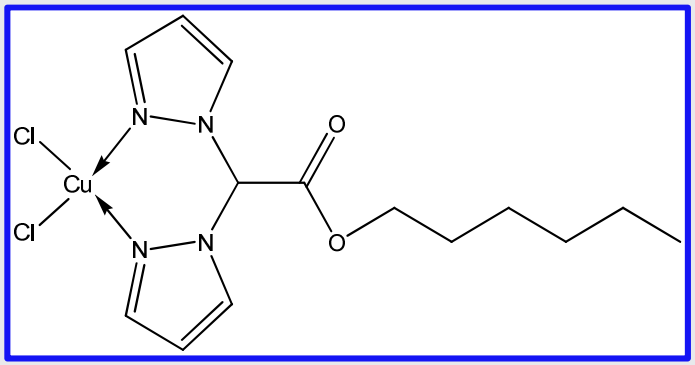

Hexyl bis(3,5-1H-pyrazol-1-yl)acetate

I. Schiestaro et al., in progress

CONTINUUM

CONTINUUM+**MXAN**

J. Phys.: Condens. Matter **19** (2007) 266206

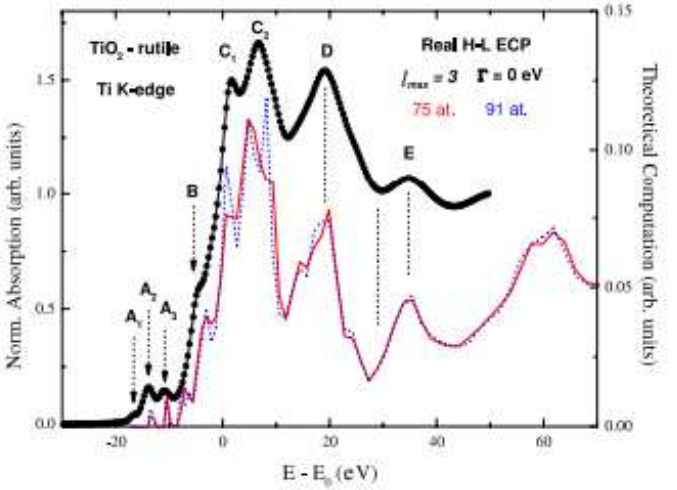

J Chaboy[1], N Nakajima[2] and Y Tezuka[3]

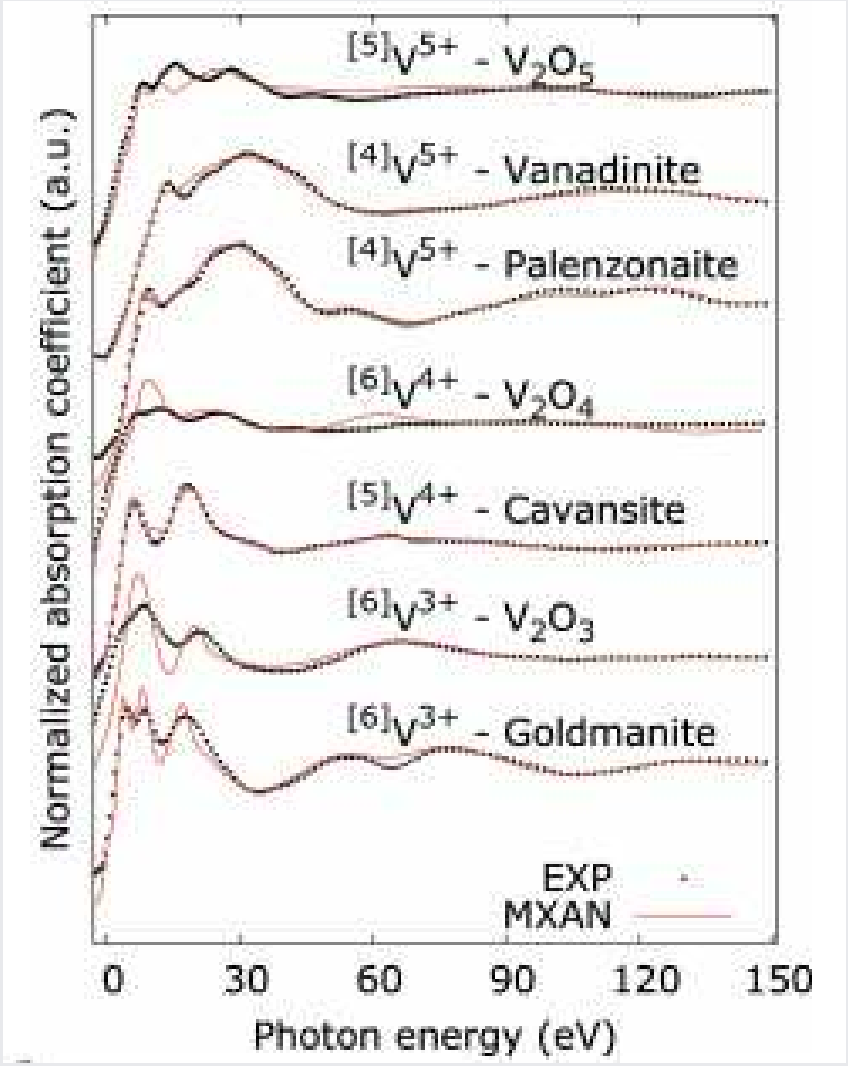

Vanadium *K*-edge XANES in vanadium-bearing model compounds: a full multiple scattering study

Federico Benzi, Gabriele Giuli, Stefano Della Longa, Eleonora Paris

First published: 15 June 2016 | https://doi.org/10.1107/S1600577516008134

CONTINUUM+MXAN

imidazolonepropionase from *Bacillus subtilis* at the zinc site

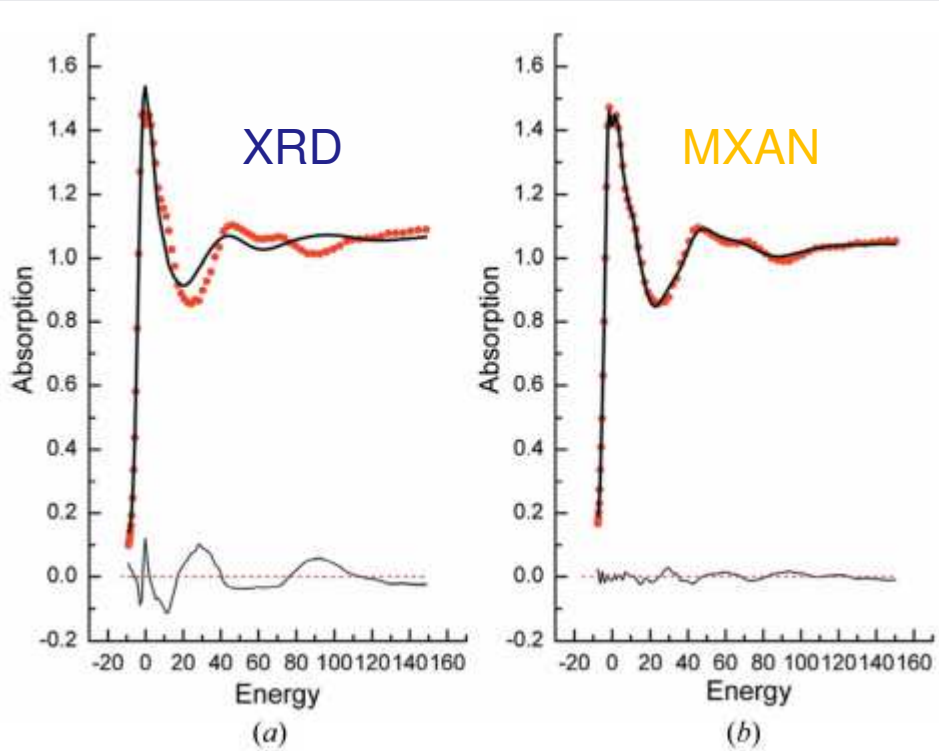

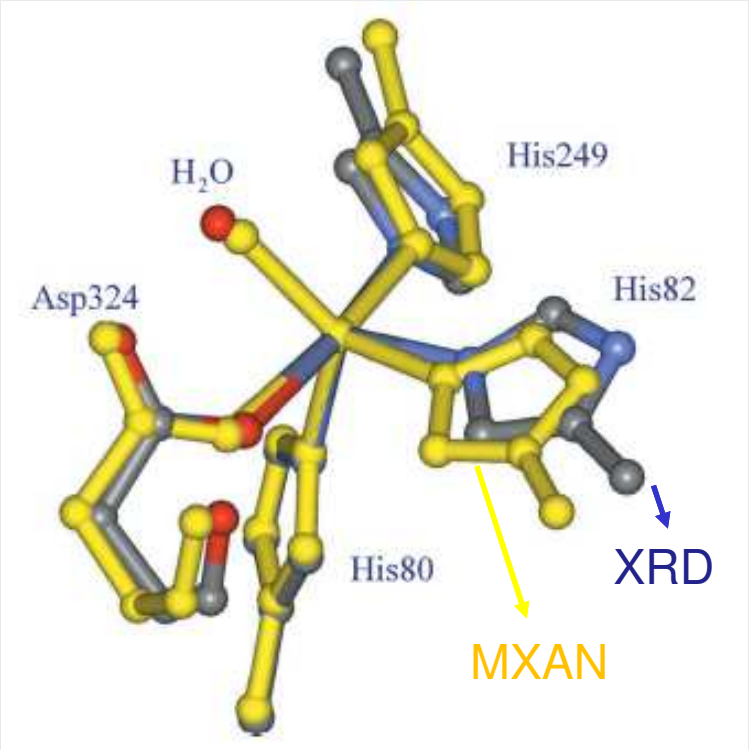

J. Synchrotron Rad. (2008). **15**, 129–133

Feifei Yang, Wangsheng Chu, Meijuan Yu, Yu Wang, Sixuan Ma, Yuhui Dong and Ziyu Wu*

XA(NE)S data collection is *conceptually* simple

Transmission geometry

$$I_t = I_o e^{-\mu \cdot x}$$

μ = Linear absorption coefficient

$$\mu x = \ln \frac{I_o}{I_t}$$

Fluorescence geometry

$$I_f \propto I_o - I_t = I_o(1 - e^{-\mu \cdot x})$$

$$\mu \cdot x \ll 1$$

$$I_f \simeq I_o \mu \cdot x$$

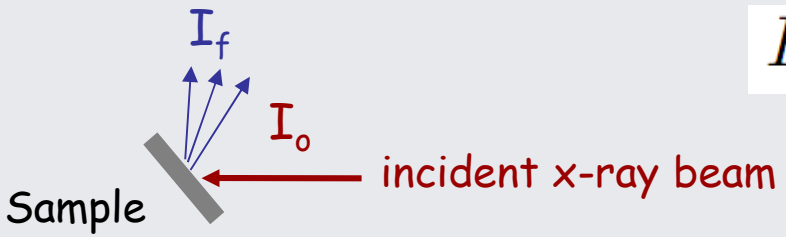

$$\mu x \simeq \frac{I_f}{I_o}$$

… but: warning to the data collection

Transmission geometry: inhomogeneous samples (i.e. holes) may determine severe distortions of the XA(NE)S spectra

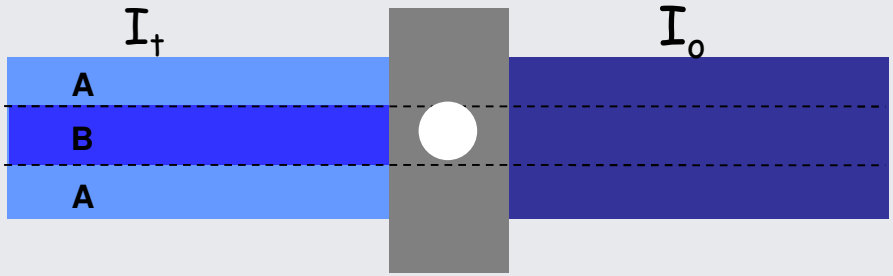

$$I_t = I_o(y_A \cdot e^{-\mu_A x} + y_B \cdot e^{-\mu_B x})$$

! $$\ln \frac{I_o}{I_t} = \ln(y_A \cdot e^{-\mu_A x} + y_B \cdot e^{-\mu_B x})$$!

S- K edge calculated for a layer of spheres

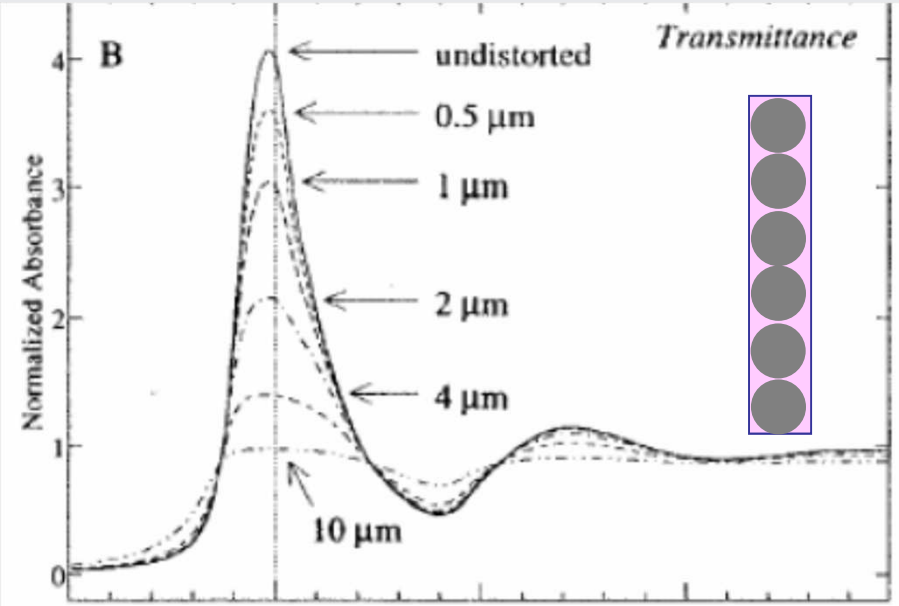

Pickering et al. Biochem 40 92001) 8138

S- K edge calculated for an ensemble of spheres

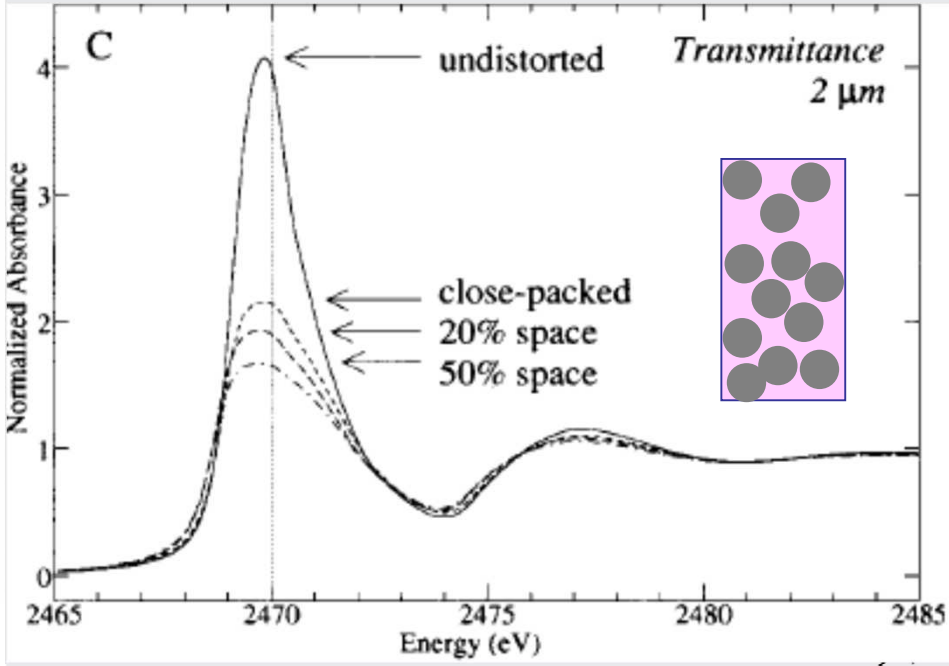

… but: warning to the data collection

Fluorescence geometry: re-absorption and detector linearity may determine severe distortions of the XA(NE)S spectra

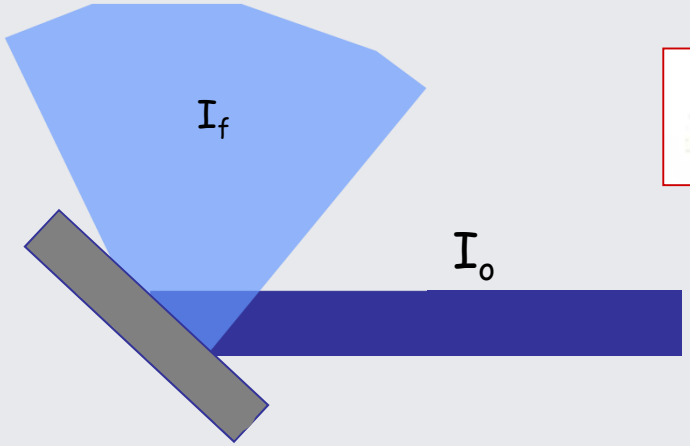

$$I_f \propto I_o - I_t = I_o(1 - e^{-\mu x}) \simeq I_o \mu x$$

$\mu x << 1$

effect of particle size (spheres) on I_f

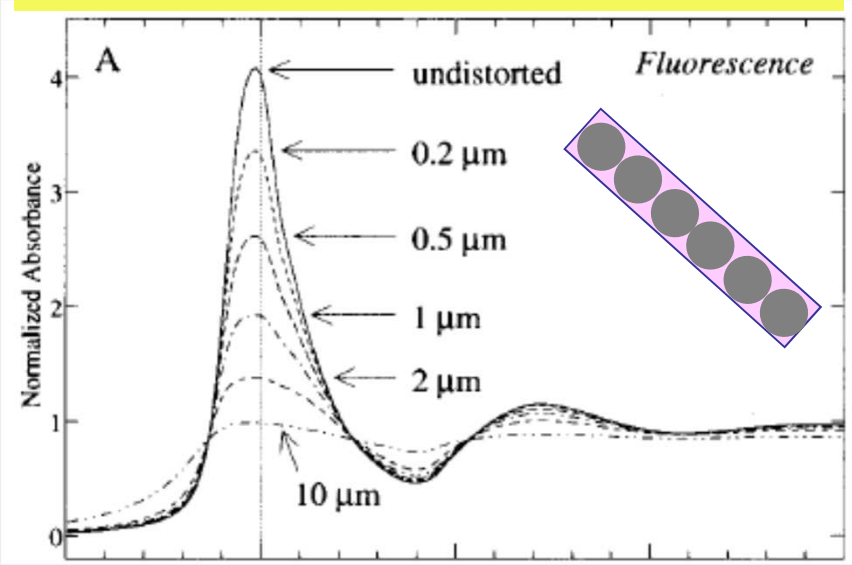

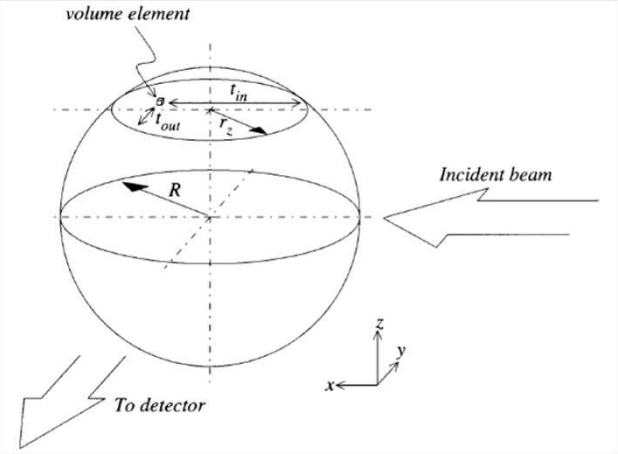

Warning to the data collection

photoreduction on Mn_4Ca PS(II) complex

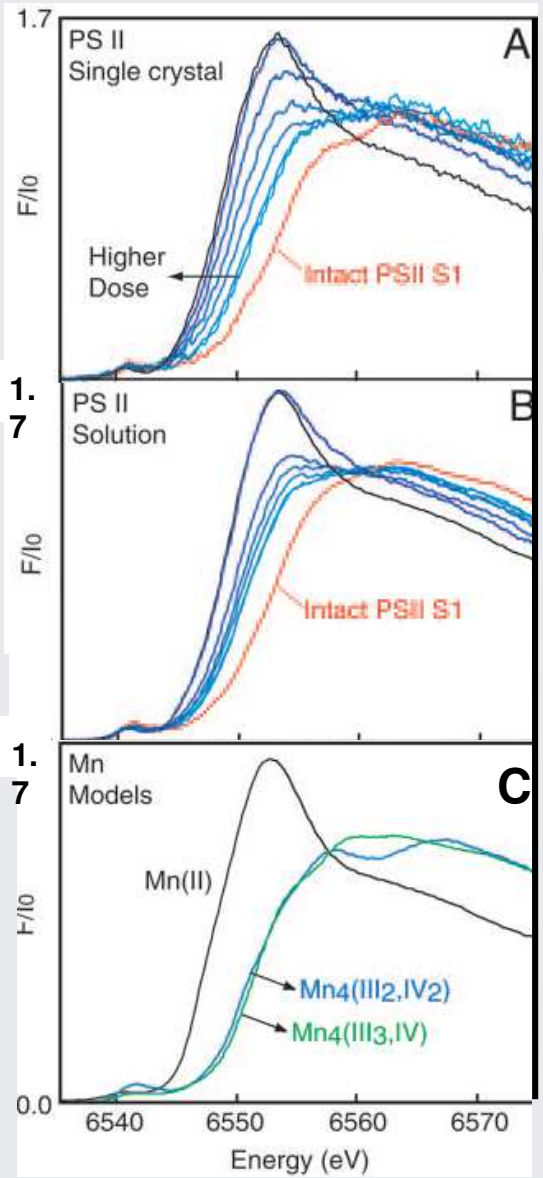

Proc. Natl. Acad. Sci. USA **102**, 12047 (2005)

Radiation Damage (RD) & photoreduction

RD is a function of exposure time/dose, provoke shift of the edge and deformation of XAFS features.

RD can be attenuated by:

- reducing the x-ray intensity
- reducing the exposure time
- collecting data at low sample temperature

RD can be very relevant in biological samples like metalloproteins.

Details about radiation damage and photoreduction can be relevant for reliable protein crystallography

Radiation Damage: XAS and Crystallography

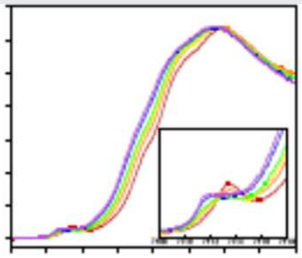

XAS

Visible Effect

- Edge shift (~ 1 eV per e-)
- Shift in EXAFS peak positions

Structural Effect

- *Can be monitored over time (repeated single scans)*
- Longer Metal-Ligand bonds and/or increased σ^2 in M-L paths
- Change in site geometry due to irradiation/chemical reaction

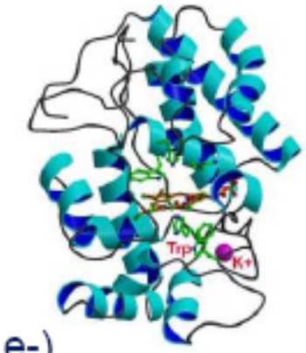

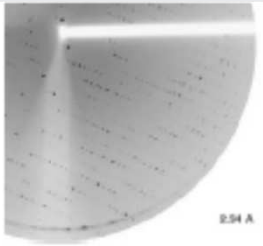

PX

Visible Effect

Loss of diffraction intensity

- Increased unit cell volume

Structural Effect

- *Not monitored over time (one cumulative data set)*
- Breakage of selected bonds
- High DW-factors
- Loss of or unexplained density

XAFS can be used to monitor (in situ) photoreduction of metals

X-ray damage to the Mn_4Ca complex in single crystals of photosystem II: A case study for metalloprotein crystallography

Junko Yano*†‡, Jan Kern§¶, Klaus-Dieter Irrgang§, Matthew J. Latimer¶, Uwe Bergmann¶, Pieter Glatzel‖, Yulia Pushkar*†, Jacek Biesiadka**, Bernhard Loll**, Kenneth Sauer*†, Johannes Messinger†‡‡‡, Athina Zouni§‡‡, and Vittal K. Yachandra*‡‡

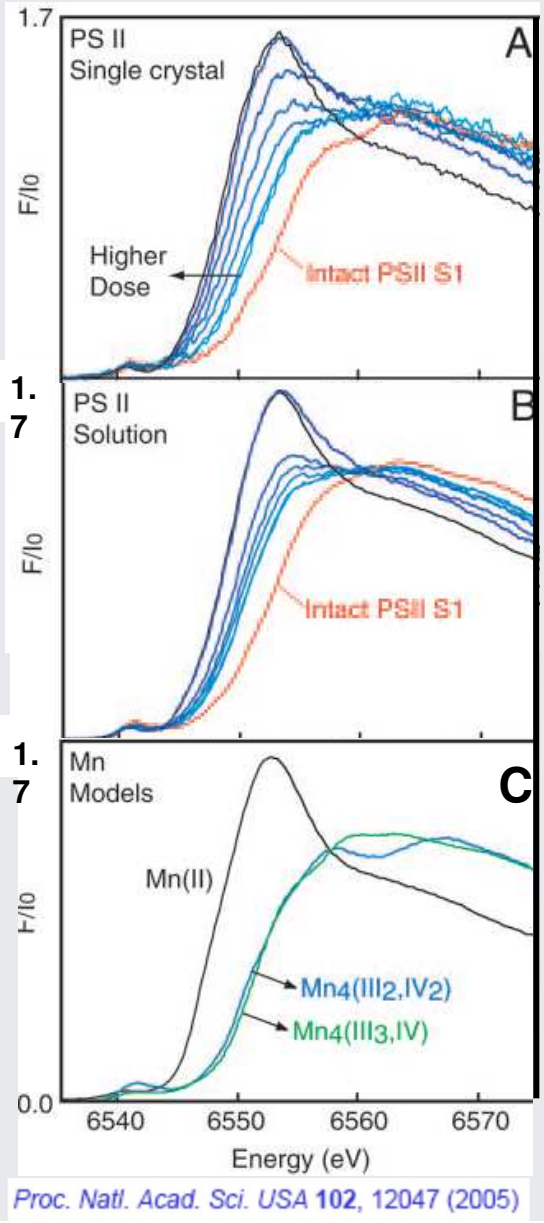

Proc. Natl. Acad. Sci. USA **102**, 12047 (2005)

Photosynthesis uses light energy to **produce O_2 and fix CO_2.** This process generates an aerobic atmosphere and produces a readily usable carbon source.

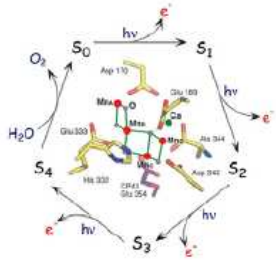

Photosystem II (PSII) reaction catalyzes the photoinduced oxidation of water so it plays an essential role in maintaining the biosphere

It is of considerable importance to elucidate its catalytic mechanisms, particularly those involved in the water oxidation process.

...at present, there are serious discrepancies among the models of the structure of the Mn_4Ca complex in the published x-ray crystallography studies, and there are inconsistencies with x-ray, EPR, and FTIR (...). **This disagreement is predominantly a function of x-ray-induced damage to the catalytic metal site** (...) Therefore, the reported **model of the Mn_4Ca complex** at atomic detail **cannot be based on the diffraction data only** (...).

Proc. Natl. Acad. Sci. USA **102**, 12047 (2005)

photo-reduction of Mn ions

Radiation Damage and photoreduction

The PDB lists 40 structures for $[Fe_2S_2]Cys_4$ ferredoxins
8 are described as oxidized, 1 is described as reduced
none include spectroscopy that would verify the redox state!

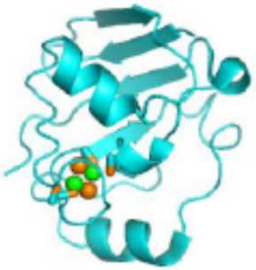

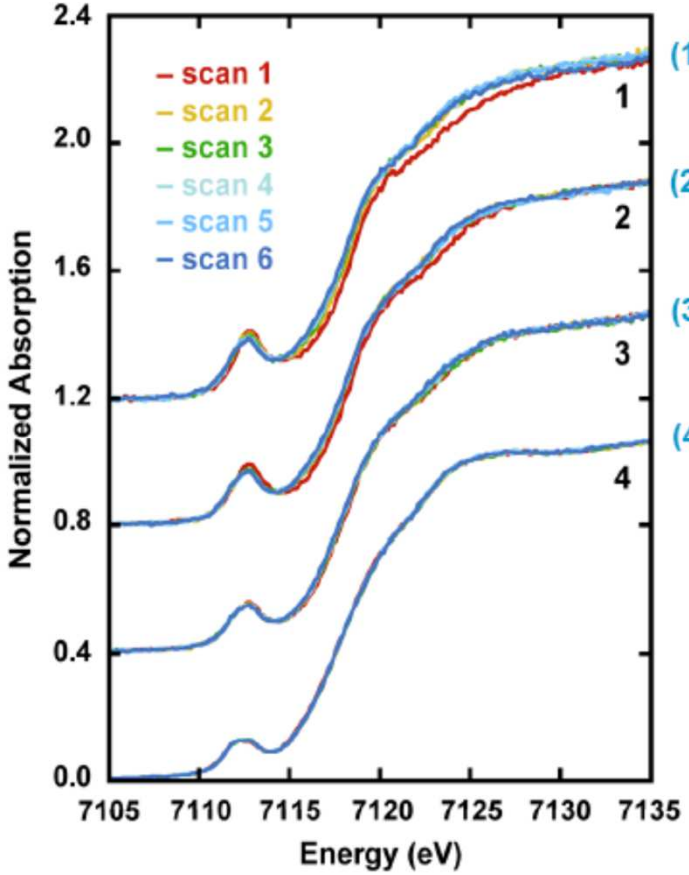

(1) oxidized crystal at ~ 110 K

Immediate photoreduction during first scan

(2) oxidized crystal at ~ 40 K

Slower photoreduction still during first scan

(3) oxidized solution at 7 K

Still slower photoreduction during first scan

(4) reduced solution at 7 K

Reduced site – no change as expected

Each set of spectra displays six consecutive scans with a ca. 20 min duration

How to cope with Radiation Damage

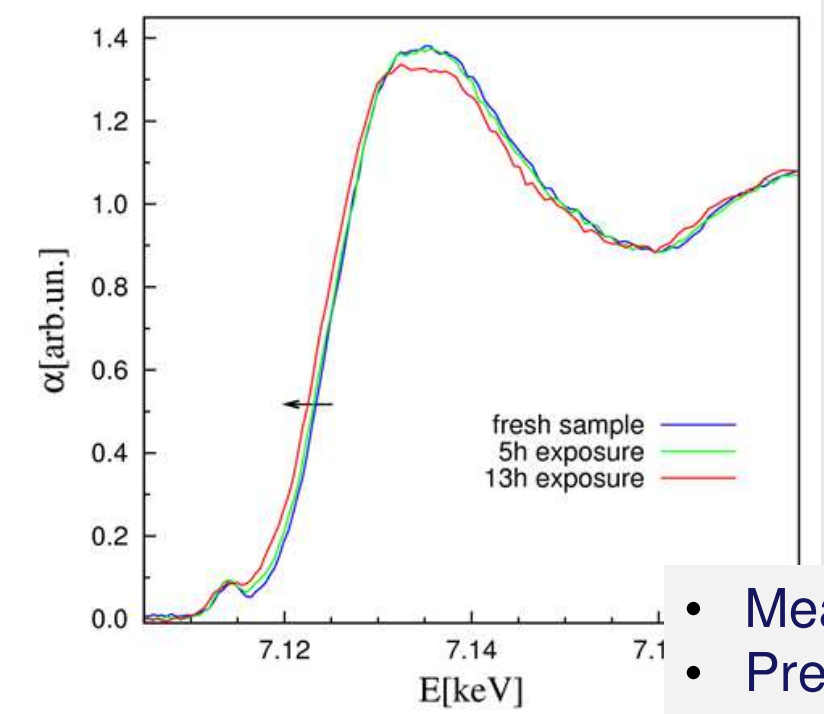

- Measure at low temperatures
- Preliminary check for the sample stability
- Acquire several fast spectra on fresh sample regions.

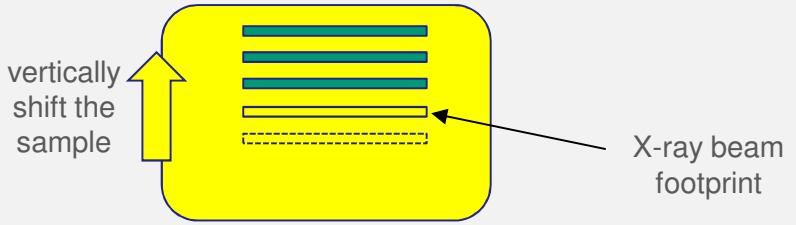

Special Applications of XANES spectroscopy: μ-XANES & mapping

XAS vs XRF
XRF= elemental sensitivity
XAS= **elemental sensitivity + chemical speciation**

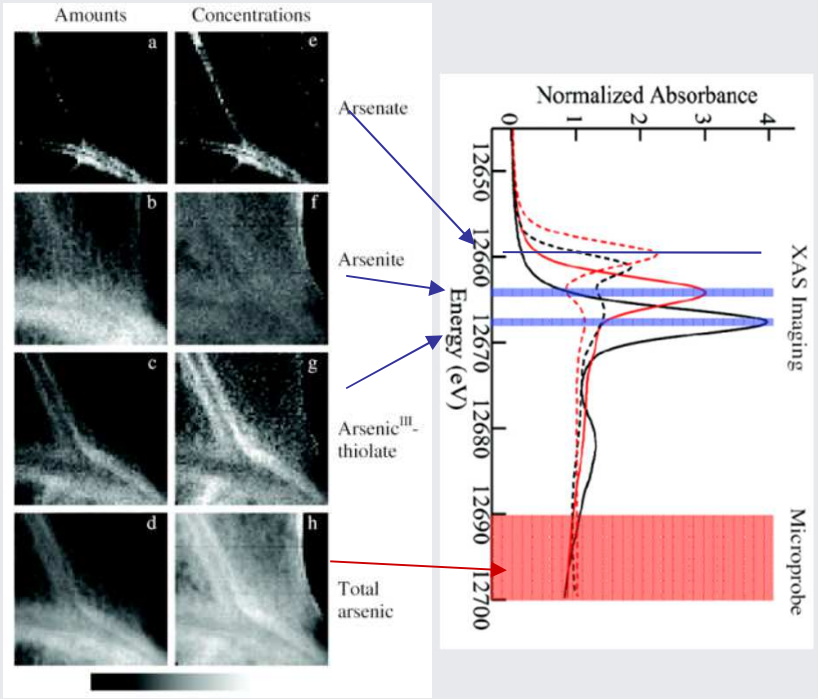

I. J.Pickering & G. N. George Proc. XAFS13 conference (2006)

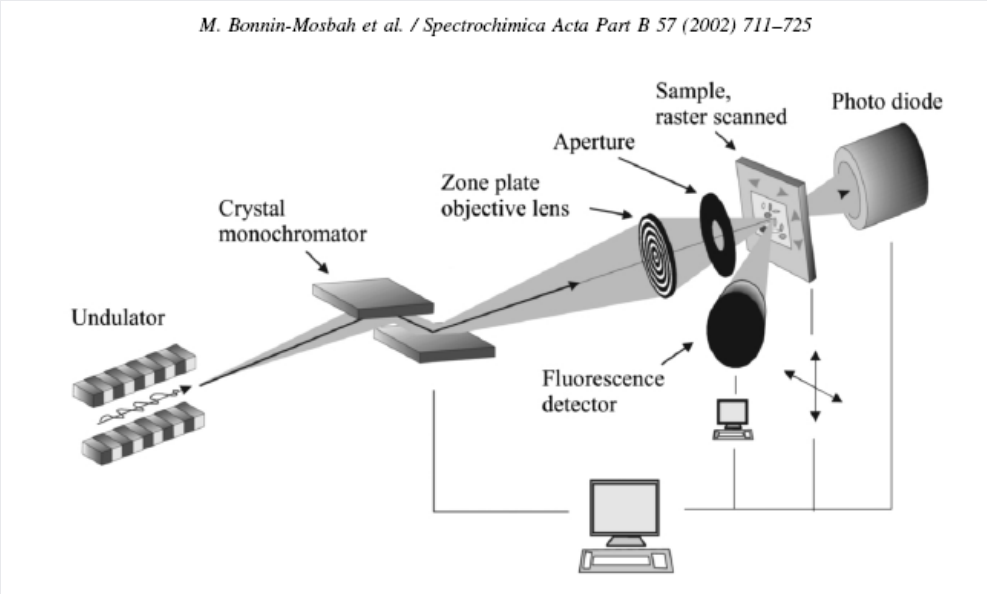

NOTE: X-ray lenses and zone plates work in a reduced energy window, therefore the EXAFS region is often not accessible to micro and nano probes

Bio- e Fito-Remediation or:
Plants and (micro-)organisms employed to regulate pollutant mobility (i.e. heavy metals) within the ecosystem and environment

Elphidium

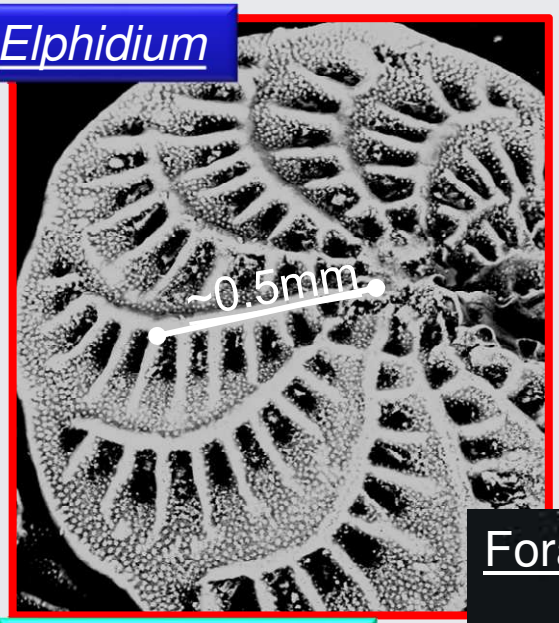

μ-XANES mapping

4x4 μm spot
@ ESRF BM23

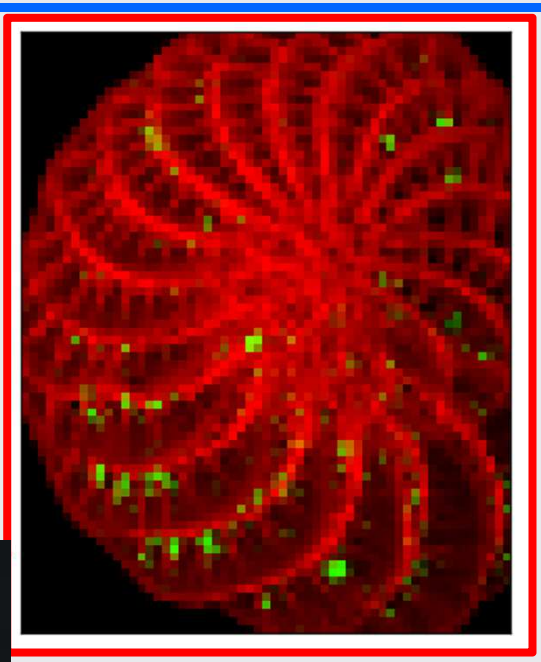

Foraminifers

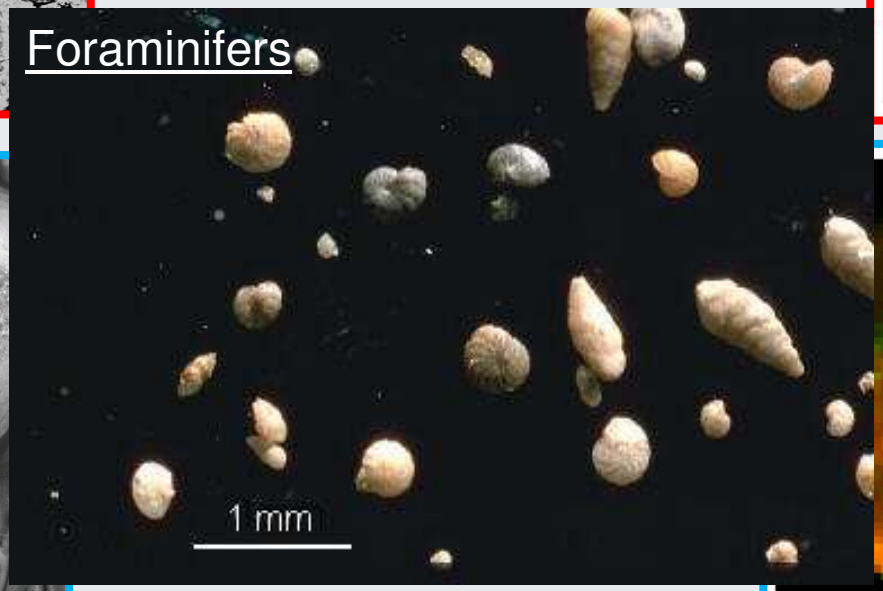

Quinquenoculina

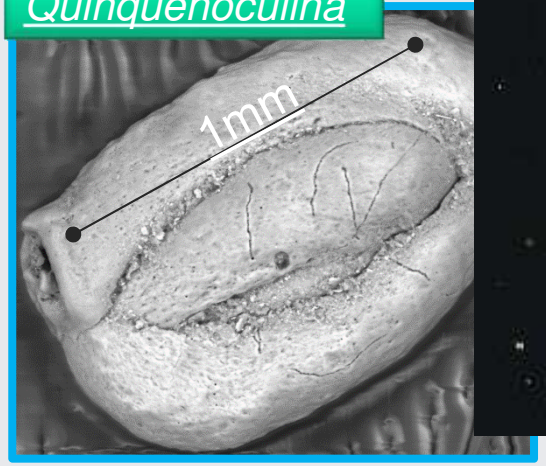

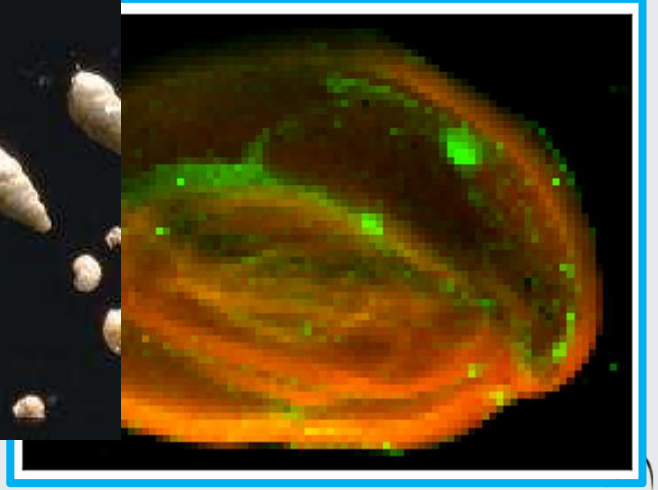

Chemical Geology 477 (2018) 100–111

Bio- e Fito-Remediation or:
Plants and (micro-)organisms employed to regulate pollutant mobility (i.e. heavy metals) within the ecosystem and environment

Elphidium

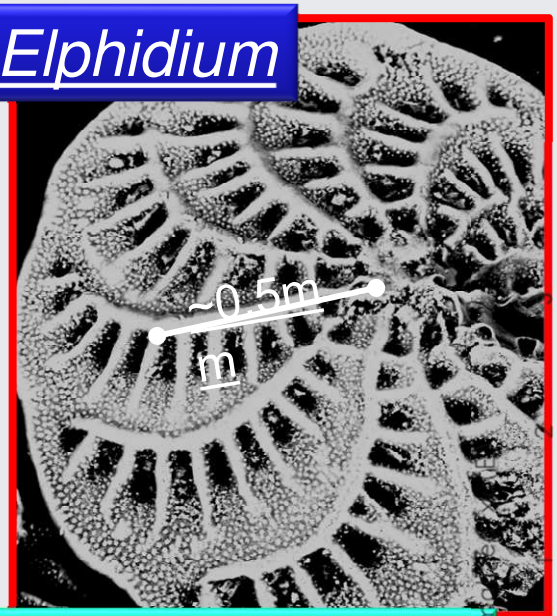

Quinquenoculina

XANES & mapping

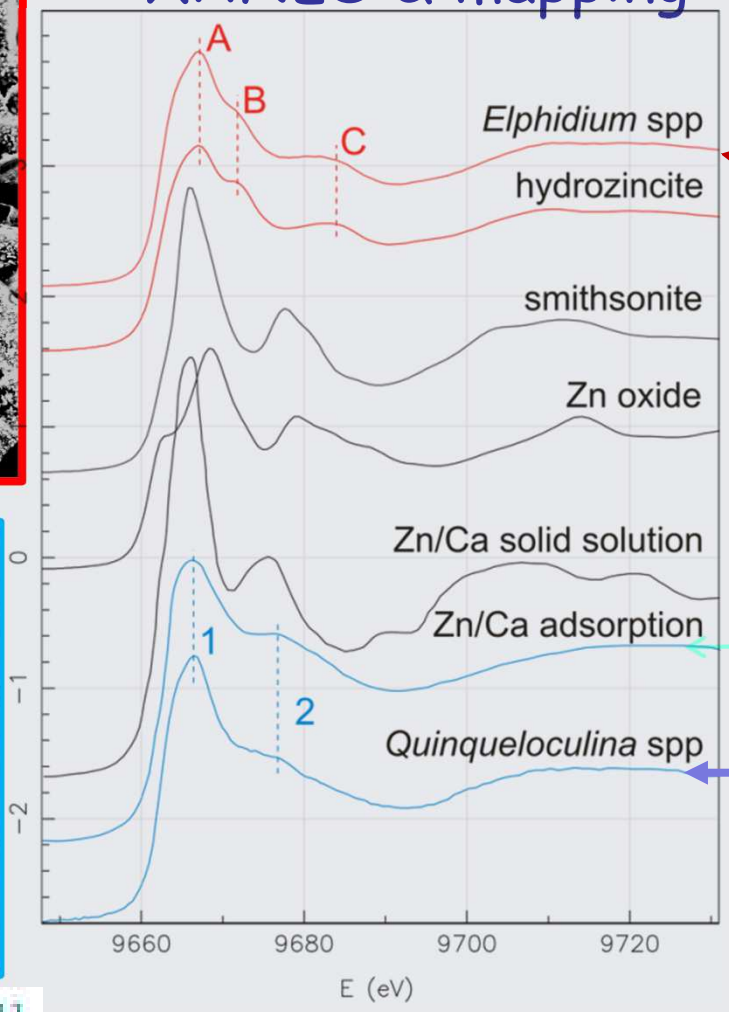

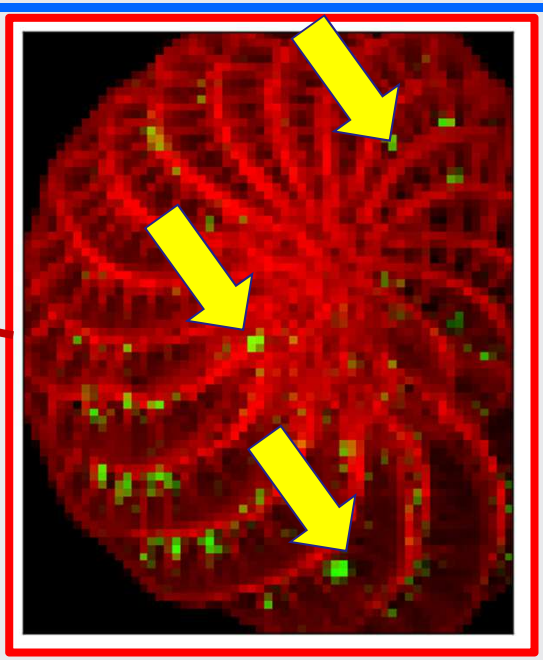

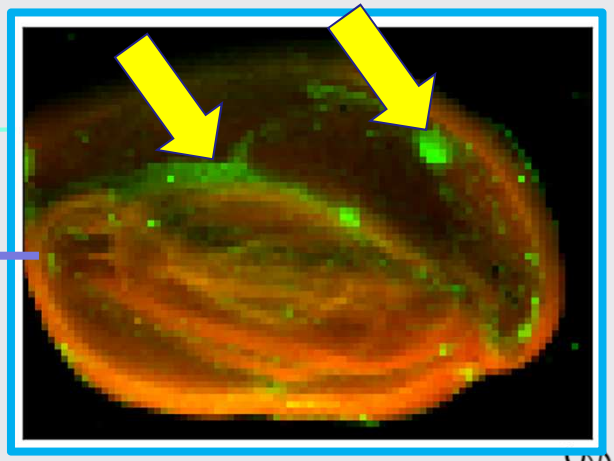

Chemical Geology 477 (2018) 100–111

Bio- e Fito-Remediation or:
Plants and (micro-)organisms employed to regulate pollutant mobility (i.e. heavy metals) within the ecosystem and environment

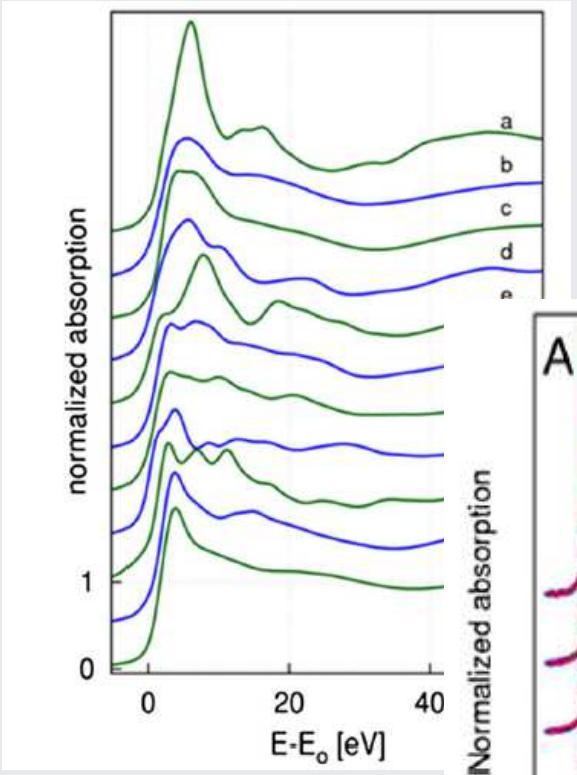

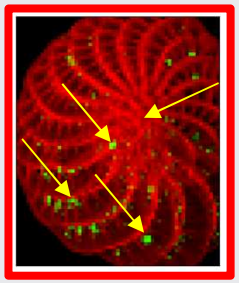

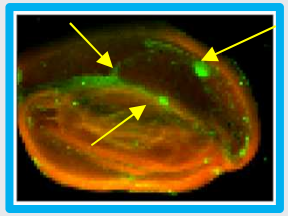

μ-XANES

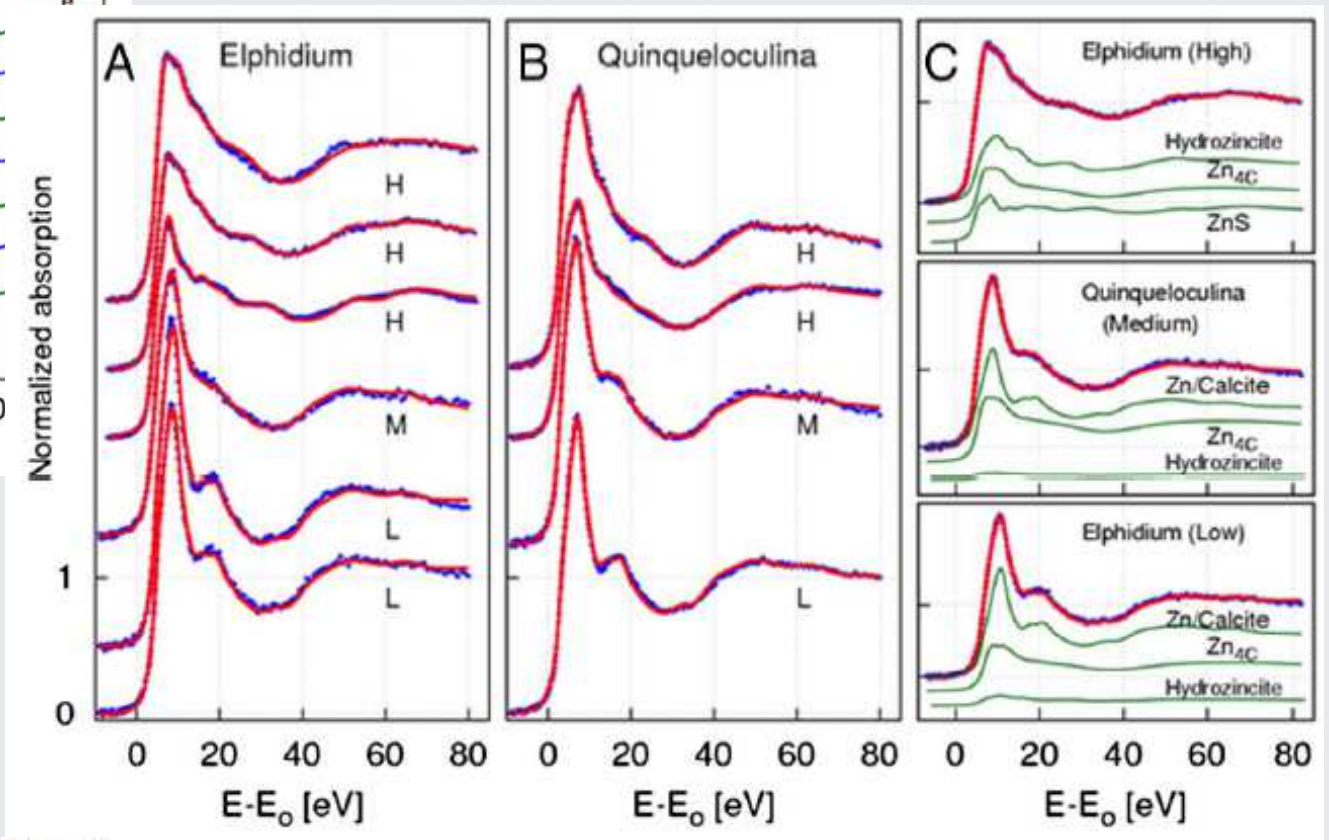

Chemical Geology 477 (2018) 100–111

Bio- e Fito-Remediation or:
Plants and (micro-)organisms employed to regulate pollutant mobility (i.e. heavy metals) within the ecosystem and environment

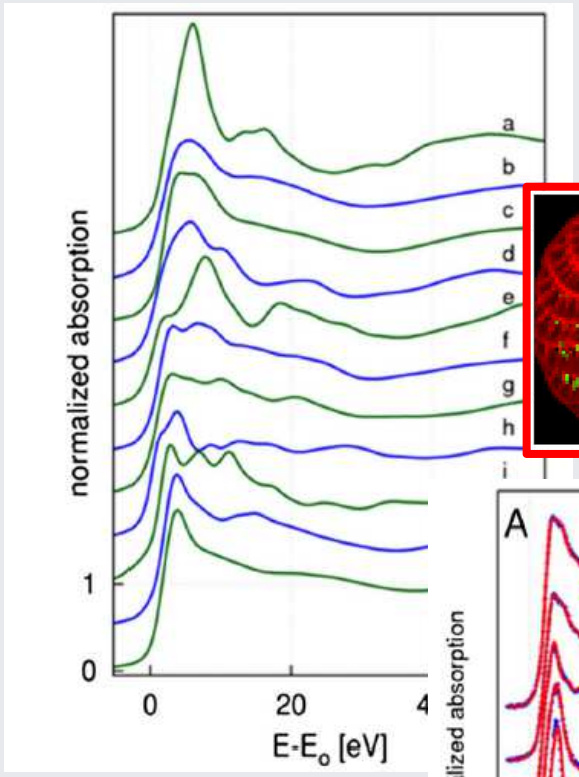

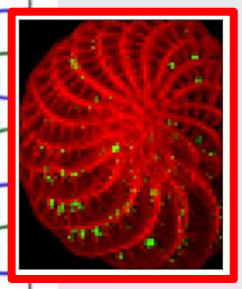

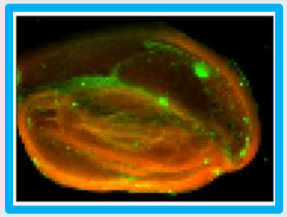

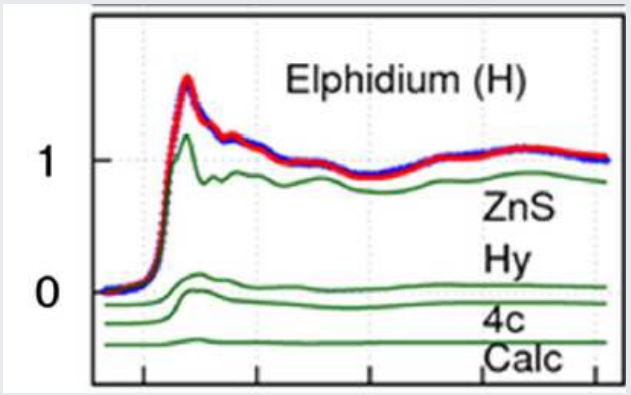

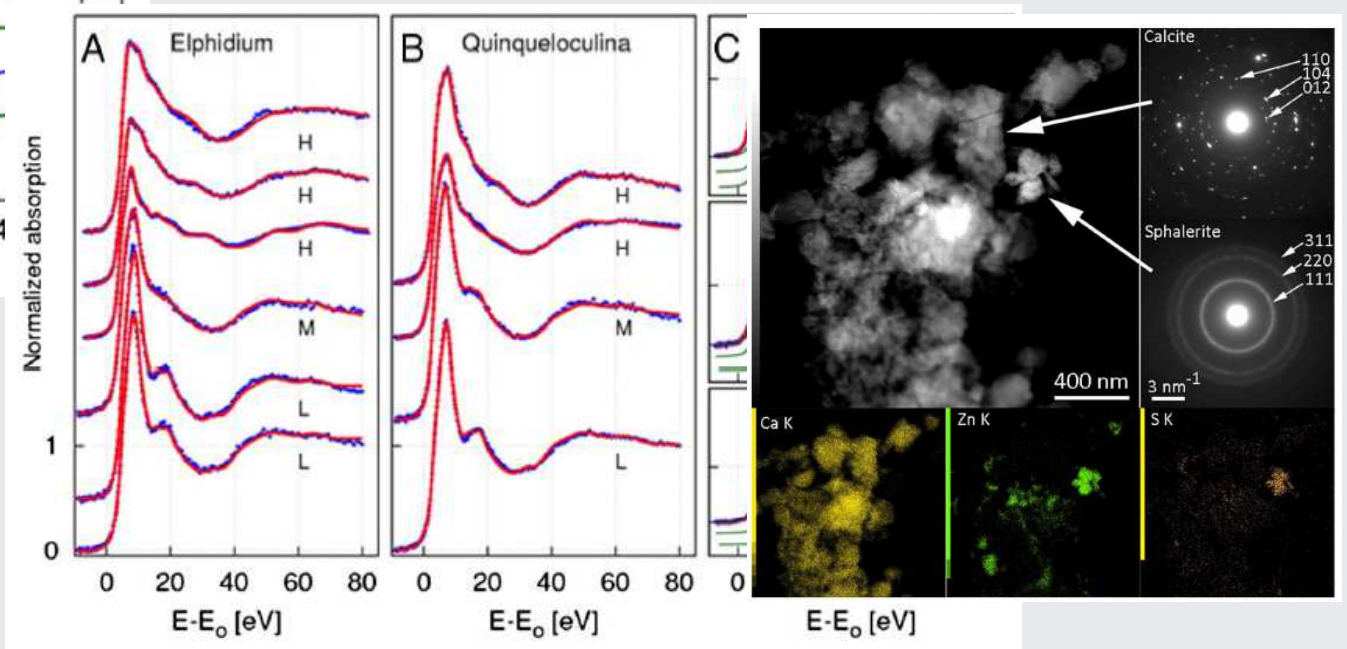

G. De Giudici, D. Medas, P. Lattanzi, C. Meneghini, et al. to be submitted (Scienze)

Time resolved XA(NE)S: experimental set-up

Quick XAFS

$\Delta t = 10\text{-}10^2 s$

any data collection geometry

Dispersive XAFS

$\Delta t = 10^{-3} - 1\ s$

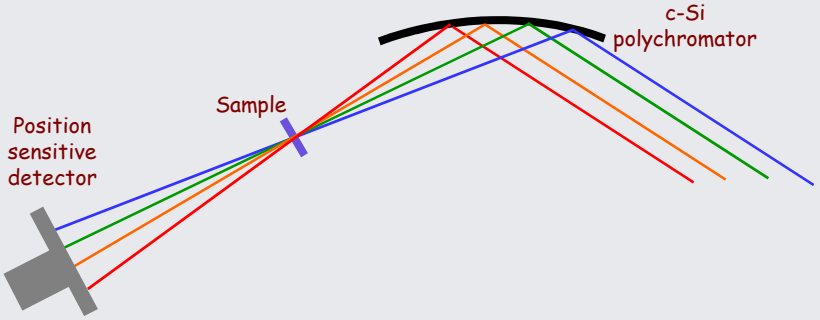

Transmission geometry

Pump probe

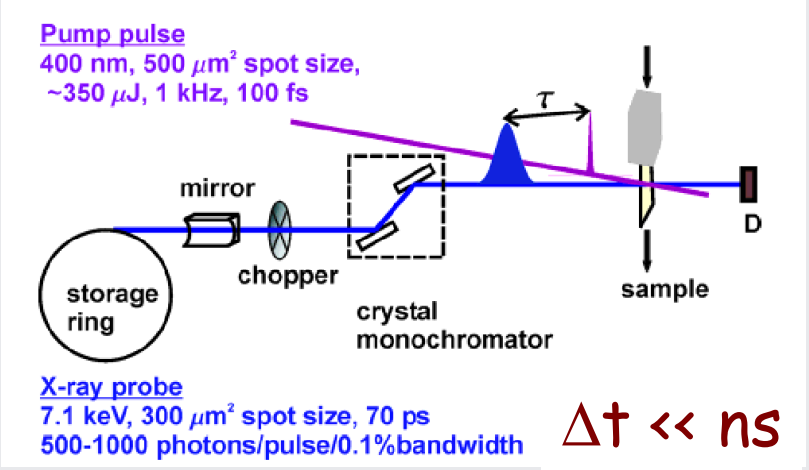

$\Delta t << ns$

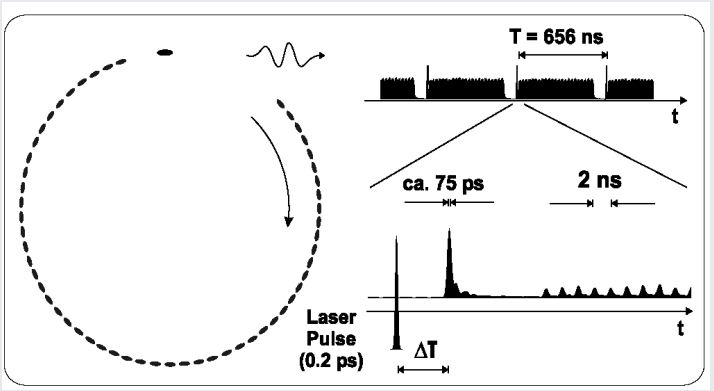

Time resolved XAS

Single Energy - XAS

Melting of In μ-particles and structure of undercooled In phase

In K edge

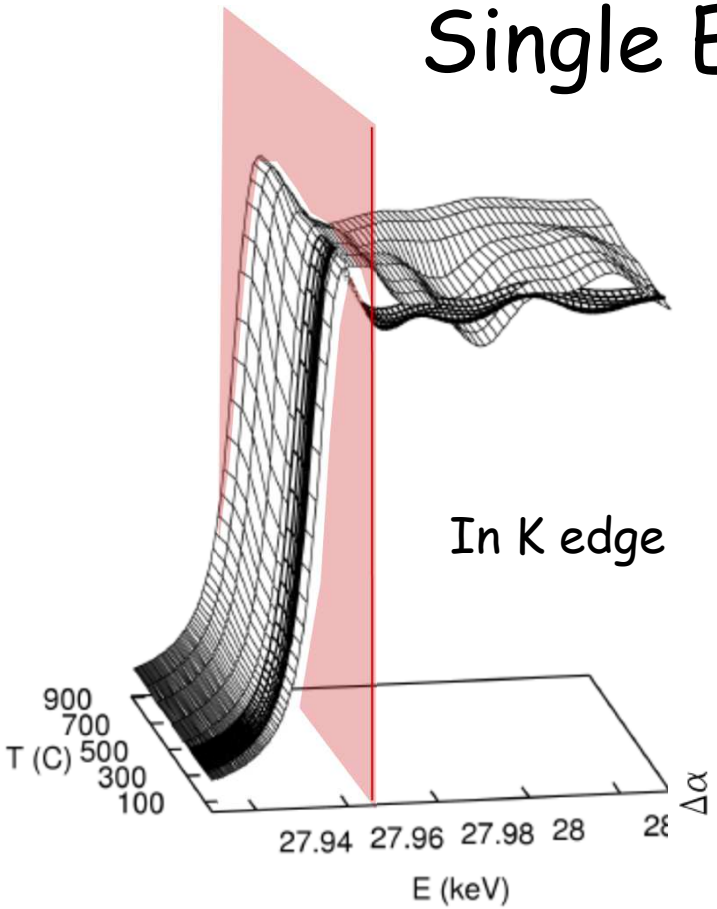

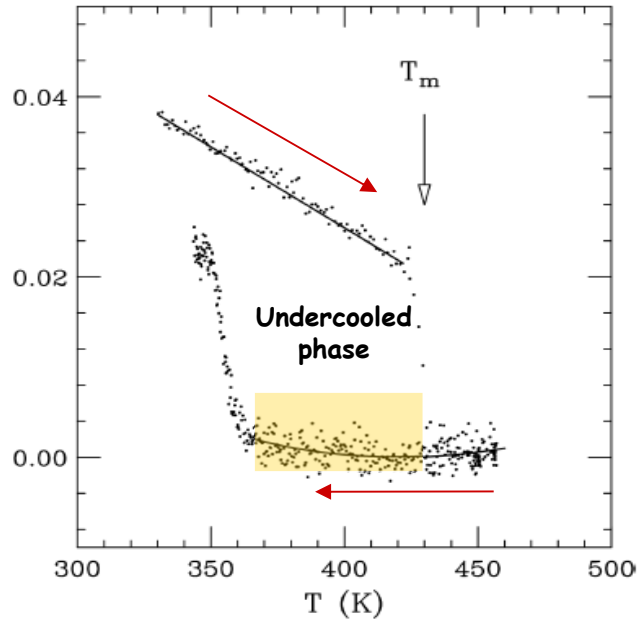

A. Filipponi et al. J. Sinchr. Rad. 8, 81 (2001)

Light elements XANES

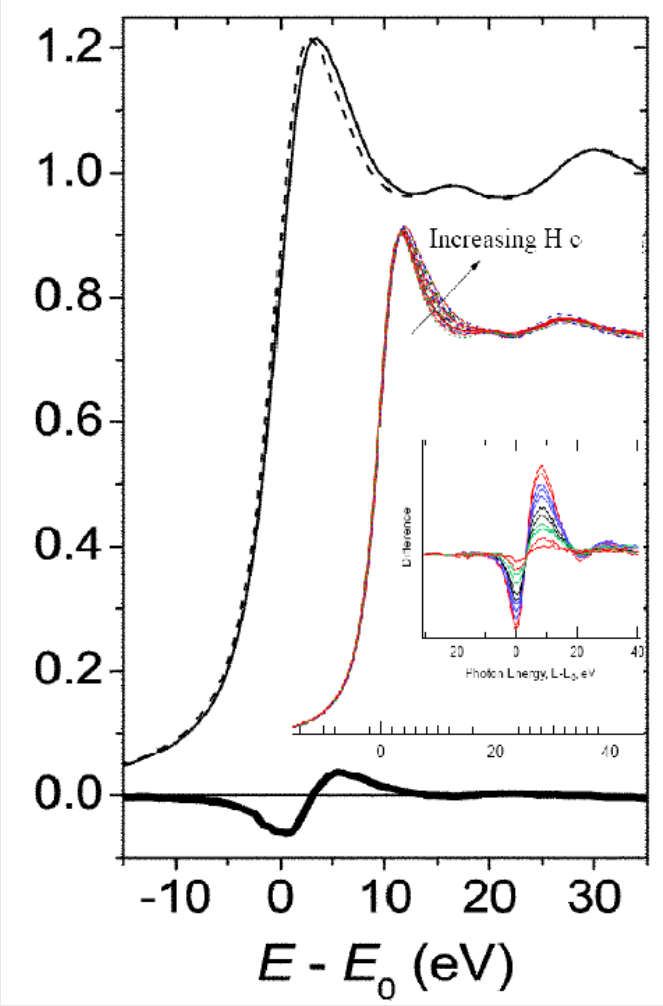

The Effect of H coverage on Pt nanoparticles:

H is notably weakly visible to x-ray

but becomes evident in the XANES region

At the Pt L_{III} edge the effect of H is evident and can be followed in-situ to monitor the catalytic activity of Pt clusters as a function of environmental parameters.

Example: transient states of photoexcited hydrated atoms Δt ~1 ns

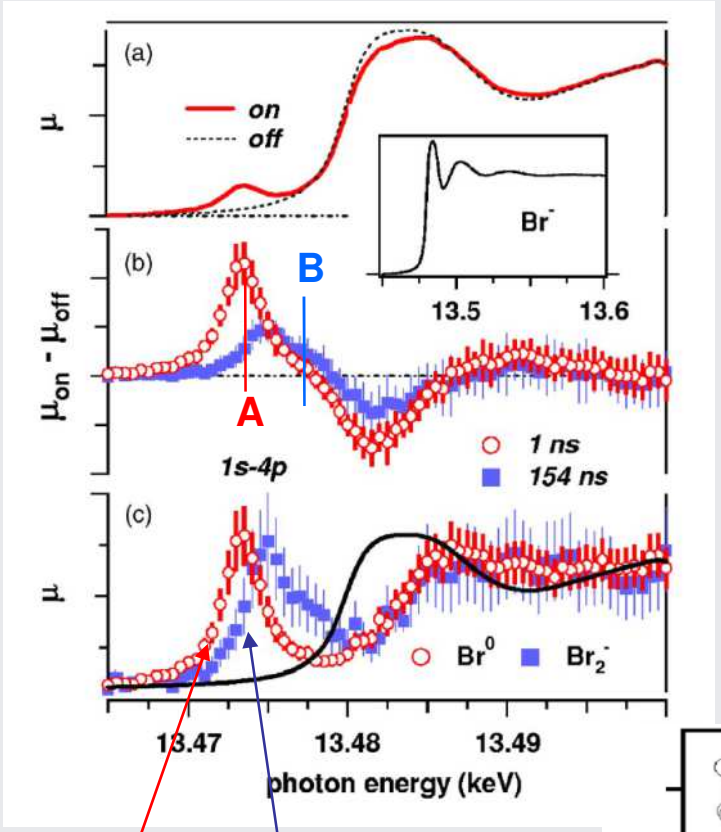

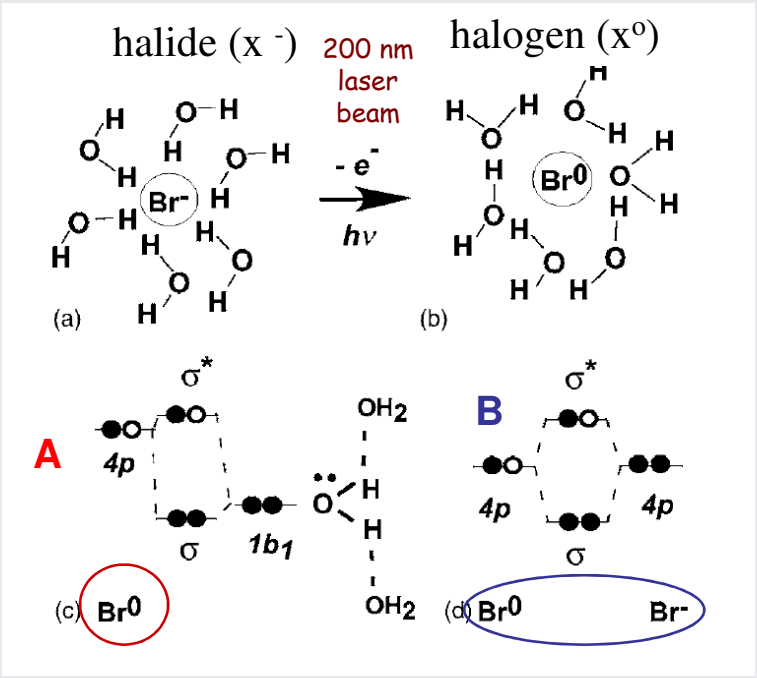

SE-XAS

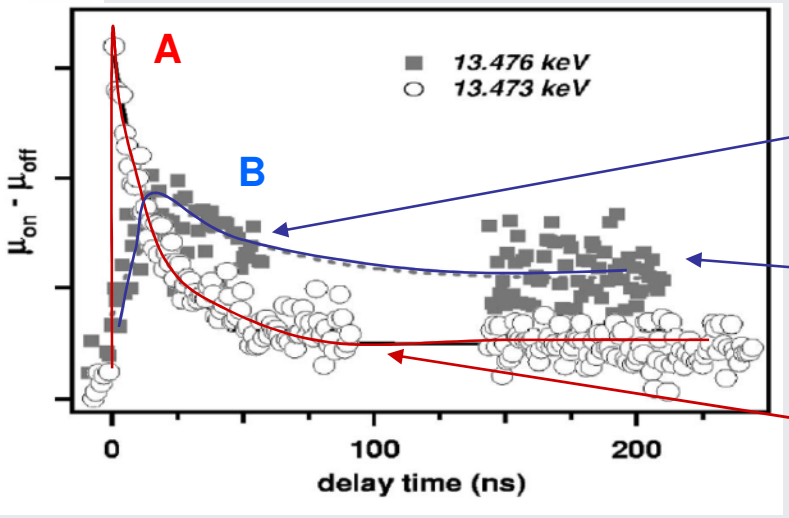

Br_0 Br_2^-

production of Br_2 (Δt ~10 ns)

Br_2 molecules survive after Δt >150 ns

Reaction with water (Δt ~ 50 ns)

THE JOURNAL OF CHEMICAL PHYSICS 128, 061102 (2008)

Transient x-ray absorption spectroscopy of hydrated halogen atom

Christopher G. Elles,[a] Ilya A. Shkrob,[b] and Robert A. Crowell[c] Dohn A. Arms and Eric C. Landahl

Polarized XANES: directional probe for not isotropic structures

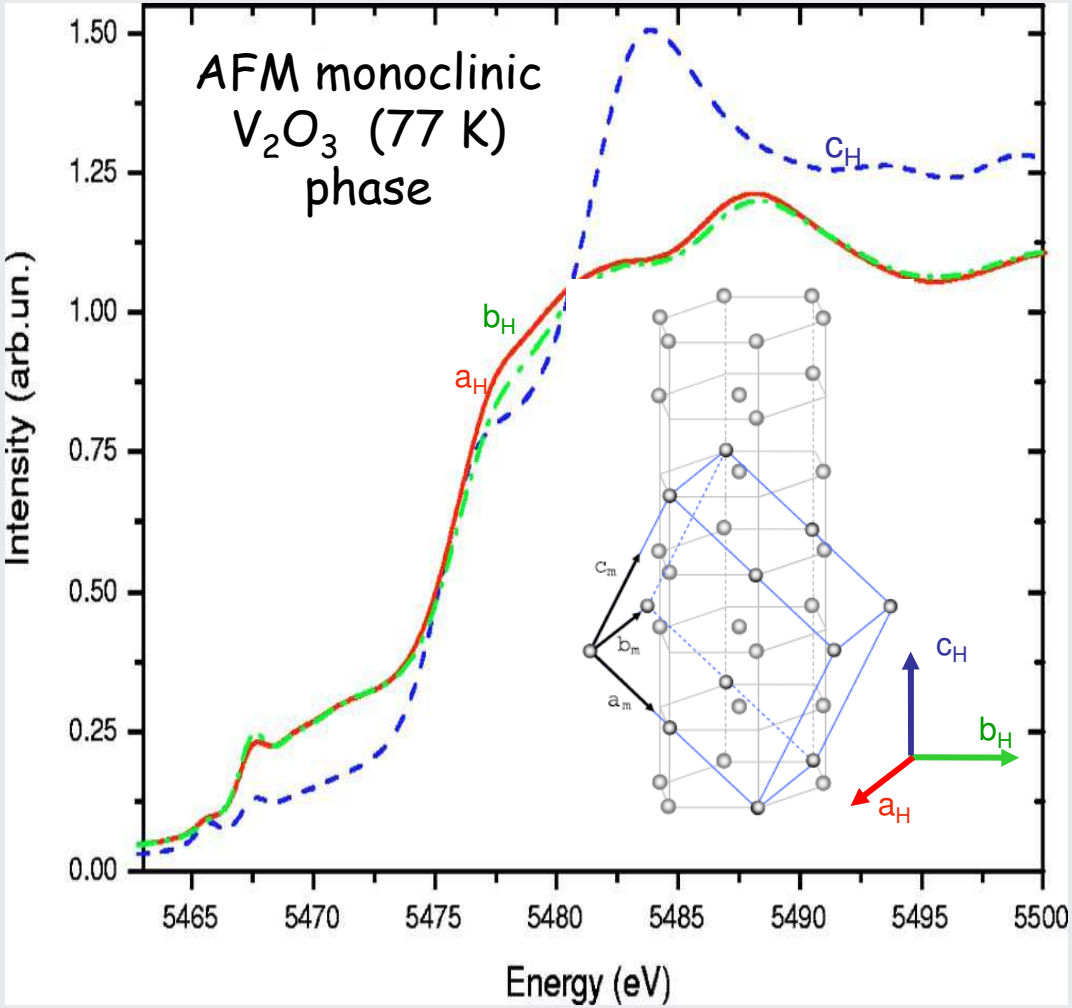

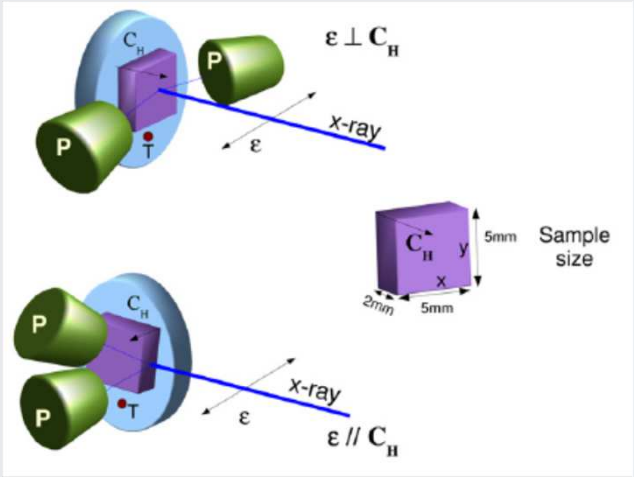

Structural dichroism (absent in hexagonal HT phase) is the fingerprint of monoclinic distortion

PHYSICAL REVIEW B 72, 033111 (2005)

Structural dichroism in the antiferromagnetic insulating phase of V_2O_3

C. Meneghini,[1] S. Di Matteo,[1,2] C. Monesi,[1] T. Neisius,[3] L. Paolasini,[3] S. Mobilio,[1,2] C. R. Natoli,[2] P. A. Metcalf,[4]

XMCD-XANES extreme condition studies

High pressure structural and magnetic diagram of phase of 3d metal alloys

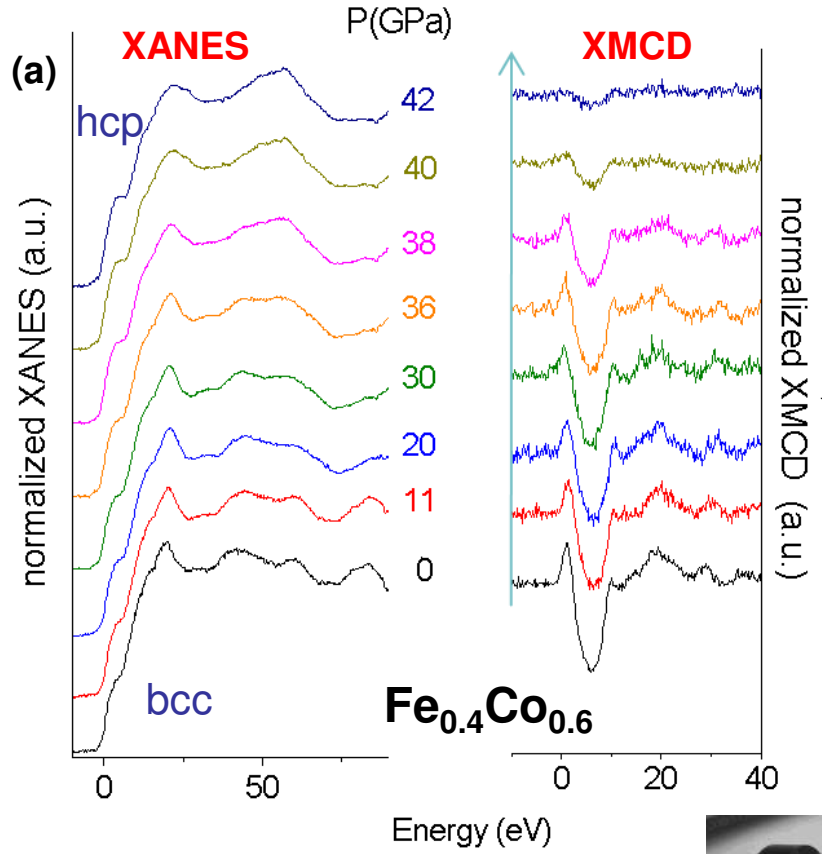

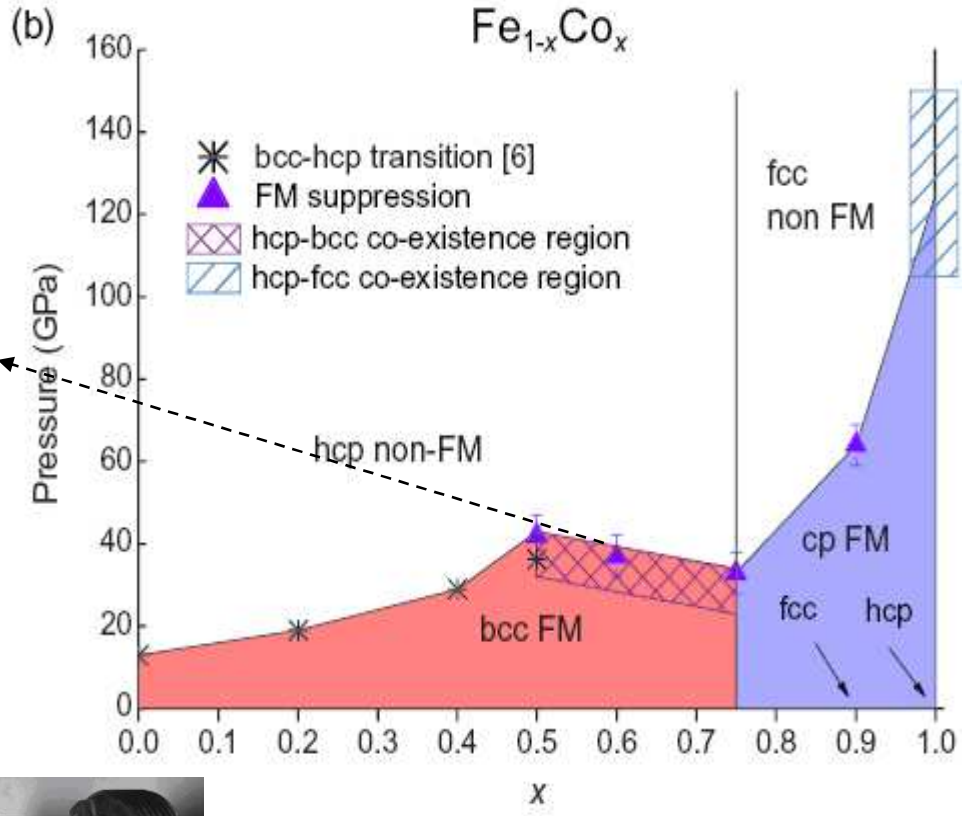

R. Torchio et al. High Pressure Research 31, 148-152 (2011)

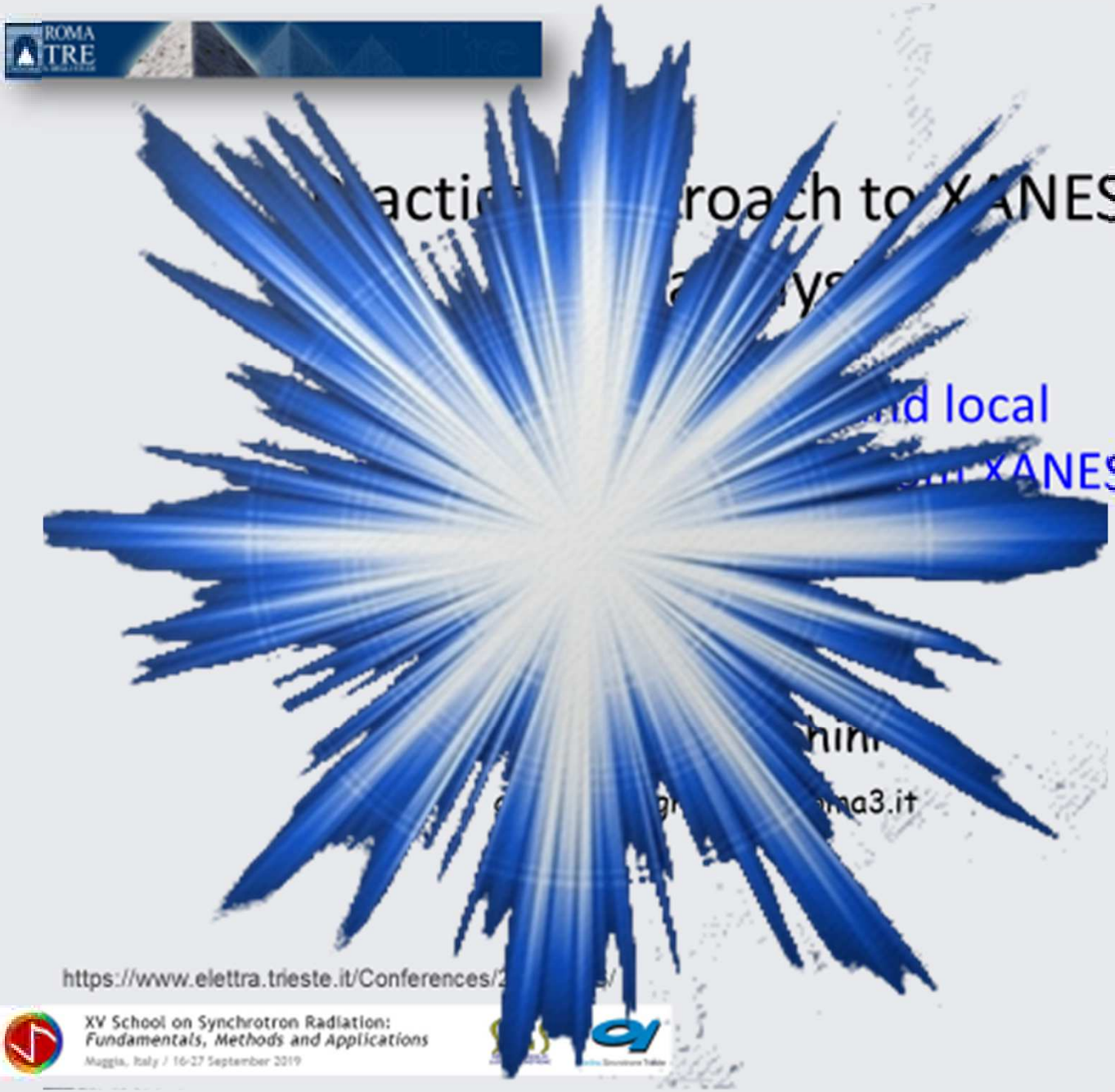
ROMA TRE
roach to XANES
nd local
XANES
hin
ma3.it
https://www.elettra.trieste.it/Conferences/2
XV School on Synchrotron Radiation:
Fundamentals, Methods and Applications
Muggia, Italy / 16-27 September 2019